



TECHNISCHE
UNIVERSITÄT
WIEN

DIPLOMARBEIT

New Data Standard for the SModelS Database Containing LHC Results for Supersymmetry Searches

ausgeführt am Atominstitut (E141) und am Institut für
Hochenergiephysik (HEPHY) der Österreichischen Akademie der
Wissenschaften (ÖAW)

eingereicht an der Technischen Universität Wien, Fakultät für Physik

unter der Anleitung von

Doz. DI Dr. techn. Claudia-Elisabeth Wulz

DI Dr. techn. Wolfgang Waltenberger

Dr. rer. nat. Suchita Kulkarni

durch

Michael Traub

September 17, 2015

Abstract

During the first phase of the LHC operation, numerous searches for Beyond the Standard model scenarios (BSM) have been conducted. As a model independent approach, it became a standard technique to interpret these searches in terms of “Simplified Models Spectra” (SMS). For a simplified model only a small number of new particles is assumed to be light. The observed result is interpreted as 95% confidence level upper limit on production cross section times branching ratio $(\sigma \times BR)_{UL}$, depending on the masses and the allowed decays of these particles. The limits can be applied to any BSM scenario that share the same simplified model topology and kinematics.

This thesis is focused on SMS interpretations of searches for supersymmetry (SUSY), done by the two general purpose experiments ATLAS and CMS. In order to estimate the reach of the searches, the experiments also plot exclusion lines on top of the upper limits on $(\sigma \times BR)_{UL}$. The exclusion lines assume 100 % branching ratio for a simplified model and are not valid for full models.

Comparing a full model to the numerous SMS results is still complicated. Therefore a tool called “SModelS” was developed. It provides an automated procedure to decompose a full model into SMS topologies. The $(\sigma \times BR)$ of these topologies are compared with the upper limits on $(\sigma \times BR)_{UL}$ obtained from the experiment. Most limits by ATLAS and CMS for Run 1 are included in the SModelS database.

During this thesis the SModelS database was validated. The framework was used to reproduce the exclusion lines given by the experimentalists. A large number of these lines were found to show very good agreement. A release database was built and shipped with the first release of SModelS 1.0.

Within the validation process improvements with respect to the implementation of the experimental data were made. In the light of new results after the restart of the LHC, a fast and reliable way for the data implementation is needed, to keep the SModelS database updated. This resulted in the development of a new framework and a new database structure, described in this thesis. The main advantages of this framework are a user friendly interface for manual data input, several safety switches and an automated recognition of off-shell SM particles for a given model. The framework and the new structure also extend the database for the implementation of efficiency maps for a future version of SModelS.

Kurzfassung

Während der ersten Operationsphase des LHC wurden zahlreiche Suchen nach neuer Physik jenseits des Standardmodells (BSM) durchgeführt. Zur Interpretation der Suchergebnisse hat sich der modellunabhängige Ansatz des “vereinfachte Modell Spektrums” (SMS) als Standardtechnik etabliert, wobei nur eine kleine Anzahl leichter neuer Teilchen für eines dieser Modelle angenommen wird. Die experimentellen Ergebnisse können im Rahmen des Modells in Abhängigkeit der Teilchenmassen und der erlaubten Zerfälle, als obere Grenzwerte für das Produkt aus Wirkungsquerschnitt der Teilchenproduktion und Zerfallswahrscheinlichkeit $(\sigma \times BR)_{UL}$ interpretiert werden. Diese oberen Grenzwerte können prinzipiell auf jedes BSM Szenario angewandt werden, solange es das entsprechende vereinfachte Modell beinhaltet.

Die vorliegende Diplomarbeit beschäftigt sich mit SMS Interpretationen von Suchen nach Supersymmetrie (SUSY), durchgeführt von den beiden multifunktionalen Experimenten ATLAS und CMS. Um die Reichweite der bisherigen Suchen abzuschätzen, werden zusätzlich zu den Werten für $(\sigma \times BR)_{UL}$ auch Grenzlinien für die Massenbereiche der neuen Teilchen angegeben. Zur Berechnung dieser Grenzlinien wird angenommen, dass die Zerfallswahrscheinlichkeit für ein vereinfachtes Modell 100 % beträgt, diese sind daher nicht für komplette BSM Szenarien gültig.

Der Vergleich kompletter Modelle mit den verschiedenen SMS Resultaten ist aufwendig. Daher wurde zu diesem Zweck ein Programm namens SModelS entwickelt. Dieses ist in der Lage, ein komplettes BSM Modell in seine SMS Topologien zu zerlegen und die theoretischen Werte von $(\sigma \times BR)$ für diese Topologien mit den experimentellen Werten von $(\sigma \times BR)_{UL}$ zu vergleichen. Zu diesem Zweck verwendet SModelS eine Datenbank in welcher die meisten SMS Resultate von ATLAS und CMS gespeichert sind.

Im Zuge der vorliegenden Diplomarbeit wurde diese Datenbank validiert, indem SModelS verwendet wurde um die von den Experimentalphysikern angegebenen Grenzlinien zu reproduzieren. Eine große Anzahl dieser Grenzlinien konnten mit guter Übereinstimmung reproduziert werden. Schließlich wurde eine validierte Datenbank erstellt, welche gemeinsam mit SModelS 1.0 veröffentlicht wurde.

Die Validierung zeigte auch Verbesserungsmöglichkeiten für die Implementierung der experimentellen Daten auf. Weiters muss in Hinblick auf die zweite Operationsphase des LHC, eine schnelle und zuverlässige Implementierung neuer Resultate gewährleistet sein um die SModelS Datenbank auf dem neuesten Stand zu halten. Dies führte zur Entwicklung eines neuen Hilfsprogramms zur Datenimplementierung und einer neuen

Datenbankstruktur. Die wesentlichen Vorteile des neuen Programms sind: eine benutzerfreundliche Schnittstelle für die Datenimplementierung, eine Überprüfung der neu implementierten Daten, so wie eine automatische Erkennung von virtuellen SM Teilchen innerhalb eines vereinfachten Modells. Die neue Datenbankstruktur und das Datenimplementierungsprogramm ermöglichen zudem eine Implementierung von Effizienzdiagrammen, welche für eine zukünftige SModelS Version benötigt werden.

Acknowledgement

First of all, I would like to thank all members of the SModelS group, in particular Wolfgang Waltenberger for being my supervisor not only for the diploma thesis, but also for the preceding project work. Moreover, I want to express my gratitude to Suchita Kulkarni for being always there to answer my questions, teaching me a lot about SUSY phenomenology and for proof reading this thesis.

In addition, I would like to thank Claudia-Elisabeth Wulz for all her effort during the final stage of my diploma thesis and also Wolfgang Adam for the nice tour at CERN.

Furthermore, I want to thank my parents for the financial support allowing me to finish my diploma studies. Eventually I'm thankful to my flatmates for their support and company. Special thanks go to Veronika Magerl for working, studying and living together - you were a great support during all this time.

Contents

1	Introduction	1
2	The Large Hadron Collider	3
2.1	LHC and the CERN Accelerator Complex	3
2.2	The General Purpose Detectors	5
2.2.1	ATLAS	6
2.2.2	CMS	8
3	The Standard Model And Physics Beyond	10
3.1	The Standard Model	10
3.1.1	Particle Content of the Standard Model	10
3.1.2	Mathematical Formulation of the Standard Model	13
3.1.3	Problems of the Standard Model	16
3.2	Supersymmetry	19
3.2.1	Motivation	20
3.2.2	The MSSM	21
4	SUSY Searches at the LHC	25
4.1	SUSY signals at the LHC	25
4.1.1	Sparticle Productions	25
4.1.2	Sparticle Decays	26
4.1.3	SUSY Searches at ATLAS and CMS	28
4.2	The Simplified Models Approach	29
4.2.1	The Concept of Simplified Models	30
4.2.2	SMS Topologies	30
4.2.3	Interpretation of SMS Results	33
4.3	CMS Summary Plots	36
5	SModelS	38
5.1	The SModelS Framework	38
5.1.1	SModelS Language	39
5.1.2	SModelS Database	42
5.1.3	Decomposition Procedure	42

5.1.4	Confronting a Full Model with Experimental Results	46
5.2	Validation of the SModelS Database	47
5.2.1	Validation Procedure	47
5.2.2	Discussion of Results	52
5.2.3	Conclusion	57
6	The New SModelS-Database	59
6.1	Motivation	59
6.2	Database Structure	64
6.2.1	General Structure	64
6.2.2	Analysis Folder	65
6.3	Implementation of Data - the dataPreparation package	69
6.3.1	Preparatory Settings	70
6.3.2	Convert File	71
6.3.3	Creating the Database	79
7	Conclusion	83
A	Content Of The SModelS Database Files	85
A.1	Information Comprised in the globalInfo.txt File	85
A.2	Naming Convention For the Exclusion Lines Stored in the sms.root File . .	86
A.3	Information Comprised in the txName.txt File	87
A.4	Information Comprised In the dataInfo.txt File	88

Chapter 1

Introduction

During the twentieth century the standard model (SM) of particle physics was developed and experimentally proofed. In 2012 a particle compatible with the properties of the SM Higgs boson was observed by the ATLAS [1] and CMS [2] experiments at the Large Hadron Collider (LHC). With this discovery not only the last particle predicted by the SM was found, but also the question what stabilises the mass of the SM Higgs boson at the weak scale, the so called hierarchy problem becomes more important. Within the SM this question can not be answered. Also the nature of dark matter, which was introduced to explain the behaviour of observable matter in the universe can not be expanded within the SM, since it provides no dark matter candidate. These and other open questions of modern particle physics give rise to the development of new theories beyond the standard model (BSM).

One of the most promising of these theories is called supersymmetry (SUSY). It extends the SM by assigning a new particle, the so called superpartner, to each SM particle. If SUSY was an exact symmetry the superpartners would be of same mass as the SM particles and would have been observed already. Due to the lack of experimental evidences SUSY must be broken. Nevertheless, the masses of the superpartners should be of $\mathcal{O}(TeV)$, if SUSY is a natural solution to the hierarchy problem. This leads to the assumption that SUSY signatures should be observable at the LHC.

During the first phase of the LHC operation numerous SUSY searches were performed by the ATLAS and CMS collaborations. To interpret the outcome of these searches the simplified model approach became a standard technique. A simplified model is defined by an effective Lagrangian describing the behaviour of a small set of relatively light new particles, whereas all other particles, predicted by a full BSM model are assumed to be very heavy.

This thesis focuses on simplified model interpretations of searches assuming R-parity conserving SUSY scenarios. Within this assumption the proton-proton collisions at the LHC lead to typical SUSY signals, containing a certain number of leptons, jets and missing transverse energy (\cancel{E}_T). To suppress the SM background for the expected SUSY signals various signal regions are defined by the experimentalists.

In order to interpret the outcome of a search in terms of a simplified model, an efficiency map is calculated for each signal region. These efficiency maps contain the acceptance times efficiency ($A \times \epsilon$) for different masses of the assumed SUSY particles. The efficiency maps together with background estimations are used to derive upper limits on the production cross section times branching ratio $(\sigma \times BR)_{UL}$ at statistical 95 % confidence level. These $(\sigma \times BR)_{UL}$ for different SUSY particle masses are presented as upper limit maps. Eventually the experimentalists calculate exclusion lines showing limits for the masses of the involved sparticles.

Furthermore, the $(\sigma \times BR)_{UL}$ derived for a specific simplified model can be applied to any BSM model giving rise to this simplified model, as long as $(A \times \epsilon)$ depends mainly on the masses of the new particles and the kinematics of their decays and is not affected by specific details of a BSM model (e.g. spin). This assumption is the guiding principle for the development of a computational framework called SModelS. It provides a general procedure to decompose any \mathbb{Z}_2 symmetric BSM model into its simplified model spectra (SMS) topologies. It can compare $(\sigma \times BR)$ of these topologies with $(\sigma \times BR)_{UL}$ obtained from the experiment, in order to constrain the parameter space of the full model.

It is obvious that SModelS needs access to the $(\sigma \times BR)_{UL}$ published by the collaborations to perform this comparison. Therefore the results of SUSY search interpretations in terms of various SMS topologies were collected and stored inside a database during the development of SModelS.

Within the scope of this thesis the SModelS database was validated. A computational working environment was built, which used SModelS to derive an exclusion line for each upper limit map stored inside the database. This exclusion line was compared with the official exclusion line as given by the experimentalists. All results showing a good agreement between the two exclusion lines were comprised in a release database which was shipped with the first public version of SModelS 1.0. and all following versions.

Based on the findings of the validation a data standard for a newly structured database and an object orientated python package for the implementation of new data into this database was developed. The new database offers a clear structure to store efficiency maps for different signal regions and thus opens the possibility to use them within a future version of SModelS. The new python package called `dataPreparation` provides a fast and reliable way to implement new search results interpreted in terms of simplified model, as are expected in the light of the $\sqrt{s} = 13$ TeV run of the LHC.

The rest of this thesis is structured as follows. After a short description of the LHC and its two general purpose detectors ATLAS and CMS (cf. [chapter 2](#)) an introduction to the SM and SUSY is given (cf. [chapter 3](#)). In [chapter 4](#) the different search strategies for SUSY signatures and the interpretations of these searches in terms of simplified models are discussed. The working scheme of SModelS and the validation of the SModelS database is explained in detail at [chapter 5](#). Eventually [chapter 6](#) is dedicated to the new SModelS database and the `dataPreparation` Package.

Chapter 2

The Large Hadron Collider

The Large Hadron Collider (LHC) is located at the European Organisation for Nuclear Research (CERN) which is based on the Franco-Swiss border. CERN was founded in 1954 as an European joint venture and brings together physicists from 21 member states. Today CERN is one of the world's most prestigious centres for fundamental physics researches and it pushed forward our understanding of matter and the universe. Among many others the discovery of the W and Z bosons in 1983 as well as the observation of a particle consistent with the Higgs boson in 2012 are mile stones of physics history. A complete time line of the history of CERN can be found elsewhere [3].

This chapter gives a short overview of the CERN acceleration complex (cf. [section 2.1](#)) and the two general purpose experiments ATLAS and CMS (cf. [section 2.2](#)).

2.1 LHC and the CERN Accelerator Complex

The LHC was designed to search for possible answers for the most fundamental questions of physics, like the origin of the mass of the elementary particles or the questions about the nature of dark matter and the possible existence of undiscovered new particles, as predicted by e.g. supersymmetric theories. While the Higgs boson could be observed during the first run, which took place from 30th March 2010 to 13th February 2013 with a center of mass energy up to $\sqrt{s} = 8$ TeV, no other new particles or evidence for dark matter could be found. After a long period of maintaining and upgrading the LHC was restarted on 3rd June 2015 to continue its search for new physical phenomena at a highly increased energy of $\sqrt{s} = 13$ TeV.

In order to answer the questions mentioned above, the CERN accelerator complex is designed to accelerate protons to a center of mass energy up to $\sqrt{s} = 14$ TeV in a process involving several steps and brings them to collision. First 50 MeV protons are produced by the LINAC 2. The energy of the protons is further increased by a series of accelerators and finally they are injected into the LHC. [Figure 2.1](#) shows the entire accelerator complex. The subsystems as well as the associated energies are listed in [Table 2.1](#).

The main part of the complex, the LHC, consists of a 27 kilometre ring located in

<i>Accelerator</i>	<i>Energy of the Proton</i>
LINAC 2	50 MeV
Proton Synchrotron Booster (PSB)	1.4 GeV
Proton Synchrotron (PS)	25 GeV
Super Proton Synchrotron (SPS)	450 GeV
Large Hadron Collider (LHC)	7 TeV

Table 2.1: Acceleration steps at CERN accelerator complex

a tunnel approximately 100 m below ground level. To bend the beam on the ring a magnetic field of 8.33 T is necessary. This field can only be provided by superconducting electromagnets, therefore a total number of 1232 dipoles, cooled down to a temperature of 1.9 K, are used. To shape the particle beam a large variety of other magnets, e.g. quadrupoles are used. The particles are accelerated by eight radio frequency cavities, resulting in well defined bunches of particles. The bunches travel inside two separated beam pipes in opposite directions. Inside the beam pipes a vacuum of 10^{-13} atm is necessary to prevent collisions with gas molecules. Finally the bunches can be brought to collision at four interaction points. At these points the four experiments ALICE, ATLAS CMS and LHCb are located.

Luminosity

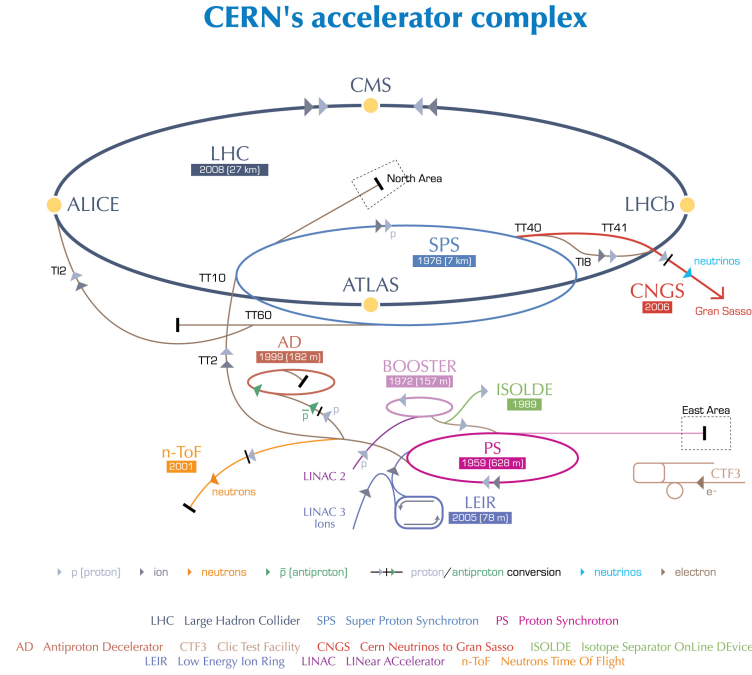
Every bunch contains about 10^{11} protons and is squeezed to a width of about $16 \mu\text{m}$ at the interaction points. The spacing between the bunches is 25 ns. Regarding the fact, that there are several bigger gaps in the pattern of bunches this leads to a frequency of 31.6 MHz. Using these numbers the maximum luminosity of the LHC can be calculated according to [Equation 2.1](#), where ν_n denotes the frequency of the bunches, N the amount of protons per bunch and A the transverse section of each bunch. This leads to a maximum luminosity of about $10^{34} \text{ cm}^{-2}\text{s}^{-1}$.

$$\mathcal{L} = \nu_n \frac{N^2}{A} \quad (2.1)$$

The luminosity is used to characterise the performance of a collider. The count rate of a given process dN/dt with cross section σ can be calculated from the luminosity by using [Equation 2.2](#).

$$\frac{dN}{dt} = \mathcal{L}\sigma \quad (2.2)$$

To obtain the total number of events, the integrated luminosity $L = \int \mathcal{L} dt$ is calculated.



European Organization for Nuclear Research | Organisation européenne pour la recherche nucléaire

© CERN 2008

Figure 2.1: The CERN accelerator Complex [4]

2.2 The General Purpose Detectors

The detectors of the LHC are built and operated by large collaborations of physicists from all over the world. While the ALICE and LHCb detectors are designed for a specific purpose, ATLAS and CMS cover a wide range of purposes, ranging from more precise measurements of the Standard Model parameters to the search of physics beyond the Standard Model (BSM). The different tasks of the detectors as well as the conditions given by the pp-collisions at the LHC lead to the following requirements for the detector design:

- Detection of muons and precise measurement of their charge and energy over a wide range of momenta.
- A full-coverage hadronic calorimetry for high resolution of jet and missing-transverse-energy \cancel{E}_T measurements.
- Very good electromagnetic calorimetry for measurement of photon and electron energy with wide geometric coverage.
- Good charged particle momentum resolution and track reconstruction near the interaction point.

- Fast and radiation-hard electronics and sensor elements.

Especially the requirement of a full-coverage leading to the so called “barrel plus end-caps” design where a cylindrical detector surrounds the central region and two end-caps cover the angles close to the beam. The subdetectors are arranged in a shell structure, starting with the inner tracking system close to the interaction point. This tracking system is surrounded by the electromagnetic-calorimeter (ECAL) followed by the hadronic-calorimeter (HCAL) for measurement of the energy of the photons, electrons and hadrons. Because muons can penetrate the ECAL and the HCAL without interacting, the muon system is located at the outermost part of the detector. For the measurement of the momentum in the inner tracking system and in the muon system a strong magnetic field is necessary in order to curve the trajectory of the charged particles.

Both general purpose experiments ATLAS and CMS are built with respect to these construction principles in mind but differ in details, as will be explained below.

2.2.1 ATLAS

The ATLAS collaboration consists of approximately 3000 members from 177 institutes in 38 countries. It has published the imposing number of about 380 papers [5], covering a wide range of physics fields. Among these there are 80 publications on searches for supersymmetry, which are of particular interest for this thesis. The ATLAS detector is depicted in Figure 2.3, it is 46 m long, 25 m in diameter and weighs about 7000 t. The main parts of the detector are described below. A more detailed description can be found elsewhere [6].

Inner Tracker

The inner tracker is 7 m long and 2.3 m in diameter. It combines two silicon sensor systems with discrete high resolution readout and one transition radiation tracker (TRT) providing a continuous tracking. In the innermost region silicon pixel detectors are used, followed by silicon strip detectors with less precision. The TRT is the outermost component of the inner tracker and allows to distinguish between electrons and hadrons.

Electromagnetic Calorimeter

For the electromagnetic calorimeters ATLAS uses liquid argon as the sensing element. As absorber material copper and stainless steel are used. The electrons produced in the liquid argon by the electromagnetic shower are collected by accordion shaped electrodes.

Hadron Calorimeter

In the barrel a sampling calorimeter is used. It consists of layers of steel and scintillating plastic. In the far forward section liquid argon is used as the active material, while copper and tungsten are used as absorbers.

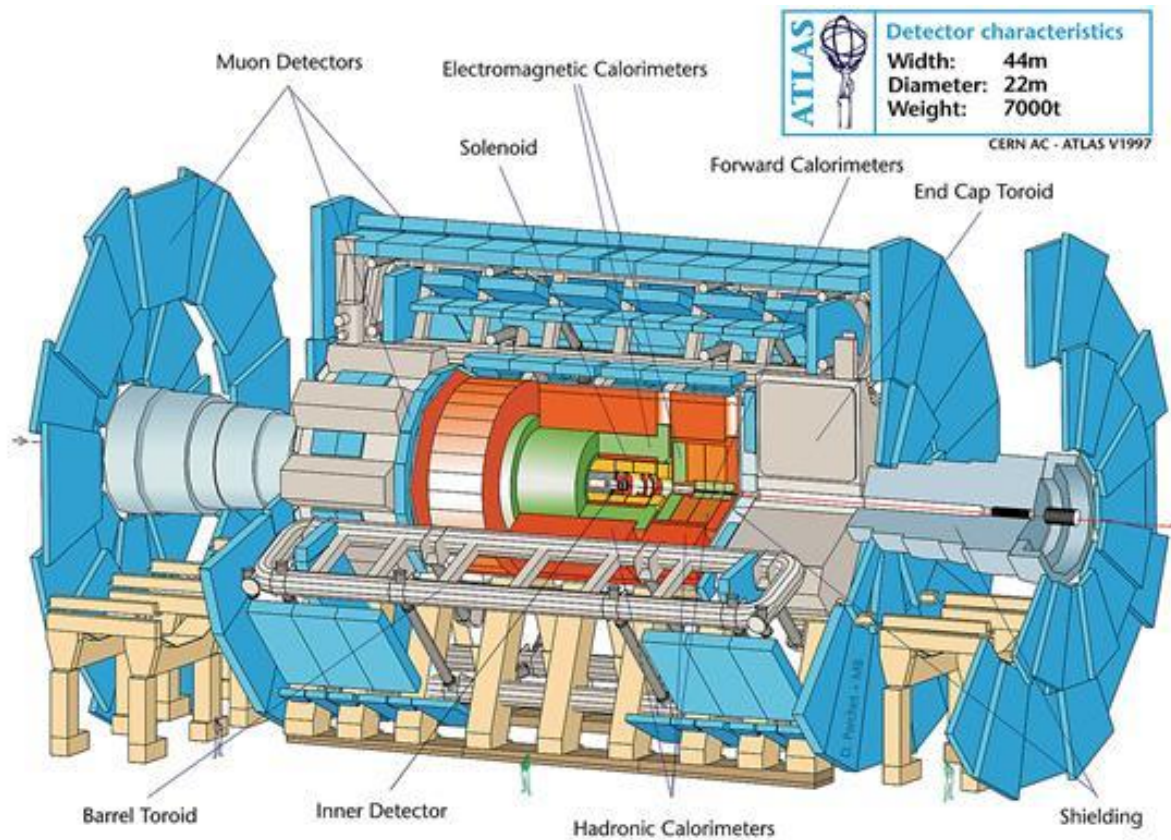


Figure 2.2: Overview of the ATLAS detector [7]

Muon System

The muon system is by far the biggest part of the detector. It starts at a radius of 4.5 m and extends to the full radius of the detector. The system consists of 1200 separate muon chambers to measure the tracks of the muons and a set of triggering chambers providing very fast signals for event selection.

Magnet System

Two large superconducting magnet systems are used. A solenoid is located right after the inner tracker and provides a nearly uniform magnetic field, which is necessary to measure the momentum of the particles in the inner tracker. The outer toroidal magnetic field is used for the momenta measurement in the muon system. It is produced by eight air-core superconducting barrel loops and two end-caps air toroidal magnets.

2.2.2 CMS

With 2680 members from 182 institutes in 42 countries the CMS collaboration is nearly as big as the ATLAS collaboration. It published a total number of 385 [8] physics papers until March 2015, whereas 49 papers focused on searches supersymmetry for s. The CMS detector is depicted in Figure 2.3. With a length of 21 m, a diameter of 15 m and a weight of 12500 t, it is much more compact than the ATLAS detector. Hence the name CMS which means Compact Muon Solenoid. The main parts of the detector are described below. A more detailed description can be found elsewhere [9].

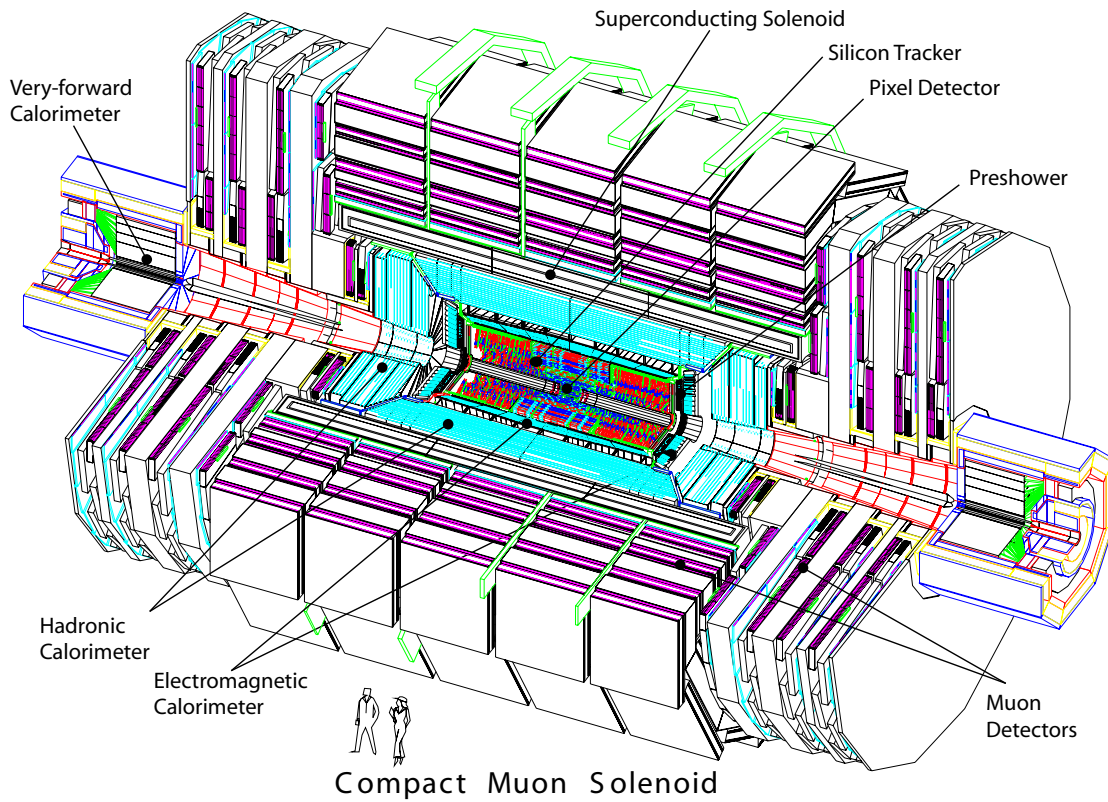


Figure 2.3: Overview of the CMS detector [7]

Inner Tracker

CMS uses a full silicon tracker of 5.4 m length and a diameter of 2.4 m. The barrel region consists of thirteen and the end-caps consist of fourteen layers of silicon detectors. The first four layers next to the beam are made of pixel sensors. All other layers consist of silicon stripe detectors.

Electromagnetic Calorimeter

To measure the energy of photons and electrons a homogeneous calorimeter made of lead tungstate ($PbWO_4$) crystals is used. The barrel region contains 61200 whereas the end-caps consists of 14648 crystals. To each crystal an avalanche photo diode (APD) is attached to read out the scintillation light. To discriminate between pions and photons a preshower detector on the inner surface of the end-cap ECAL is used.

Hadron Calorimeter

Similar to ATLAS a sampling calorimeter with plastic scintillators is used for the bigger part of the hadron calorimeter. The absorber is made of brass (70% Cu, 30% Zn). To allow a better separation of particles in the forward region, the very-forward Hadron Calorimeter (HF) uses an iron absorber and quartz fibres for readout.

Muon System

The biggest volume of the detector is occupied by the muon system. To measure the track of the muons CMS uses drift tubes (DT) in the barrel region and cathode stripe chambers (CSC) at the end-caps. For triggering resistive plate chambers (RPC) are used in both regions.

Magnet System

The magnet system makes the biggest difference between ATLAS and CMS. Unlike ATLAS, CMS uses only one superconducting solenoid. The solenoid is the central feature of the detector, it is 13 m long, 6 m in diameter and provides a magnetic field of 4 T. This very strong field leads to a big curvature of the particle tracks and allows high precision measurement of the momenta in the inner tracker and the muon system.

Both collaborations ATLAS and CMS announced the observation of a particle compatible with the properties of the Higgs boson in 2012 [1, 2]. With this discovery the last missing particle predicted by the standard model of particle physics, which will be introduced in [chapter 3](#), was experimentally observed. One of the main tasks of the two general purpose experiments during the second run of the LHC, the search for supersymmetric particles is discussed in [chapter 4](#).

Chapter 3

The Standard Model And Physics Beyond

This chapter is dedicated to the theoretical basis of particle physics. In [section 3.1](#) the Standard Model of particle physics (SM) is discussed and [section 3.2](#) introduces the concept of supersymmetry as a probable extension of the SM.

3.1 The Standard Model

The SM was developed during the late twentieth century. It is the result of contributions of different theoretical physicists and an immense experimental effort. The behaviours of the elementary particles and their interactions, discussed in [subsection 3.1.1](#), are well described within the theory. A very short overview of the mathematical formulation of the SM, which is based on quantum field theory (QFT), is given in [subsection 3.1.2](#)

As mentioned in [chapter 2](#) the Higgs boson was most likely discovered in 2012. With this discovery not only the last missing particle predicted by the SM was observed, but also the so called hierarchy problem becomes more important. This hierarchy problem and other problems which can not be solved within the SM are discussed in [subsection 3.1.3](#).

3.1.1 Particle Content of the Standard Model

The SM contains a total number of 18 elementary particles¹ and an equal number of antiparticle. Each Antiparticle has the same spin state and mass as the associated particle but carries opposite electric charge. The particles are depicted in [Figure 3.1](#). They can be divided into two groups. Fermions obey Fermi-Dirac statistics and have a half integer spin. Particles with integer spin are called bosons and obey Bose-Einstein statistics. While matter consists of fermions with spin one half, the interactions are mediated by spin one bosons as will be described in greater detail below.

¹Including the graviton, which is strictly speaking not part of the SM.

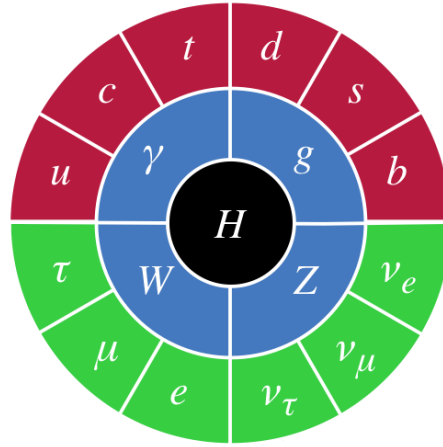


Figure 3.1: Particle content of the SM [10]. The outer ring depicts the fermions. Quarks are depicted in red and leptons in green. The inner blue ring shows the bosons and in the centre the Higgs boson is depicted in black.

Matter Sector

The fundamental constituents of matter are of two types, leptons and quarks. Each of these can be sub-grouped further into three generations. Every generation contains two particles leading to six leptons and six quarks. The particles of different generations carry the same quantum numbers and mainly differ in their mass.

Leptons: Figure 3.1 depicts the leptons in green. Each lepton generation consists of one electrically charged lepton with charge -1 and one massless neutrino (ν) without charge. One lepton number for each generation (L_e, L_μ, L_τ) is introduced. Leptons carry lepton number one and antileptons minus one. This number is conserved within a generation of leptons.

Quarks: The quarks, depicted in red in Figure 3.1, are organized into three generations as follows:

$$\begin{pmatrix} u \\ d \end{pmatrix}, \begin{pmatrix} c \\ s \end{pmatrix}, \begin{pmatrix} t \\ b \end{pmatrix}$$

The upper ones are called up-type quarks and the lower ones down-type quarks. Up-type quarks carry the electric charge $+\frac{2}{3}$ and down-type quarks the electric charge $-\frac{1}{3}$. Similar to the lepton number a so called baryon number is introduced, which is conserved. But in contrast to the leptons, there is only one baryon number for all quarks. Each quark carries the baryon number $\frac{1}{3}$ and each antiquark $-\frac{1}{3}$. In addition quarks have another property, which is the so called colour charge. There are three colours, red (r), blue (b) and green

(g) complimented by an anticolour for each. Quarks only occur in two different colour neutral bound states called baryons and mesons. Mesons consist of one quark and one antiquark, carrying a colour and the respective anticolour. Baryons consist of three quarks of different colours. Examples of baryons are protons and neutrons, the constituents of the atomic nucleus.

Force Sector

All interactions in physics can be reduced to four fundamental forces. Except gravity all of these forces are described within the SM. Each of these fundamental interactions of the SM is carried by one or more gauge bosons. They are depicted in [Figure 3.1](#) in blue and will be described below. [Table 3.1](#) lists the three fundamental interactions of the SM, their range, source and coupling constant, as well as the associated gauge bosons.

<i>Interaction</i>	<i>Range</i>	<i>Source</i>	<i>Coupling Constant</i>	<i>Mediator</i>
electromagnetic	∞	electric charge	α_F	photon γ
strong	10^{-15} m	colour charge	α_s	gluon G
weak	10^{-18} m	weak hypercharge	α_W	W^\pm, Z^0

Table 3.1: Overview of the three fundamental interactions in the SM.

electromagnetic interaction: It is mediated by a massless photon and is therefore of infinite range. The electromagnetic interaction acts on all particles carrying an electric charge. The most common example for this interaction is the binding of the electrons to the atomic nucleus.

strong interaction: It acts only on quarks. The strong interaction is mediated by eight massless gluons. Gluons are the only gauge bosons which carry the source of the interaction, the colour charge. This leads to gluon-gluon interactions and the very short range of the strong force.

weak interaction: The most common example for a weak interaction is the beta-decay of the proton. There are three gauge bosons, associated to this interaction, as can be seen in [Table 3.1](#). These are very heavy, leading to a short range of the interaction. All fundamental fermions couple to the weak interaction which is characterised by the weak isospin.

Weak Isospin

Concerning the weak interaction, all fundamental fermions form left-handed (LH) isospin doublets and right-handed isospin singlets², as depicted in [Table 3.2](#). The LH doublets carry an isospin of $\frac{1}{2}$ and a third component of the weak isospin of $\pm\frac{1}{2}$, whereas

²except the neutrinos, which only occur in the LH lepton doublets

the RH singlets carry an isospin of 0. The weak hypercharge Y is defined by the electric charge Q and the third component of the weak isospin I_3 as $Y = 2(Q - I_3)$. The weak interaction only couples to the LH isospin doublets. While the mass eigenstates for all other fermions are mixtures of LH and RH isospin states, the massless neutrinos only occur in pure LH states. This leads to the parity violation of the weak interaction.

	<i>first generation</i>	<i>second generation</i>	<i>third generation</i>
<i>leptons</i>	$\begin{pmatrix} \nu^e \\ e^- \end{pmatrix}_L$ e_R^-	$\begin{pmatrix} \nu^\mu \\ \mu^- \end{pmatrix}_L$ μ_R^-	$\begin{pmatrix} \nu^\tau \\ \tau^- \end{pmatrix}_L$ τ_R^-
<i>quarks</i>	$\begin{pmatrix} u \\ d \end{pmatrix}_L$ u_R, d_R	$\begin{pmatrix} c \\ s \end{pmatrix}_L$ c_R, s_R	$\begin{pmatrix} t \\ b \end{pmatrix}_L$ t_R, b_R

Table 3.2: SM lepton and quark fields grouped into the three generations.

Higgs Sector

The Higgs boson originates from the Higgs field. It is a scalar particle with spin 0. As will be described in more detail below, the Higgs field is needed to break the electroweak symmetry into the gauge symmetry of the quantum electrodynamics. The massive fundamental particles gain their masses by interacting with the Higgs field.

3.1.2 Mathematical Formulation of the Standard Model

The SM is a spontaneously broken gauge theory based on QFT. In QFT the particles occur as quantisations of the fundamental fields. The propagation and interactions of these fields are described in terms of Lagrangian densities. Because the SM is a gauge theory, the Lagrangian is invariant under global and local gauge transformations, represented by the underlying symmetry groups. The gauge structure of the SM is $SU(3)_C \otimes SU(2)_L \otimes U(1)_Y$. Where $SU(3)_C$ is the gauge group of the quantum chromodynamics (QCD) which describes the behaviour of quarks and gluons. $SU(2)_L \otimes U(1)_Y$ refers to the unification of weak and electromagnetic interaction, the so called electroweak interaction. The gauge symmetry of the electroweak group is spontaneously broken into the group $U(1)_{QED}$. Where $U(1)_{QED}$ is the group of the quantum electrodynamics (QED). This symmetry breaking generates the masses of the weak gauge bosons and leads to the Higgs boson.

Electromagnetic Interaction

The electromagnetic interaction is described by the QED. The generator of the gauge group of the QED is the electric charge Q . Equation 3.1 represents the corresponding Lagrangian.

$$\mathcal{L}_{QED} = \bar{\psi} (i\gamma^\mu \mathcal{D}_\mu - m) \psi - \frac{1}{4} F_{\mu\nu} F^{\mu\nu} \quad (3.1)$$

$$\mathcal{D}_\mu = \partial_\mu + ieA_\mu \quad (3.2)$$

$$F_{\mu\nu} = \partial_\mu A_\nu - \partial_\nu A_\mu \quad (3.3)$$

In order to make the Lagrangian invariant under transformations of $U(1)_{QED}$, the so called covariant derivative \mathcal{D}_μ , given in Equation 3.2, is introduced. This leads to an interaction between the field spinor of the Dirac fermions ψ and the electromagnetic field A_μ . Therefore the first term in the Lagrangian describes the kinetic energy of the free fermion and its interaction with the field, as well as the rest mass of the fermion. The second term describes the kinetic energy of the free field, with $F_{\mu\nu}$ being the electromagnetic field strength tensor (cf. Equation 3.3). Because a mass term of the electromagnetic field would violate the gauge invariance the photon is massless.

Strong Interaction

The QCD was introduced by Fritzsch, Gell-Mann and Leutwyler in 1972 [11]. The generator of the corresponding gauge group is the colour charge C . The Lagrangian (cf. Equation 3.4) can be written in a very similar way to the one of the QED.

$$\mathcal{L}_{QCD} = \bar{q} (i\gamma^\mu \mathcal{D}_\mu - m) q - \frac{1}{4} G_{\mu\nu}^a G_{\mu\nu}^a \quad (3.4)$$

$$\mathcal{D}_\mu = \partial_\mu + ig_s \frac{\lambda_a}{2} G_\mu^a \quad (3.5)$$

$$G_{\mu\nu}^a = \partial_\mu G_\nu^a - \partial_\nu G_\mu^a - g_s f_{abc} G_\mu^b G_\nu^c \quad (3.6)$$

In this Lagrangian q denotes the quark fields in a vector representation in colour space. The covariant derivative shown in Equation 3.5 involves the eight matrices λ_a which form the algebra of the $SU(3)_C$ and leads to an interaction of the quarks and the gluons. As one can see in Equation 3.6 the third term of the field strength tensor of the gluonic field $G_{\mu\nu}^a$ includes the structure constant f_{abc} . This third term makes the biggest difference between QED and QCD. It results in gluon self interactions. Like in the QED, a mass term for the gluon is forbidden, in order to keep the Lagrangian gauge invariant.

Electroweak Interaction

The construction of a Lagrangian for the electroweak interaction is more complex. As already mentioned, the weak interaction only couples to LH doublets. Therefore the $SU(2)_L$ only acts on LH fermionic fields as indicated by the index L . The $SU(2)_L$ is generated by the weak isospin I_3 . To include the electromagnetic interaction an additional group is needed. The $U(1)_Y$ applies to all fermions in the same way and is generated by the hypercharge Y . A naive identification of the $U(1)_Y$ with $U(1)_{QED}$ is not possible due to the fact that the $U(1)_{QED}$ is generated by the electric charge. The gauge theory of the electroweak interaction, based on $SU(2)_L \otimes U(1)_Y$ is known as the Salam-Weinberg theory. To fulfil the local gauge invariance the theory includes three gauge fields W_μ^a ($a = 1, 2, 3$) for the $SU(2)_L$ and one field B_μ for the $U(1)_Y$. With these fields one can define a covariant derivative as given in Equation 3.7.

$$\mathcal{D}_\mu = \partial_\mu + ig\frac{\sigma_a}{2}W_\mu^a + ig'\frac{Y}{2}B_\mu \quad (3.7)$$

Where g denotes the coupling strength of the $SU(2)_L$ and g' the one of the $U(1)_Y$. The four gauge fields of the electroweak interaction carry the same quantum numbers. Therefore they can be mixed in order to form the neutral Z_μ and A_μ fields, as well as the charged W_μ^\pm fields (cf. Equation 3.8 - 3.10), where Θ_W is the so called Weinberg angle.

$$Z_\mu = \cos \Theta_W W_\mu^3 - \sin \Theta_W B_\mu \quad (3.8)$$

$$A_\mu = \sin \Theta_W W_\mu^3 + \cos \Theta_W B_\mu \quad (3.9)$$

$$W_\mu^\pm = \frac{1}{\sqrt{2}}(W_\mu^1 \mp W_\mu^2) \quad (3.10)$$

Because the photon corresponding to the field A_μ is massless, whereas the Z^0 and W^\pm bosons are heavy, the electroweak symmetry must be broken.

Symmetry Breaking

In order to gain mass the electroweak symmetry has to be broken spontaneously. This symmetry breaking can be done by constructing an invariant Lagrangian with a potential providing non-vanishing ground state energy. Such a potential is given in Equation 3.11. If $\mu^2 < 0$ and $\lambda > 0$ the minimal value for this potential is non-vanishing. Where μ is the mass parameter and λ the quartic coupling.

$$V = \mu^2 |\Phi^\dagger \Phi| + \lambda (|\Phi^\dagger \Phi|)^2 \quad (3.11)$$

Figure 3.2 depicts this so called “sombbrero potential”. As one can see there are an infinite number of degenerate states with minimal energy. By choosing one specific ground state the symmetry is spontaneously broken.

As mentioned above the weak gauge bosons are massive particles, whereas the photon is massless. Therefore a doublet of complex scalar fields (cf. Equation 3.12) is introduced in order to break the electroweak symmetry without breaking the symmetry of the electromagnetic subgroup $U(1)_{QED}$.

$$\Phi = \begin{pmatrix} \phi^+ \\ \phi^0 \end{pmatrix} \quad (3.12)$$

This doublet couples to the gauge fields as described by the Lagrangian given in Equation 3.13. Where \mathcal{D}_μ is the electroweak covariant derivative defined in Equation 3.7.

$$\mathcal{L}_S = (\mathcal{D}_\mu \Phi)^\dagger \mathcal{D}_\mu \Phi - V(\Phi) \quad (3.13)$$

The potential $V(\Phi)$ has a non-vanishing minimum. With v being the vacuum expectation value (VEV):

$$\langle \Phi \rangle = \frac{1}{\sqrt{2}} \begin{pmatrix} 0 \\ v \end{pmatrix} \quad (3.14)$$

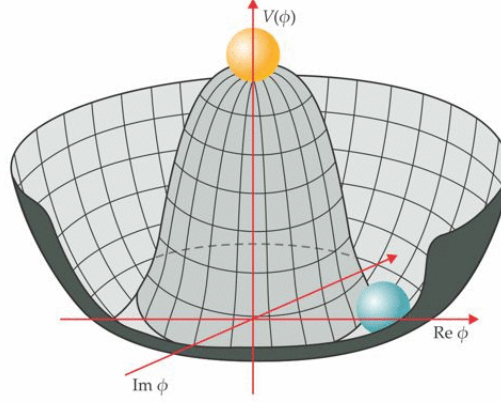


Figure 3.2: Illustration of the Higgs potential [12]. The blue pellet indicates the stable, non vanishing ground state, whereas the yellow pellet marks the unstable vanishing vacuum expectation value.

The gauge freedoms of the $SU(2)_L$ can be used to set $\phi^+ = 0$ and make ϕ^0 a real quantity. Describing the ground state with perturbation theory leads to a small fluctuation around the VEV.:

$$\Phi = \frac{1}{\sqrt{2}} \begin{pmatrix} 0 \\ v + H(x) \end{pmatrix} \quad (3.15)$$

Together with the Lagrangian from Equation 3.13 this results in a new massive scalar particle with mass $m_H = \sqrt{-2\mu^2}$, the Higgs boson. The covariant derivative \mathcal{D}_μ of the Lagrangian contains the gauge fields of the electroweak interactions. This leads to mass terms for the weak boson fields W_μ^\pm and Z^μ , while the photon stays massless, due to the fact that the $U(1)_{QED}$ is unbroken. The coupling of the W and Z bosons to the Higgs field is shown in Equation 3.16.

$$\mathcal{L}_{HG} = m_W^2 W_\mu^+ W^{-\mu} \left(1 + \frac{2}{v}H + \frac{1}{v^2}H^2\right) + \frac{1}{2}m_Z^2 Z^\mu Z^\mu \left(1 + \frac{2}{v}H + \frac{1}{v^2}H^2\right) \quad (3.16)$$

Where $m_W^2 = \frac{1}{4}g^2 v^2$ and $m_Z^2 = \frac{1}{4}(g^2 + g'^2) v^2$ denote the W and Z boson masses.

3.1.3 Problems of the Standard Model

Today the SM is a well established theory. Nevertheless there are some experimental hints and open issues which currently cannot be answered within the theory. This section lists a few of these issues without the claim of completeness. Some of them are of special interest for this thesis and will be discussed further in section 3.2, others are only mentioned to give an overview of current fields of researches linked to the SM and shall only be introduced in a few words.

Unification of Interactions

In QFT the physical quantities can be calculated using perturbation theory. In perturbation terms of higher order so called virtual particles occur. Virtual particles do not obey conservation of energy and momenta, which can lead to unphysical infinities. To get rid of these infinities the concept of renormalisation is used. This concept can be understood if one thinks of a “bare” particle which is “dressed” by the virtual particles. Therefore the values for the parameters of the “bare” particle can not be measured. The physically measurable value is described by the renormalised value of the parameter.

The renormalisation leads to a logarithmic dependency of the coupling constants on the energy scale. The coupling constants for the different interactions of the SM tend to converge at higher energies. This gives rise to the idea of the grand unified theory (GUT) where all couplings would coincide at a certain point at high energies. Unfortunately this is not the case if the SM is extended up to higher energies. Therefore a unification of all interactions described in the SM is not possible within the theory.

Gravity

Gravity is described by the theory of general relativity, it is the only fundamental force which so far can not be described in terms of quantum mechanics and consequently is not part of the SM. Because the coupling strength of the gravitational interaction is very weak in comparison to the other three interactions, gravitation is negligible in most experiments of particle physics. But for very small distances and high masses a description of gravity in terms of quantum mechanics becomes important to describe the behaviour of the elementary particles. The Planck mass $M_{Pl} = \sqrt{\frac{1}{G}} = 1.2 \cdot 10^{19}$ GeV, with G being the gravitational constant, defines the energy scale where this unification becomes important.

Hierarchy Problem

The energy scale up to which the SM is valid is given by the ultraviolet cutoff $\Lambda_{UV} < M_{Pl}$. In perturbation theory the mass of the measurable Higgs boson is given by Equation 3.17. Where m_{hbar}^2 is the “bare” mass of the Higgs and Δm_h^2 refers to the correction obtained from higher order perturbation theory.

$$m_h^2 = m_{hbar}^2 + \Delta m_h^2 \quad (3.17)$$

For the coupling of the Higgs boson to a Dirac fermion the corrections can be written as:

$$\Delta m_{h,f}^2 = -\frac{Y_f^2}{8\pi^2} \left(\Lambda^2 - m_f^2 \ln \frac{\Lambda^2}{m_f^2} \right) + \dots \quad (3.18)$$

Where Y_f is the Yukawa coupling describing the Higgs coupling to the fermions. A similar expression can be found for the bosons. If one extends the cutoff scale Λ close to the M_{Pl} the first term in Equation 3.18 leads to a value of order 10^{38} eV. In order to protect the

measured Higgs mass of about 125 GeV this very high value has to be cancelled by the “bare” mass, which therefore must be of the same order of magnitude. This kind of fine tuning seems to be very unnatural.

Dark Matter

There are several hints from cosmological observations that only 4.6 % of the universe consists of “ordinary” matter as described by the SM. According to these observations 24 % of the Universe consists of non-luminous matter, so called dark matter (DM) and 71.4 % of dark energy (DE), a hypothetical form of energy used to describe the accelerated expansion of the universe. One of these evidences for DM are the rotation curves of the galaxies. The rotation velocity of stars at the outer region of the galaxies can be explained only by a halo of DM, not by the gravitational force of visible matter. The fractions of matter, DM and DE can be obtained from e.g. the anisotropies in the cosmic microwave background (CMB), as measured by e.g. WMAP [13] and the Planck-satellite [14].

Neutrino Masses

Neutrinos in the SM are assumed to be massless. Several experiments were performed to measure the abundance of the different neutrino flavours from various sources like the sun or cosmic rays. One of the earliest of these experiments was the Homestake experiment at South Dakota, which measured the flux of electron neutrinos from the sun [15]. The results of these experiments give rise to the fact that neutrinos can oscillate between their flavour eigenstates, which is only possible if neutrinos have mass.

Matter - Antimatter Asymmetry

According to the Big Bang theory matter and antimatter was produced in equal amounts. It is assumed that in the early Universe a process known as baryogenesis produced the huge dominance of matter over antimatter of about $N_{matter}/N_{antimatter} > 10^4$, observed in the current Universe. Andrei Sakharov formulated three conditions necessary to explain the matter-antimatter asymmetry:

- baryon number violating interactions
- deviation from thermal equilibrium
- charge (C) and charge-parity (CP) violation

While CP violating processes could be observed (e.g. decay of the K_L^0 -meson), there is no observation of baryon number violating interactions which would lead to a decay of the proton. The sum of all known processes which can result in a matter - antimatter asymmetry are not enough to explain the massive asymmetry in the Universe.

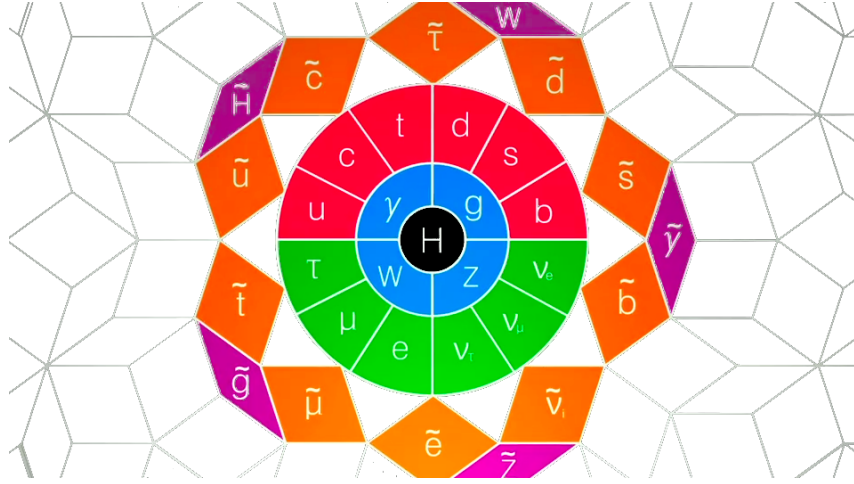


Figure 3.3: Extension of Figure 3.1. The particles of the SM shown in the circle are extended by their superpartners. The new particles are denoted by the symbol of their SM partner with a tilde. [10]

3.2 Supersymmetry

During the last decades numerous theories were introduced for possible physics beyond the Standard Model (BSM). Since this thesis is based on searches for supersymmetry (SUSY) only this approach shall be introduced. Various SUSY models were developed since the seventies of the last century and a detailed description would go far beyond the scope of this thesis. Therefore only some basics are mentioned in this section. A more detailed introduction can be found elsewhere [16].

SUSY is one of the most promising theories to answer some of the already mentioned open issues, as will be discussed in subsection 3.2.1.

The name supersymmetry is motivated by a symmetry between fermion and boson fields introduced by the theory. In every supersymmetric extension of the SM a superpartner is assigned to every SM particle. One of these extensions, the so called minimal supersymmetric extension of the SM (MSSM) is introduced in subsection 3.2.2. The spin of the superpartners differ by $\frac{1}{2}$. They are arranged in so called supermultiplets containing fermionic and bosonic fields. Figure 3.3 extends Figure 3.1 by the superpartners of the SM particles. The naming convention for them adds the prefix “s”, short for scalar, to the name of the related SM fermions and the postfix “ino” to the SM boson names. For example the partner of the electron is the selectron and the one for the photon is the photino.

As long as SUSY is an exact symmetry the superpartners are of same mass as the SM particles and would have been observed already, which is not the case. Therefore SUSY has to be broken which is done by adding symmetry breaking terms to the Lagrangian. This so called soft breaking comes at the cost of more than one hundred new parameters. Hereby the term “soft” refers to the maximal mass scale for these parameters,

capable of providing the observed Higgs boson mass without severe cancellations (c.f. [subsection 3.2.1](#)).

3.2.1 Motivation

In this section the open issues mentioned in [subsection 3.1.3](#) linked to SUSY are discussed.

Hierarchy Problem

The hierarchy problem is one of the strongest motivations for SUSY. [Equation 3.19](#) and [Equation 3.20](#) show the higher order corrections to the Higgs boson mass resulting from virtual fermions and their scalar superpartners. Where λ_s denotes the coupling strength of the scalar particles to the Higgs field and Y_f is the fermionic Yukawa coupling.

$$\Delta m_{h,f}^2 = -\frac{Y_f^2}{8\pi^2} \left(\Lambda^2 - m_f^2 \ln \frac{\Lambda^2}{m_f^2} \right) + \dots \quad (3.19)$$

$$\Delta m_{h,s}^2 = \frac{\lambda_s^2}{8\pi^2} \left(\Lambda^2 - m_s^2 \ln \frac{\Lambda^2}{m_s^2} \right) + \dots \quad (3.20)$$

The higher order corrections to the Higgs boson mass are given by the sum of $\Delta m_{h,f}^2$ and $\Delta m_{h,s}^2$. If $Y_f = \lambda_s$ the first terms proportional to the squared cutoff scale cancel and only the logarithmic ones are left. These logarithmic divergences are harmless even for $\Lambda = M_{Pl}$. As long as the boson mass stays close to the fermion mass the correction Δm_h^2 is sufficiently small to provide a natural solution to the hierarchy problem.

Unification of Interactions

The MSSM leads to a unification of the coupling constants. This unification only depends on the quantum numbers but not on the details of the particle spectrum. [Figure 3.4](#) shows the running coupling constants within the SM and the MSSM. As shown in the left plot the coupling constants coincide in a certain point considering an MSSM scenario. In the SM scenario this is not the case, as shown in the left plot.

Dark Matter

To avoid lepton and baryon violation R-parity (cf. [subsection 3.2.2](#)) can be introduced within SUSY models. One of the consequences of the R-parity conservation is a stable lightest supersymmetric particle which can not decay further. Thus the MSSM provides a dark matter candidate if this lightest supersymmetric particle is assumed to be an electrically neutral, only weakly interacting particle.

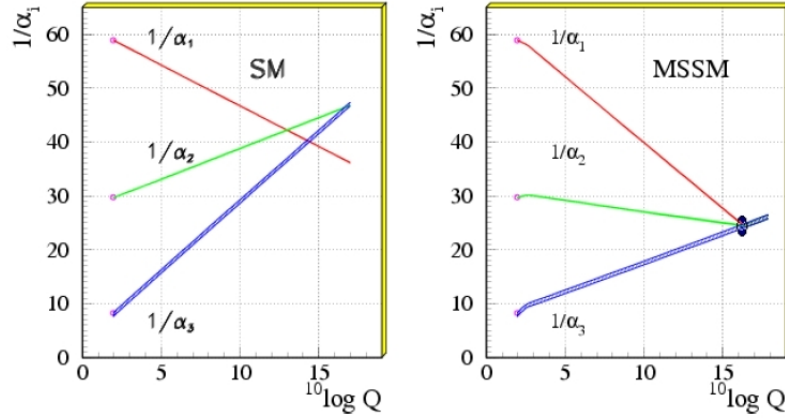


Figure 3.4: Dependency of the coupling constants for the electromagnetic α_1 , weak α_2 and strong interaction α_3 on the energy scale Q in the SM (left) and the MSSM (right). [17]

Gravity

As discussed in subsection 3.1.2 in QED the claim for local gauge invariance leads to a massless spin 1 particle, the photon. In a similar way the claim for local SUSY gauge invariance leads to a massless spin 2 particle, the graviton. Even if this theory is not renormalisable it gives an idea of how the unification of the gravitational interaction with the other three interactions can be done.

3.2.2 The MSSM

In order to construct the minimal supersymmetric extension of the SM for every degree of freedom in the SM a partner degree of freedom is introduced, leading to 19 new parameters. Due to the symmetry breaking over one hundred more parameters occur as discussed above. The MSSM is based on the gauge group $SU(3)_C \otimes SU(2)_L \otimes U(1)_Y$ like the SM.

The fields of the SM are extended to supermultiplets. The fermion fields are grouped in chiral supermultiplets (cf. Table 3.3). Hereby charge conjugated LH fermion fields are used instead of RH fermion fields. To avoid inconsistencies in the Higgs sector two Higgs supermultiplets are introduced. The SM gauge bosons are extended to gauge supermultiplets (cf. Table 3.4).

R-Parity

The construction of supermultiplets leads to the problem that the gauge invariance of the Lagrangian allows baryon and lepton number violating processes. This would lead to the decay of the proton which is not observed. In order to avoid this violation of baryon

and lepton number conservation a discrete symmetry known as R-parity is introduced (c.f. Equation 3.21).

$$P_R = (-1)^{3(B-L)+2s} \quad (3.21)$$

The R-parity number +1 is assigned to SM particles and -1 to their superpartners, the sparticles. The conservation of this number results in two important consequences: Sparticles can only be produced and annihilated pairwise and the lightest supersymmetric particle is stable.

<i>Names</i>	<i>Supermultiplet</i>	<i>spin</i> $\frac{1}{2}$	<i>spin</i> 0
quarks, squarks ($\times 3$ families)	Q \bar{u} \bar{d}	$\begin{pmatrix} u_L \\ d_L \end{pmatrix}$ $\bar{u}_L \sim (u_R)^c$ $\bar{d}_L \sim (d_R)^c$	$\begin{pmatrix} \tilde{u}_L \\ \tilde{d}_L \end{pmatrix}$ $\tilde{\bar{u}}_L, \tilde{u}_R$ $\tilde{\bar{d}}_L, \tilde{d}_R$
leptons, sleptons ($\times 3$ families)	L ℓ	$\begin{pmatrix} \nu_L \\ e_L \end{pmatrix}$ $\bar{\ell}_L \sim (\ell_R)^c$	$\begin{pmatrix} \tilde{\nu}_L \\ \tilde{e}_L \end{pmatrix}$ $\tilde{\bar{\ell}}_L, \tilde{\ell}_R$
Higgs, higgsinos	H_U H_D	$\begin{pmatrix} \tilde{H}_U^+ \\ \tilde{H}_U^0 \end{pmatrix}$ $\begin{pmatrix} \tilde{H}_D^0 \\ \tilde{H}_D^- \end{pmatrix}$	$\begin{pmatrix} H_U^+ \\ H_U^0 \end{pmatrix}$ $\begin{pmatrix} H_D^0 \\ H_D^- \end{pmatrix}$

Table 3.3: chiral supermultiplets in the MSSM

<i>Names</i>	<i>spin</i> 1	<i>spin</i> $\frac{1}{2}$
gluons, gluinos	g	\tilde{g}
W bosons, winos	W^\pm, W^0	$\tilde{W}^\pm, \tilde{W}^0$
B boson, bino	B	\tilde{B}

Table 3.4: gauge supermultiplets in the MSSM

Particle Content of the MSSM and Mixing

Except for the gluino fields all fermionic fields of the gauge supermultiplets and of the Higgs supermultiplets carry the same quantum numbers. Therefore they can mix to mass eigenstates. This leads to neutralinos and the charginos. The four scalar fields of the Higgs supermultiplets form three electrically neutral scalars h^0 , H^0 , A^0 and two charged

scalars H^+ , H^- in the Higgs sector. Also the bosonic squarks and slepton fields can mix to mass eigenstates. Due to the fact that the gluino is the only colour octet fermion it can not mix with other fermions.

For this thesis, especially for [section 5.2](#), the mixing matrices for neutralinos, charginos and the third generation squarks and sleptons are of interest and shall be introduced below:

neutralinos: The four electrically neutral neutralinos $\tilde{\chi}_i^0$ ($i = 1, 2, 3, 4$) are the mass eigenstates of the gauge eigenstates \tilde{B}^0 , \tilde{W}^0 , \tilde{H}_D^0 and \tilde{H}_U^0 . The masses of the four neutralinos are ordered by their indices. The lightest neutralino ($\tilde{\chi}_1^0$) is often assumed to be the lightest supersymmetric particle (LSP). The LSP is stable in an R-parity conserving scenario. In the basis of the gauge eigenstates the mass matrix can be written as shown in [Equation 3.22](#).

$$\mathbf{M}_{\tilde{\chi}^0} = \begin{pmatrix} M_1 & 0 & -m_Z s_W c_\beta & m_Z s_W s_\beta \\ 0 & M_2 & m_Z c_W c_\beta & m_Z c_W s_\beta \\ -m_Z s_W c_\beta & m_Z c_W c_\beta & 0 & -\mu \\ m_Z s_W s_\beta & -m_Z c_W s_\beta & -\mu & 0 \end{pmatrix} \quad (3.22)$$

Whereby m_Z is the mass of the Z boson and μ is the higgsino mass parameter. The symbols s_W , c_W , c_β and s_β are abbreviations for $\sin \theta_W$, $\cos \theta_W$, $\cos \beta$ and $\sin \beta$. Where $\tan \beta$ is the ratio of the Higgs VEVs.

The matrix $\mathbf{M}_{\tilde{\chi}^0}$ can be diagonalized by a unitary matrix \mathbf{N} in order to obtain the mass eigenstates $\tilde{\chi}_i^0$:

$$\tilde{\chi}_i^0 = N_{i1} \tilde{B}^0 + N_{i2} \tilde{W}^0 + N_{i3} \tilde{H}_D^0 + N_{i4} \tilde{H}_U^0 \quad (3.23)$$

charginos: the gauge eigenstates \tilde{H}_U^+ , \tilde{H}_D^- , \tilde{W}^+ and \tilde{W}^- can be used to form the electrically charged mass eigenstates $\tilde{\chi}_1^\pm$ and $\tilde{\chi}_2^\pm$ called charginos. The mass matrix in the gauge basis can be written as a diagonal block matrix. The off diagonal elements are given by the 2×2 matrices \mathbf{X} and \mathbf{X}^T while the diagonal blocks are zero.

$$\mathbf{X} = \begin{pmatrix} M_2 & \sqrt{2} m_W s_\beta \\ \sqrt{2} m_W c_\beta & -\mu \end{pmatrix} \quad (3.24)$$

The matrices \mathbf{X} and \mathbf{X}^T can be diagonalized leading to the mass eigenstates $\tilde{\chi}_1^\pm$ and $\tilde{\chi}_2^\pm$:

$$\begin{pmatrix} \tilde{\chi}_1^+ \\ \tilde{\chi}_2^+ \end{pmatrix} = \mathbf{V} \begin{pmatrix} \tilde{W}^+ \\ \tilde{H}_U^+ \end{pmatrix} \quad \begin{pmatrix} \tilde{\chi}_1^- \\ \tilde{\chi}_2^- \end{pmatrix} = \mathbf{U} \begin{pmatrix} \tilde{W}^- \\ \tilde{H}_D^- \end{pmatrix} \quad (3.25)$$

squarks and sleptons: The superpartners of the quarks and leptons are often referred to as sfermions. Since the fermions are bosons they have no chiral eigenstates. The

indices L and R indicate the chiral eigenstates of the assigned SM fermionic fields.

Similar to the neutralinos the mixing of sfermions (cf. Equation 3.26) can be obtained by diagonalising the mass matrix $\mathbf{M}_{\tilde{f}}$ of the bosonic fields $(\tilde{f}_L, \tilde{f}_R)$.

$$\begin{pmatrix} \tilde{f}_1 \\ \tilde{f}_2 \end{pmatrix} = \begin{pmatrix} \cos \theta_{\tilde{f}} & -\sin^* \theta_{\tilde{f}} \\ \sin \theta_{\tilde{f}} & \cos \theta_{\tilde{f}} \end{pmatrix} \begin{pmatrix} \tilde{f}_L \\ \tilde{f}_R \end{pmatrix} \quad (3.26)$$

Whereby $\tilde{f}_1 < \tilde{f}_2$ and $\theta_{\tilde{f}}$ is the mixing angle. The off-diagonal elements of the mass matrix $\mathbf{M}_{\tilde{f}}$ depend on the Yukawa couplings of the fermions. Because the Yukawa coupling of the first two generations of fermions is negligible this mixing is sizeable in the third generation of squarks and sleptons only.

The neutralinos and charginos may occur as bino-like, wino-like or higgsino-like particles. The terms wino and bino refer to \widetilde{W}^{\pm} , \widetilde{W}^0 and \widetilde{B} , the superpartners of the electroweak gauge fields. The fermionic partners of the Higgs scalars are called higgsinos. As described above neutralinos can have admixtures from winos, binos and higgsinos and charginos only from winos and higgsinos. The terms bino-like, wino-like or higgsino-like particles refer to this admixture. For example for a bino-like neutralino the admixture of bino is much bigger than the wino and higgsino admixtures.

Chapter 4

SUSY Searches at the LHC

As pointed out in the last chapter, the masses of the sparticles should be of $\mathcal{O}(TeV)$ at most, if SUSY is a natural solution to the hierarchy problem. This leads to the assumption that sparticles can be produced at the LHC. In this chapter only R-parity conserving scenarios are considered and the $\tilde{\chi}_1^0$ is assumed to be the LSP. Furthermore charge and parity (CP) conservation as well as flavour conservation is assumed. These assumptions lead to characteristic production and decay modes of the sparticles at the LHC (c.f. [section 4.1](#)). Based on the different production and decay processes specific detector signals are expected at ATLAS and CMS. One of the standard techniques to interpret these signals are simplified models, discussed in [section 4.2](#).

4.1 SUSY signals at the LHC

In order to search for SUSY signatures at the LHC it is essential to know the signals produced by SUSY interactions at a hadron collider. Therefore the possible production modes for SUSY particles and their decay modes are discussed in [subsection 4.1.1](#) and [subsection 4.1.2](#). These two subsections follow the discussion of sparticle decays and experimental signals for SUSY in [\[16\]](#) where a more detailed description can be found.

The production and decay modes lead to characteristic signals in the detectors and different search strategies for SUSY at the LHC (cf. [subsection 4.1.3](#)).

4.1.1 Sparticle Productions

Considering an R-parity conserving SUSY scenario sparticles can only be produced pairwise from proton-proton collisions. For light squarks and gluinos this production is dominated by the strong interaction. If the mass of squarks and gluinos get higher the production of neutralinos, charginos and sleptons becomes important. These sparticles are produced by the electroweak interaction. Finally one can also have production modes of mixed strong and electroweak strength, although these modes are suppressed.

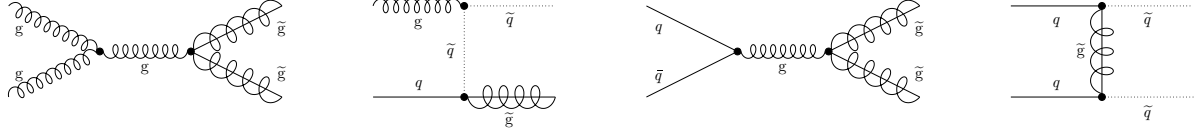


Figure 4.1: Examples for strong particle productions. From the left to the right: gluon-gluon fusion in s-channel, gluon-quark fusion in t-channel, quark-antiquark annihilation in s-channel, quark-quark scattering in t-channel.

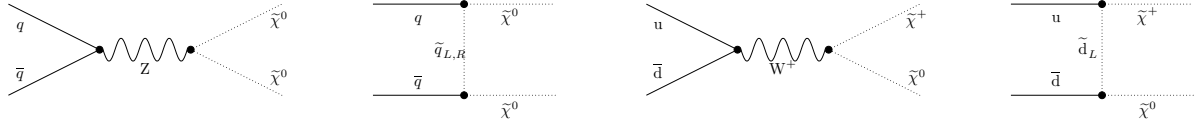


Figure 4.2: Examples for production of electroweak particles. From the left to the right: neutralino pair production in s- and t-channel, chargino-neutralino associated production in s- and t-channel

Strong Production

The most dominant production modes at the LHC are gluino and squark productions from gluon-gluon ($gg \rightarrow \tilde{g}\tilde{g}, \tilde{q}\tilde{q}$) and gluon-quark ($gq \rightarrow \tilde{g}\tilde{q}$) fusion. Gluinos and squarks can also be produced by quark-antiquark annihilation ($q\bar{q} \rightarrow \tilde{g}\tilde{g}, \tilde{q}\tilde{q}$) and quark-quark scattering ($qq \rightarrow \tilde{q}\tilde{q}$). The production cross sections of squarks and gluinos depend on their mass only. Figure 4.1 depicts some example Feynman diagrams for these production modes.

Electroweak Production

Neutralinos, charginos and sleptons can be produced from quark-antiquark annihilation. The production cross sections of these particles depend both on their mixing (cf. subsection 3.2.2) and their masses. The different production processes are listed below. Figure 4.2 shows some typical Feynman diagrams.

$$\begin{aligned}
 q\bar{q} &\rightarrow \tilde{\chi}^{\pm}\tilde{\chi}^{\mp}, \tilde{\chi}^0\tilde{\chi}^0 & q\bar{q} &\rightarrow \tilde{\ell}^{\pm}\tilde{\ell}^{\mp}, \tilde{\nu}_L\tilde{\nu}_L \\
 u\bar{d} &\rightarrow \tilde{\chi}^+\tilde{\chi}^0 & u\bar{d} &\rightarrow \tilde{\ell}_L^+\tilde{\nu}_L \\
 d\bar{u} &\rightarrow \tilde{\chi}^-\tilde{\chi}^0 & d\bar{u} &\rightarrow \tilde{\ell}_L^-\tilde{\nu}_L
 \end{aligned}$$

4.1.2 Sparticle Decays

Due to R-parity conservation sparticles typically decays into SM particles and one other sparticle. This can lead to long decay chains ending up with the $\tilde{\chi}_1^0$ that is assumed to be the LSP. Sparticles can decay via strong or electroweak interactions. The different decay

modes mediated by the strong interaction are controlled by the masses of the involved particles. For decays of electroweak strength the situation is more complex. Due to the fact that only LH sfermions couple to winos, LH and RH sfermions may prefer different decays. Decays including neutralinos and charginos strongly depend on their mixing.

This subsection discusses the possible decays of the different sparticles. This discussion mainly focusses on the mass-dependence of the decays .

Squark Decays

If the strong decay of squarks to quarks and gluinos ($\tilde{q} \rightarrow q\tilde{g}$) is kinematically allowed it is favoured. If not the decay to charginos and neutralinos via the electroweak interaction occurs ($\tilde{q} \rightarrow q\tilde{\chi}^0, \tilde{q} \rightarrow q\tilde{\chi}^\pm$). Especially for the stop it is possible that the decays $\tilde{t} \rightarrow t\tilde{g}$ and $\tilde{t} \rightarrow t\tilde{\chi}^0$ are forbidden, due to the high top mass. In this case the stop can decay in a flavour-violating manner and in addition to three-body decay ($\tilde{t} \rightarrow bW\tilde{\chi}^0$) and four-body ($\tilde{t} \rightarrow b\bar{q}q\tilde{\chi}^0, \tilde{t} \rightarrow b\ell\bar{\nu}\tilde{\chi}^0$) decays.

Gluino Decays

The gluino couples only via the strong interaction and can therefore decay via on- and off-shell squarks only ($\tilde{g} \rightarrow q\tilde{q}, \tilde{g} \rightarrow q\bar{q}\tilde{\chi}^0, \tilde{g} \rightarrow q\bar{q}\tilde{\chi}^\pm$). The two body decay via on-shell squark occurs if the gluino is heavier than the sum of the masses of quark and squark, otherwise it decays through the three body decay via an off-shell squark.

Slepton Decays

The sleptons decay to charginos and neutralinos via the electroweak interaction. The direct decay to LSP ($\tilde{\ell} \rightarrow \ell\tilde{\chi}_1^0, \tilde{\nu} \rightarrow \nu\tilde{\chi}_1^0$) is almost always kinematically allowed, because leptons are typically very light. If the sleptons are sufficiently heavy, decays to the second lightest neutralinos or to the lightest charginos can also be important.

Chargino and Neutralino Decays

Neutralinos and charginos can decay via electroweak interaction only. If sleptons and squarks are sufficiently light they can decay to leptons and sleptons ($\tilde{\chi}^0 \rightarrow \ell\tilde{\ell}, \nu\tilde{\nu}, \tilde{\chi}^\pm \rightarrow \ell\tilde{\nu}, \nu\tilde{\ell}$) or quarks and squarks ($\tilde{\chi}^0 \rightarrow q\tilde{q}, \tilde{\chi}^\pm \rightarrow q\tilde{q}$). Other possibilities for neutralinos and charginos are the decays to any lighter neutralino or chargino plus a Higgs scalar (e.g. $\tilde{\chi}_i^0 \rightarrow h^0\tilde{\chi}_j^0$) or an electroweak gauge boson (e.g. $\tilde{\chi}_i^0 \rightarrow Z\tilde{\chi}_j^0$). Which decay is dominant heavily depends on the gauge-higgsino mixture and on the mass spectrum of the sparticles. For example sleptons are often lighter than squarks, therefore the decay to leptons-sleptons is favoured against the decay to quark-squarks.

4.1.3 SUSY Searches at ATLAS and CMS

The processes discussed above typically lead to pair-produced sparticles, decaying through decay chains of arbitrary length to the LSP. The LSP can not be detected in the detector but carries away energy. In particle detectors a variable called missing transverse energy (\cancel{E}_T) is measured. It is defined as the negative of the vector sum of the transverse momenta of all final state particles reconstructed in the detector (cf. Equation 4.1). Typical SUSY searches assume signals containing a certain number of leptons, jets and \cancel{E}_T .

$$\cancel{E}_T = - \sum_i \vec{p}_T(i) \quad (4.1)$$

Unfortunately, these signals are not exclusive for sparticle decays. There are some SM processes which can mimic the SUSY signals. A common example is the production of vector bosons by SM processes. Both of them can decay to final states including neutrinos ($W \rightarrow \ell \bar{\nu}$, $Z \rightarrow \nu \bar{\nu}$). The neutrinos leave the detector unrecognised, thus also leading to signals including \cancel{E}_T .

In a first step a signal region is defined by a number of jets, leptons and \cancel{E}_T . In order to reduce the SM background additional requirements can be imposed on the signal region. This can be done by setting cuts on \cancel{E}_T and additional kinematic variables. A common example for such a kinematic variable is H_T . Equation 4.2 gives the definition of H_T , where X is the set of objects included in the sum (e.g. jets). The ideal signal region contains a low SM background and a strong signal from the expected SUSY process.

$$H_{T,X} = \sum_{i \in X} |\vec{p}_T(i)| \quad (4.2)$$

Without the claim of completeness a selection of search strategies used by the ATLAS and CMS collaborations is given below. This selection mainly follows the description of analyses in [18]. A short description of the experimental signals for SUSY at the LHC can also be found in [16] and a list of SUSY searches performed by the ATLAS and CMS collaborations can be found in [19] and [8], respectively.

All-Hadronic

Events containing at least two jets with high p_T and significant \cancel{E}_T are selected. Significant background comes from $t\bar{t}$, W and Z production. The background can be reduced by a veto on isolated leptons. In order to define a signal region a selection of kinematic variables like \cancel{E}_T and H_T is used. This type of analysis is applicable to squark and gluino searches.

Single Lepton plus Jets

Events are selected with jets, one high p_T isolated lepton and significant \cancel{E}_T . The main background originates from $t\bar{t}$ and W production. Again signal regions can be defined by

using cuts on \cancel{E}_T and H_T . Furthermore the kinematic variable $m_T = \sqrt{2p_T\cancel{E}_T(1 - \cos \Delta\phi)}$ is often used to reduce the background from the SM production of W bosons, where $\Delta\phi$ is the difference in azimuthal angle between missing transverse momentum and the lepton. This class of analyses can have large contributions from various sparticle production modes and is very sensitive to sparticles decaying via W -bosons, e.g. chargino decay.

Opposite- and Same-Sign Dileptons

This event selection requires two leptons, jets and significant \cancel{E}_T . It can be distinguished further between analyses searching for leptons having electric charge with opposite sign (OS) and those searching for same sign leptons (SS). The largest SM background for isolated lepton pairs originates from $t\bar{t}$ and always leads to OS leptons. Therefore the SM background for the SS lepton searches is very low. Typically in an OS analysis a search for a characteristic kinematic edge in the dilepton mass distribution is performed. \cancel{E}_T and H_T can be used in both analyses to suppress the background. Examples for this class of analyses are the searches for sparticle decay chains including neutralinos decaying to Z bosons (OS) or directly produced sleptons decaying to leptons (SS).

Multileptons

Events are selected containing three or more leptons, jets and \cancel{E}_T . Signal regions are selected by several kinematic variables including \cancel{E}_T and H_T . The SM background from $t\bar{t}$ can be reduced further by identifying jets originating from bottom quarks, so called b-tagged jets, and rejecting them. Multilepton searches are very suitable for neutralinos and charginos decaying to leptons and sleptons as well as for sparticle decays with SM vector bosons in the final state.

4.2 The Simplified Models Approach

In principle the outcomes of a SUSY search, which are mostly event counts, can be interpreted in terms of any theory providing the selected signature. Most BSM theories like the MSSM involve a great number of free parameters. In order to reduce the number of free parameters more specific models which constrain the parameter space by certain assumptions can be used. An example of such a model is the phenomenological minimal supersymmetric standard model (pMSSM). The pMSSM is defined at the weak scale and the reduction of parameters is driven by experimental constraints. Experimental data can then be used to exclude particular regions of the parameter space. This approach is very demanding and computationally expensive. Therefore interpreting SUSY searches within the framework of simplified models spectra (SMS) became a standard technique.

4.2.1 The Concept of Simplified Models

Within the simplified model approach SUSY searches are interpreted in terms of simple models involving relatively few light new particles. All other sparticles are considered to be decoupled, meaning their masses are set to very high values. A simplified model is defined by an effective Lagrangian describing the interactions of these few particles. It can be described by a small number of parameters, which are directly related to the observables in the particle detectors. These parameters are the masses of the new light particles (m_i), the branching ratios of their decays (BR) and the production cross section (σ).

For example, one of the most simplest SMS models assumes only two new non-decoupled particles, the gluino \tilde{g} and the neutralino $\tilde{\chi}_1^0$. Considering the SUSY decay modes discussed in [subsection 4.1.2](#) the only possible decay for the gluinos is $\tilde{g} \rightarrow q\bar{q}\tilde{\chi}_1^0$. Here again the $\tilde{\chi}_1^0$ is assumed to be the LSP. The BR for this decay therefore is 100 %. The model is parametrized by $m_{\tilde{g}}$, $m_{\tilde{\chi}_1^0}$ and the production cross section for the pair-produced gluinos.

A model that includes the additional particle $\tilde{\chi}^\pm$ enables the cascade decay $\tilde{g} \rightarrow q\bar{q}\tilde{\chi}^\pm \rightarrow q\bar{q}(W^\pm\tilde{\chi}_1^0)$. This leads to two new parameters: $m_{\tilde{\chi}_1^\pm}$ and $BR(\tilde{g} \rightarrow q\bar{q}\tilde{\chi}^\pm)$. In order to reduce the number of parameters of the simplified model the branching ratio can be set to 100 %.

The example above is described in more detail in [\[20\]](#) where explanations of numerous simplified models can be found. A simplified model and the included decays can be described in terms of so called SMS topologies (c.f. [subsection 4.2.2](#)). On the basis of the results of a SUSY search experimental upper limits on the production cross section times branching ratio at statistical 95 % confidence level (C.L.) can be calculated for a simplified model. Also limits for the masses of the involved new particles (cf. [subsection 4.2.3](#)) can be obtained.

Simplified models are not completely model independent. They assume that the kinematic of particles introduced by the model mainly depend on their masses, BR and σ . All other specific properties, e.g. the spin of these particles, have to be negligible. Nevertheless, interpretations of SUSY searches in terms of SMS are more general than an interpretation in terms of a full model like the pMSSM. The limits obtained using SMS can be applied to every model giving rise to the same topology, as long as the assumptions, mentioned above, are not violated.

4.2.2 SMS Topologies

Each simplified model can be depicted by a Feynman graph showing the primary produced new particles, also called mother particles, and the associated decays. One of these Feynman diagrams represents one SMS topology. Due to R-parity conservation each topology consists of two branches. Each branch originates from one of the pair-produced sparticles which decays to the LSP.

This thesis follows the “TNx” naming convention used by CMS. In this convention T indicates that it is an SMS topology. The variable N holds an integer or string which indicates the sparticles produced by proton-proton collision and the length of the decay chain to the LSP. The different possibilities for N and their meanings is listed below.

gluino production: Odd numbers indicate gluino pair production by strong interaction, whereby $N = 1$ indicates a direct decay of both gluinos to the LSP. $N = 3$ is used for asymmetric topologies where one gluino decays directly and the other one via a two step decay to the LSP. Finally $N = 5$ means that both gluinos decay via two step decays.

squark production: Even numbers indicate squark pair production by strong interactions. Similar to the gluino case, $N = 2, 4, 6$ indicates topologies with direct decays in both branches, asymmetric topologies and symmetric topologies with two step decays, respectively.

electroweak production: Electroweakly produced sparticles are indicated by a string. The string “Chi” denotes neutralinos and charginos. This can be specified further by using “Chipm” for charginos. Also the charge of the chargino can be indicated by using “p” or “m” instead of “pm” as postfix. For direct production of sleptons the abbreviation “Slep” is used.

The last variable -x- in the “TNx” naming convention can be used for more detailed descriptions of the decay if necessary. For clarification some topologies are explained in greater detail below.

Gluino Production

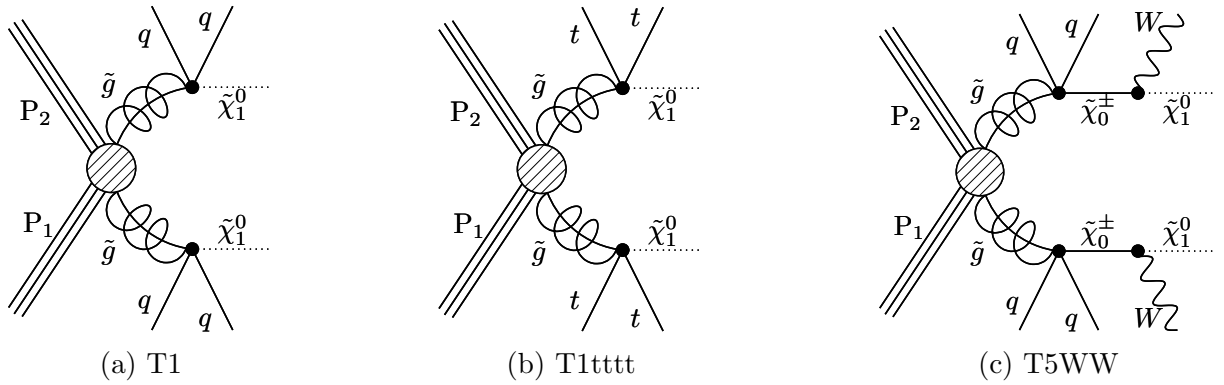


Figure 4.3: Feynman graphs for topologies with gluino productions

The simplest topology which stems from gluino pair production is based on the three body decay $\tilde{g} \rightarrow q\bar{q}\tilde{\chi}^0$. In contrary to [section 4.1](#) where all quarks were denoted by q , in this section and in all following sections q denotes a light flavoured quark only. The

number 1 in the name T1 indicates the direct decays into the LSP in both branches. The decay into light flavour quarks is chosen as the standard decay within the naming convention. Therefore no further description of the decay is needed. If both gluinos decay into a top-antitop pair as shown in Figure 4.3b this is indicated by the postfix “tttt” leading to the name T1tttt. Figure 4.4c shows a symmetric topology including two step decays via on-shell charginos. This topology is named T5WW. Where $N = 5$ indicates the symmetric two step decays and the postfix “WW” the two W bosons in the final state.

Squark Production

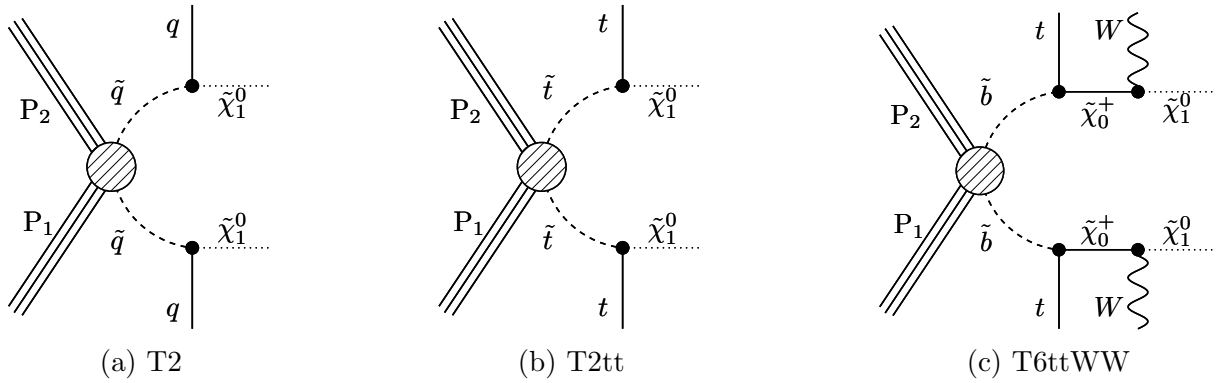


Figure 4.4: Feynman graphs for topologies with squark productions

In analogy to the gluino topologies the simplest topology that originates from squark pair production is called T2. Figure 4.4a shows this topology consisting of two branches each described by the decay $\tilde{q} \rightarrow q\tilde{\chi}_1^0$. If instead of the light flavoured squarks a stop pair is produced, each decaying directly to top and the LSP, the topology is called T2tt (cf. Figure 4.4b). The decay of pair produced sbottoms to a final state including tops, W bosons and the LSP via on-shell chargino is depicted in Figure 4.4c. It is called T6ttWW where the number 6 and the SM particles in the final state are used to describe the cascade decays of both sbottoms.

Electroweak Production

The topology in Figure 4.5a is named TChiWW and the one in Figure 4.5b TChiWZ. Even if the mother particles differ, both topologies are labelled with “Chi” which does not distinguish between neutralinos and charginos. Due to the fact that the W boson can only origin from a chargino and the Z boson only from a neutralino the topologies are clearly described by their names containing the SM particles in the final states. Figure 4.5c shows the associated production of a neutralino and a chargino, indicated by the string “ChiChipm”. Both particles decay via on-shell sleptons into the finale state leading to the name TChiChipmSlepSlep. In contrast to the first two topologies the clarification of the exact type of the mother particles is necessary in order to make the name unambiguous.

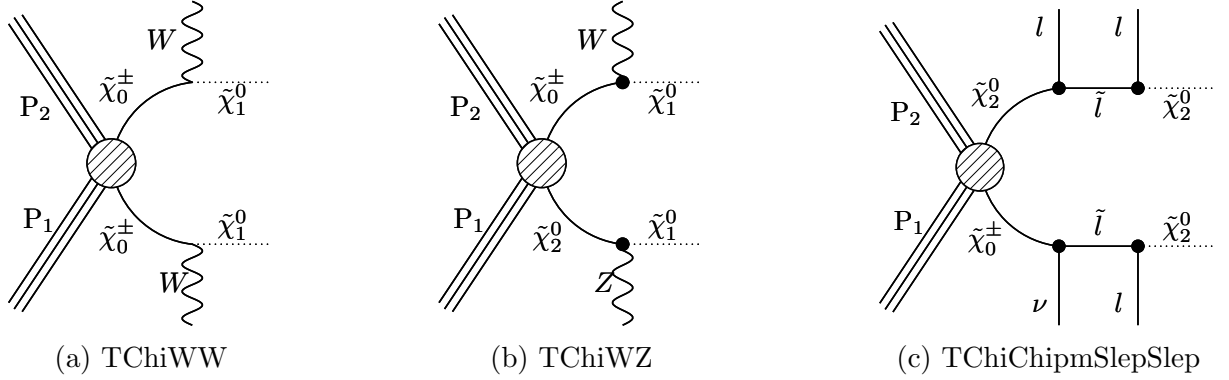


Figure 4.5: Feynman graphs for topologies with neutralino and chargino production

4.2.3 Interpretation of SMS Results

So far no experimental evidence for SUSY could be found. Therefore SUSY searches interpreted in terms of simplified models are used to set limits on the masses of the sparticles. Often these limits are presented as exclusion lines printed on top of so called upper limit maps. The concept of these limit setting procedure is introduced below.

Upper Limit Maps

As discussed in [subsection 4.1.3](#) searches for SUSY assume specific detector signatures. In order to suppress the background additional restrictions can be applied on the signal region. For one given signal region a so called efficiency map can be calculated. To that end simplified model events are simulated. $(A \times \epsilon)$ can be determined by the ratio of selected to generated events. Where A is named acceptance and describes the fraction of events that actually reach the detector. The variable ϵ is the so called efficiency that describes the ratio of selected events to the events that reach the detector. The calculation of $(A \times \epsilon)$ is repeated for different sparticle masses and the derived values are plotted as a two dimensional histogram called efficiency map. [Figure 4.6a](#) shows the efficiency map of the T1tttt topology for one specific signal region.

The values of $(A \times \epsilon)$ and background estimations, together with their uncertainties and the integrated luminosity (cf. [section 2.1](#)) can be used to derive the 95 % C.L. experimental upper limits on production cross section times branching ratio $(\sigma \times BR)_{UL}$. The C.L. (confidence level) technique is a statistical method which is based on hypothesis tests. The background (B) hypothesis assume that the event yield in the signal region stems from background only. Whereas the signal plus background (B+S) hypothesis assumes also contributions from SUSY signals. In order to derive $(\sigma \times BR)_{UL}$ the B hypothesis is tested against the B+S hypothesis as a function of the signal cross section. More details of this statistical method can be found elsewhere [\[21\]](#). Roughly speaking $(\sigma \times BR)_{UL}$ denotes the maximally possible production cross section for a certain topology that is compatible with measurement .

The upper limit map is a two dimensional histogram showing $(\sigma \times BR)_{UL}$ as a function of two particle masses. Contributions from efficiency maps from different signal regions can be combined to one upper limit map. Figure 4.6b shows a combined upper limit map for the topology T1tttt. The upper limits are overlaid by the exclusion line, indicating limits for the particle masses.

For SMS topologies including more than only two particles e.g. T5WW, also the masses of the other sparticles have influence on $(\sigma \times BR)_{UL}$. In order to define the masses of the other sparticles so called “slicing methods” are used. An upper limit map together with the slicing method defines a mass plane, as described below.

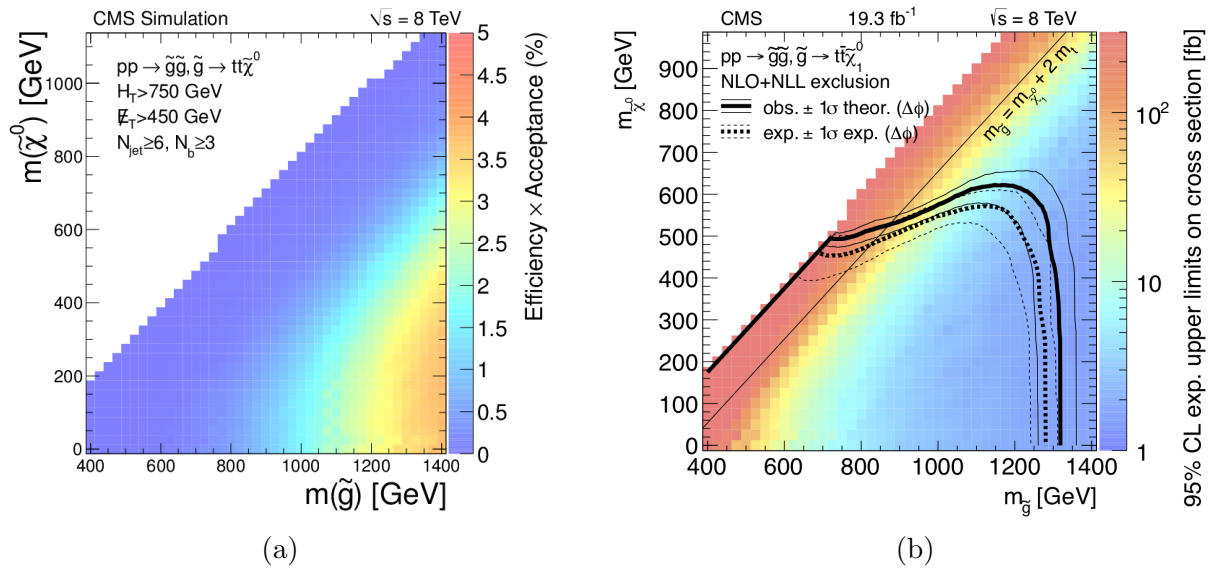


Figure 4.6: Efficiency map (a) and upper limit map including exclusion line (b) for the T1tttt topology from CMS-SUS-13-007 [22] in the gluino-LSP mass plane. Figure (a) shows $(\epsilon \times A)$ for a signal region determined by jets and selections on \cancel{E}_T and H_T . Figure (b) shows the 95 % C.L. upper limits on the production cross section assuming $BR = 100\%$, obtained from the combination of different signal regions. For the exclusion lines, next to leading logarithmic (NLL) SUSY production cross sections are computed and compared with the 95 % CL upper limits. To this end, a BR of 100 % into the SMS topology is assumed

Mass Planes

To introduce the concept of a mass plane a symmetric topology is assumed. The mass ranges of the on-shell sparticles involved in the decay chain can be used to define a mass space. The dimension of the mass space is given by the number of these sparticles. For example the T6ttWW topology (cf. Figure 4.4c) describes a cascade decay leading to a three-dimensional mass space defined by $(m_{\tilde{b}}, m_{\tilde{\chi}^\pm}, m_{\tilde{\chi}_1^0})$.

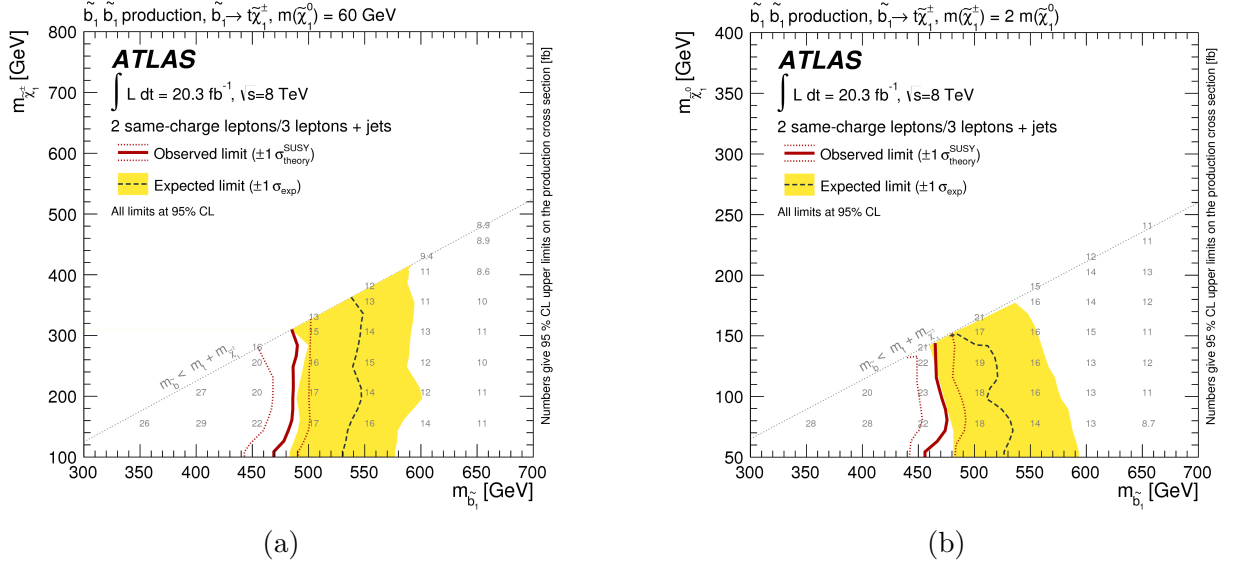


Figure 4.7: Upper limit map and exclusion lines for the T6ttWW topology from ATLAS-SUSY-2013-09 [23] in two different mass planes. Figure (a) shows a mass plane defined by the mass of the sbottom (x-axis) and the mass of the chargino (y-axis). The mass of the LSP is set to 60 GeV. Figure (b) depicts a mass plane defined by the mass of the sbottom (x-axis) and the mass of the LSP (y-axis). The mass of the chargino is set to two times the mass of the LSP.

For the presentation of SUSY search results interpreted in terms of an SMS topology it is more descriptive to consider two-dimensional subspaces of the mass space. These two-dimensional subspaces are called mass planes or slices. They are presented as two-dimensional plots. Usually the masses of two of the sparticles are printed on the x- and the y-axis. Because the masses of the other sparticles also influence the kinematics of the topology these masses have to be defined. A number of different useful methods to define them, called slicing methods, are used by the experimentalists in order to present their results. The different methods are listed below.

- The most simplest method is setting one or more masses to a fixed value. As an example the $\tilde{\chi}_1^\pm - \tilde{b}_1$ - mass plane with $m_{\tilde{\chi}_1^0} = 60$ GeV for T6ttWW from ATLAS-SUSY-2013-09 [23] is depicted in Figure 4.7a
- The difference of the masses of two adjacent sparticles can be set to a certain value (e.g. $m_{i+1} = m_i - 5$ GeV). This method is used in e.g. ATLAS-CONF-2013-048 [24] for the T6bbWW topology.
- One sparticle mass can be set to a multiple of one other sparticle mass. Figure 4.7a shows an example in the $\tilde{\chi}_1^\pm - \tilde{b}_1$ - mass plane with $m_{\tilde{\chi}_1^\pm} = 2 \cdot m_{\tilde{\chi}_1^0}$ for T6ttWW from ATLAS-SUSY-2013-09 [23].

- One of the most common methods is to set the value of a variable denoted as x with $0 \leq x \leq 1$. The mass of a sparticle B is given by $m_B = x \cdot m_A + (1 - x) \cdot m_C$ whereby m_A , m_B and m_C are the masses of the sparticles involved in the decay $A \rightarrow B \rightarrow C$. Different upper limit maps for the T6bbWW topology where the mass plane is defined by using this method can be found in e.g. CMS-SUS-13-011 [25].

Most topologies describe two- or one-step decays. In the case of an one-step decay the mass space is equal to the mass plane and no further definitions are needed. For two-step decays one of the masses has to be set by using one of the described methods. In addition there are also simplified model interpretations in terms of topologies which describe cascade decays including three or more steps. In these cases more than one mass has to be set in order to define a mass plane.

Exclusion Lines

The exclusion line is derived by comparing the upper limit cross sections σ_{UL} with a reference cross section (σ_{ref}) which refers to the production cross section of the mother particles¹. For the calculation of σ_{ref} a BR of 100 % to the topology in question is assumed. Figure 4.6b depicts the exclusion line in the gluino-LSP mass plane as bold black line. It is derived using the next-to-leading order (NLO) plus next-to-leading logarithm (NLL) gluino production cross section. By adding the theory uncertainties to σ_{ref} the thin black lines are derived. Furthermore the expected exclusion line is shown in Figure 4.6b. It is derived by comparison of σ_{ref} with the expected upper limits using the background (B) hypothesis.

4.3 CMS Summary Plots

To give an overview of the various CMS SUSY search results, the so called summary plots are presented by the CMS collaboration [26]. Within the scope of thesis the CMS summary bar plot was produced, which was presented at the 37th International Conference on High Energy Physics (ICHEP 2014) at Valencia.

This plot shown in Figure 4.8 compares the results of different SUSY searches performed by the CMS collaboration. The lower region of the plot, marked with RPV, shows the best mass limits for light and heavy flavoured squarks obtained within R-parity violating SUSY scenarios. The upper part shows the best limits for the mother particles of different SMS topologies considering R-parity conservation. For each topology only the best exclusion limit is shown. The CMS notification of the Physics Analysis Summary (CMS-PAS or CMS-SUS-PAS) which provides this best limit is shown as a string inside the respective bar. The dark shaded bars belong to the limit of the mother particle mass for LSP masses equal to zero. The light shaded bars show the limits for

¹For the comparison of σ_{UL} with σ_{ref} the C.L. method is used

$m_{\text{mother}} - m_{\text{LSP}} = 200$ GeV. For topologies describing two step decays only mother-LSP mass planes are considered. The mass of the third particle is parametrised by the variable x as described in subsection 4.2.3.

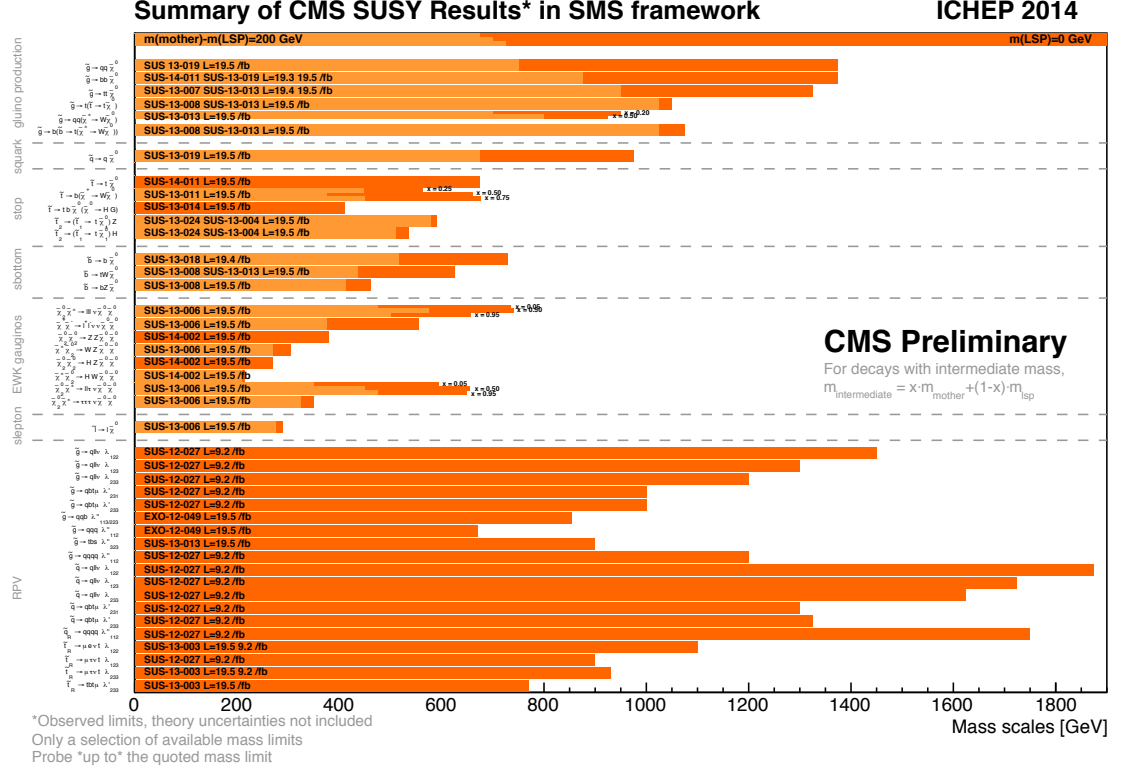


Figure 4.8: CMS summary bar plot produced for the 37th International Conference on High Energy Physics (ICHEP 2014) at Valencia. The plot shows a comparison of the exclusion limits for the mother particles of different SMS topologies. The string inside the bars refers to the CMS notification of the respective CMS Physic Analysis Summary.

The CMS summary bar plot was produced by using the data stored in the SModelS database. SModelS is a computational framework that was released during this thesis and will be described in the next chapter.

Chapter 5

SModelS

During the first run of the LHC numerous results of SUSY searches were interpreted in terms of different SMS topologies. In order to use the $(\sigma \times BR)_{UL}$ obtained by these searches to constrain the parameter space of more complex BSM models, e.g. MSSM, the SModelS framework [27] was developed (cf. [section 5.1](#)). SModelS was published in December 2014 [28] after a massive validation procedure. This validation took place during the work for this thesis and is described in [section 5.2](#).

5.1 The SModelS Framework

This section describes the working procedure of the current public version, SModelS v1.0.3. It provides a procedure to confront a full model with a \mathbb{Z}_2 symmetry, e.g. R-parity conserving SUSY models, against the experimental constraints for simplified models. SModelS can be divided into an experimental side and a theoretical side. [Figure 5.1](#) shows the working procedure of SModelS.

On the experimental side SModelS uses a database (cf. [subsection 5.1.2](#)) to store all the results from different analyses. Here an analysis means either a publication, a CMS analysis Summary (CMS-PAS or CMS-SUS-PAS) [8] or an ATLAS conference note (ATLAS-CONF or ATLAS-SUSY) [19] including SUSY search interpretations in terms of SMS topologies. The term result refers to one specific upper limit map from a given analysis which holds the $(\sigma \times BR)_{UL}$. As discussed in [subsection 4.2.3](#), $(\sigma \times BR)_{UL}$ is derived from $(A \times \epsilon)$. Within the SModelS framework it is assumed that $(A \times \epsilon)$ mainly depends on the masses of BSM particles and the kinematics of their decays and is not affected by specific details of a BSM model like the spin of the particle.

On the theoretical side this assumption leads to the possibility to reduce all properties of a BSM model to its mass spectrum, production cross sections (σ) and decay branching ratios (BR). Therefore a given point in the parameter space of a BSM model, called model point, can be decomposed into its signal topologies. The meaning of a signal topology is described in [subsection 5.1.1](#).

After the decomposition described in [subsection 5.1.3](#) the weight $(\sigma \times BR)$ of the

signal topologies can be compared to the $(\sigma \times BR)_{UL}$ of the results stored in the database (cf. subsection 5.1.4). This procedure can be used to exclude a model point, but also to identify regions of the parameter space of a BSM model which are so far unchallenged by the experiment.

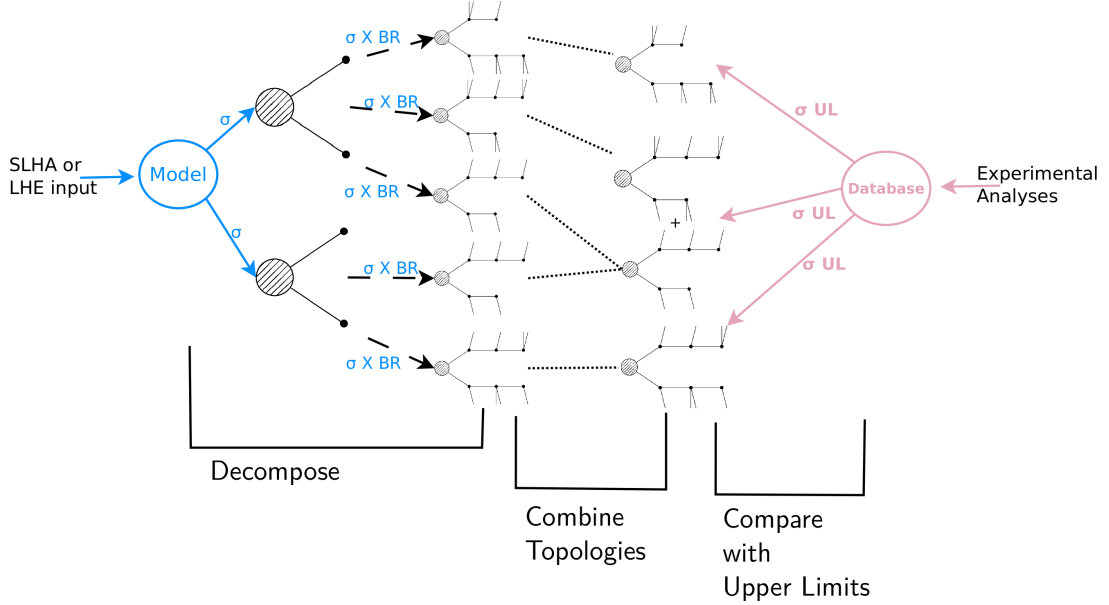


Figure 5.1: SModelS working procedure [29]. The experimental side (right) contains σ_{UL} for different SMS topologies. On the theory side (left) a BSM model can be decomposed into its signal topologies. The signal topologies can be combined and their weights are compared to σ_{UL} uppecase of the SMS topologies.

5.1.1 SModelS Language

To store experimental results in the database and to describe BSM model points as a spectrum of signal topologies SModelS uses a specific notation, which is explained below.

Signal Topologies, Mass Vector and Constraints

It is important to clearly distinguish between an SMS topology as introduced in subsection 4.2.2 used within the analyses and the decay chains as predicted by a BSM model. Hence, in this thesis the term signal topology reveres to the decay chains of a pair of BSM particles as computed by SModelS decomposition procedure, whereas as the term topology always refers to a SMS topology used in the analyses.

Within SModelS each signal topology is fully characterised by the constraint, the mass vector and the weight $(\sigma \times BR)$. To explain the constraint and the mass vector Figure 5.2 shows the topology T5WW and its signal topology analogue.

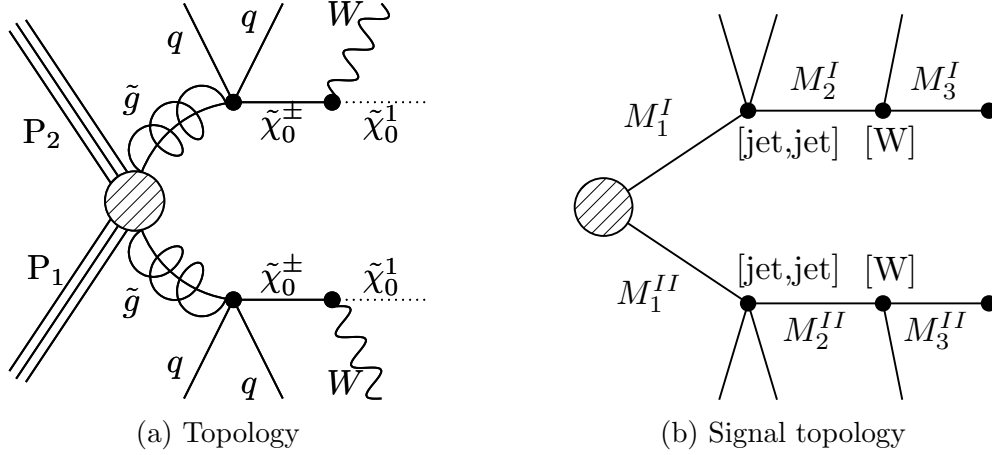


Figure 5.2: Comparison between the topology T5WW as used in the analyses and its signal topology analogue as used in SModelS. The signal topology is defined by the constraint $[[[jet, jet], [W]], [[jet, jet], [W]]]$ and the mass vector $[[M_1^I, M_2^I, M_3^I], [M_1^{II}, M_2^{II}, M_3^{II}]]$.

The constraint describes the structure of a signal topology as a system of nested brackets. The two branches of the signal topology are indicated by two brackets. For each vertex in a branch an inner bracket is inserted. Each inner bracket contains the SM particles related to the respective vertex. In the example of Figure 5.2 this leads to $[[[jet, jet], [W]], [[jet, jet], [W]]]$. The structure of the signal topology is fully described by the vertices in each branch and the SM particles in each vertex. This description holds no information about the nature of the involved BSM particles and is therefore model independent.

The only information about the BSM particles which is kept are their masses stored in the so-called mass vector. In analogy to the formalism used for the constraints the outermost structure of the mass vector is given by two brackets representing the two branches. Each bracket contains the masses of the BSM particles which occur in this branch according to their appearance. For the example of T5WW this leads to $[[M_1^I, M_2^I, M_3^I], [M_1^{II}, M_2^{II}, M_3^{II}]]$.

The weight ($\sigma \times BR$) of a signal topology is determined by the production cross sections σ of the mother particle and by the BR of all decays of the signal topology.

On the experimental side the topologies used by the analyses can also be described by means of constraints. In the simple example of T5WW the topology is described by the constraint mentioned above. It is important to note that some of these topologies comprise contributions from more than one signal topology. This will be explained below exemplified by an off-shell topology.

off-shell Topologies

The SM particles in the final state of a topology can be either on-shell or off-shell. A topology with one or more off-shell SM particles is termed *off-shell topology*. Otherwise it can be referred to as *on-shell topology*. Here only third generation fermions and the heavy vector bosons as well as the Higgs boson may occur in the off-shell regime.

The name of the off-shell topology is given by the name of the on-shell topology and the postfix “off”. For the example topology T5WW this leads to T5WWoff. The constraint for this off-shell topology can be constructed like the one for the on-shell topology replacing the off-shell particles with their decay products. The W boson in T5WW can decay into a quark pair or into a lepton-neutrino pair. Considering all these possibilities T5WWoff can comprise contributions from more than one signal topology. Some possible constraints for these signal topologies are listed below.

$$\begin{aligned} & [[[jet, jet], [e, nu]], [[jet, jet], [e, nu]]] \\ & [[[jet, jet], [jet, jet]], [[jet, jet], [e, nu]]] \\ & [[[jet, jet], [jet, jet]], [[jet, jet], [jet, jet]]] \\ & [[[jet, jet], [e, nu]], [[jet, jet], [mu, nu]]] \end{aligned}$$

It depends on the analysis which of these signal topologies contribute to the topology. For example an analysis might search for final states including two leptons. In this case only signal topologies containing two leptons should be taken into account. The constraint for T5WWoff with two leptons in the final state can be written as:

$$2.3 * ([[[jet, jet], [L, nu]], [[jet, jet], [L, nu]]])$$

Where the contributions from all charged leptons are described by the character “L”. The BR for this topology is assumed to be 100 % by the experimentalists. Due to the branching ratio of the W boson in a full model only 42 % of the T5WWoff topologies lead to final states containing two leptons. The factor 2.3 scales the BR up to 100 %.

Conditions and Fuzzyconditions

When comparing the signal topologies with a topology it is important to take into account that the detector efficiencies for, e.g. electrons and muons are not the same. The detector efficiency for muons is higher than the one for electrons. On the other hand most analyses assume flavour democratic scenarios where electrons and muons contribute equally to $(\sigma \times BR)_{UL}$. In order to be more conservative, the signal contribution from muons can be assumed to be equal or higher than the one from electrons. This can be indicated by the “conditions”.

The simplest example to describe the conditions is the topology TSlepSlep where each of the pair-produced sleptons decays into one light-flavoured lepton and the LSP.

The constraints for this topology can be written as $[[[e], [e]]] + [[[mu], [mu]]]$ ¹. Therefore the respective condition can be written as: $[[[mu], [mu]]] \geq [[[e], [e]]]$, which indicates that the contribution of the signal topology $[[[mu], [mu]]]$ should be equal or greater than the one from $[[[e], [e]]]$.

In order to compare the signal topologies against a given result the condition do not have to be fully satisfied. Therefore the fuzzyconditions were introduced. They can be defined in terms of two functions. The function $Cgtr(x, y)$ is used to measure the violation of the condition $x > y$ by mapping it into a number between 0 and 1, where 0 means full satisfaction and 1 full violation. A second function ($Csim(x, y)$) can be used to indicate that the contributions from two different signal topologies should be of same order. The violation of this condition is again mapped onto a number in the interval 0-1. SModelS provides a variable called *maxcondition* which can be set by the user to define the maximal value of allowed violation of the conditions. The default value for *maxcondition* is set to 0.2. For the TSlepSlep example the fuzzycondition can be written as $Cgtr([[[mu], [mu]]], [[[[e], [e]]]])$.

5.1.2 SModelS Database

As of September 2015 SModelS v1.0.3 database contains information from 62 results obtained by 26 CMS and ATLAS analyses. [Table 5.1](#) shows all analyses and topologies comprised in this database.

It holds all information about the results needed by SModelS. These are the constraints, conditions, fuzzyconditions and upper limit maps. Furthermore additional information about the results, e.g. luminosity and center of mass energy, is stored. SModelS is able to clearly identify each result inside the database and compare the signal topologies against these results.

The database was completely overworked and restructured within the scope of this thesis. This new database will be part of a future version of SModelS available by the end of this year. Therefore all stored objects and the structure of the new database is explained in great detail in [chapter 6](#).

5.1.3 Decomposition Procedure

If a BSM model point is given described by its mass spectrum, production cross section σ and branching ratios BR , it can be decomposed into its signal topology spectrum. For each signal topology the weight ($\sigma \times BR$) can be computed. Furthermore it might be necessary to *compress* certain signal topologies. One example where such a compression has to be performed is when a signal topology contains an decay leading only to invisible decay products, eg. $\tilde{\chi}_2^0 \rightarrow \nu \bar{\nu} \tilde{\chi}_1^0$ at the end of the decay chain. This decay is not detectable within the experiment.

¹The different signs for the sleptons are not taken into account in this example. If the respective analysis is searching for OS-leptons or SS-leptons the signs of the leptons must be written explicitly.

<i>ID</i>	<i>short description</i>	<i>L</i>	<i>Ref.</i>	<i>Tx names</i>
ATLAS-SUSY-2013-02	0 leptons + 2–6 jets + \cancel{E}_T	20.3	[30]	T1, T2
ATLAS-SUSY-2013-04	0 leptons + ≥ 7 –10 jets + \cancel{E}_T	20.3	[31]	T1tttt
ATLAS-SUSY-2013-05	0 leptons + 2 b-jets + \cancel{E}_T	20.1	[32]	T2bb
ATLAS-SUSY-2013-11	2 leptons (e, μ) + \cancel{E}_T	20.3	[33]	TChiWZ, TSlepSlep
ATLAS-SUSY-2013-12	3 leptons (e, μ, τ) + \cancel{E}_T	20.3	[34]	TChiWH, TChiWZ(off)
ATLAS-SUSY-2013-14	2 taus + \cancel{E}_T	20.3	[35]	TStauStau
ATLAS-SUSY-2013-15	1 lepton + 4(1 b-)jets + \cancel{E}_T	20.3	[36]	T2tt, T2bbWW
ATLAS-SUSY-2013-19	2 leptons + (b)jets + \cancel{E}_T	20.3	[37]	T2tt, T2bbWW, T6bbWW
ATLAS-CONF-2012-105	2 SS leptons + ≥ 4 jets + \cancel{E}_T	5.7	[38]	T1tttt
ATLAS-CONF-2013-007	2 SS leptons + 0–3 b-jets + \cancel{E}_T	20.7	[39]	T1tttt
ATLAS-CONF-2013-024	0 lepton + 6 (2 b-)jets + \cancel{E}_T	20.5	[40]	T2tt
ATLAS-CONF-2013-061	0–1 leptons + ≥ 3 b-jets + \cancel{E}_T	20.1	[41]	T1bbbb, T1tttt
ATLAS-CONF-2013-065	2 leptons + (b)jets + \cancel{E}_T	20.3	[42]	T2tt
CMS-SUS-12-024	0 leptons + ≥ 3 (1 b-)jets + \cancel{E}_T	19.4	[43]	T1bbbb, T1tttt(off), T5tttt
CMS-SUS-12-028	jets + \cancel{E}_T , α_T	11.7	[44]	T1, T1bbbb, T1tttt, T2, T2bb
CMS-SUS-13-002	≥ 3 leptons (+jets) + \cancel{E}_T	19.5	[45]	T1tttt
CMS-SUS-13-006	EW productions with decays to leptons, W, Z, and Higgs	19.5	[46]	TChiWZ(off), TSlepSlep, TChiChipmSlepL, TChiChipmSlepStau
CMS-SUS-13-007	1 lepton + ≥ 2 b-jets + \cancel{E}_T	19.3	[22]	T1tttt(off)
CMS-SUS-13-011	1 lepton + ≥ 4 (1 b-)jets + \cancel{E}_T	19.5	[25]	T2tt, T6bbWW
CMS-SUS-13-012	jet multiplicity + \cancel{H}_T	19.5	[47]	T1, T1tttt(off), T2
CMS-SUS-13-013	2 SS leptons + (b-)jets + \cancel{E}_T	19.5	[48]	T1tttt(off),
CMS-PAS-SUS-13-008	3 leptons + (b)jets + \cancel{E}_T	19.5	[49]	T6ttWW, T1tttt
CMS-PAS-SUS-13-016	2 OS leptons + ≥ 4 (2b-)jets + \cancel{E}_T	19.7	[50]	T1tttt(off)
CMS-PAS-SUS-13-018	1–2 b-jets + \cancel{E}_T , M_{CT}	19.4	[51]	T2bb
CMS-PAS-SUS-13-019	hadronic M_{T2}	19.5	[52]	T1, T1bbbb, T1tttt(off), T2, T2tt, T2bb
CMS-PAS-SUS-14-011	razor with b-jets	19.3	[53]	T1bbbb, T1tttt(off), T2tt

Table 5.1: List of analyses contained in the public database [28]. A detailed description of each analysis can be found in the respective publication.

SModelS provides two different decomposition procedures as described below. For the validation of the SModelS database, described in [section 5.2](#), the SLHA based decomposition was used and is described in greater detail. For completeness also a short description of the Monte Carlo based decomposition is given. Eventually the process of compression is described.

Monte Carlo based decomposition

This decomposition is based on parton level Monte Carlo (MC) event generation. The generated events for a given BSM model point have to be stored in an LHE event file [\[54\]](#). This file is used as input to SModelS. Each event is mapped to a signal topology, whereby more than one event can contribute to the same signal topology. The weight ($\sigma \times BR$) for a signal topology is given by the sum of the MC weights of events contributing to the signal topology.

This MC based decomposition allows to decompose any \mathbb{Z}_2 symmetric BSM model as long as it is possible to generate MC events for this model. The disadvantage of this method is the introduction of statistical MC uncertainties, which affect the result of the decomposition.

SLHA based decomposition

For SUSY models SLHA files [\[55\]](#) can be used as input. The SLHA file format provides a standard for the definition of a SUSY model point and an interface between event and spectrum generators. An SLHA file is organized in blocks. Each block describes different types of information like the mixing of the sparticles or their mass spectrum. The decomposition of SModelS needs the following blocks of an SLHA file:

mass block: This block describes the mass spectrum of the model point. Each particle is defined by the Monte Carlo particle numbering scheme (PDG-code) [\[56\]](#). Inside the mass block the mass of each sparticle is defined in units of *GeV*.

decay table: The decay table lists the possible decays for the sparticles. [Listing 5.1](#) shows an example decay table for the gluino decaying via three-body decay into the first generation quarks and the lightest neutralino. The line indicated with “DECAY” holds the PDG code of the decaying particle and its decay width. The two other lines show the possible decays for this particle. For each decay mode the branching ratio (BR), the number of decay products (NDA) and the PID codes of the final state particles (ID1-ID3) are given.

xsection block: The cross section block holds information about the production modes of the sparticle and the respective σ . [Listing 5.1](#) shows two example xsection blocks for gluino pair-production. The upper block shows the production cross sections calculated at LO (leading order) and the lower block at NLL. A more detailed description of the xsection block can be found elsewhere [\[57\]](#).

Listing 5.1: Example decay table for the three body decays $\tilde{g} \rightarrow d\bar{d}\tilde{\chi}^0$ and $\tilde{g} \rightarrow u\bar{u}\tilde{\chi}^0$ with $BR = 50\%$

#	PDG	Width			
DECAY	1000021	1.00000000E+00			
#	BR	NDA	ID1	ID2	ID3
	0.50000000E+00	3	1000022	-1	1
	0.50000000E+00	3	1000022	-2	2

Listing 5.2: Example XSECTION table for gluino pair-production with $\sqrt{s} = 8$ TeV at NLO and NLL

XSECTION	8.00E+03	2212	2212	2	1000021	1000021	# Nevts: 10000
0 0 0 0 0 0		7.84569100E-04	SModelS	v1.0.3			
XSECTION	8.00E+03	2212	2212	2	1000021	1000021	# Nevts: 10000
0 2 0 0 0 0		2.12775140E-03	SModelS	v1.0.3			

To calculate the mass spectrum and the decay table for the SLHA file a wide range of public codes are available, e.g. SOFTSUSY [58], SUSY-HIT [59] and SPheno [60]. The cross section blocks can be computed by using SModelS's internal cross section computer, which uses Pythia 6.4.27 [61] for calculation of σ at LO. If an MSSM model is decomposed into its signal topologies the precision of σ for QCD produced sparticles has to be increased. For squarks and gluinos this can be done using NLL-fast versions 1.2 and 2.1 [62] (see also [63–69]).

For the generation of the signal topologies and the calculation of $(\sigma \times BR)$ the production cross section σ from the cross section block and the corresponding branching ratios BR from the decay table are used. The mass vector for each signal topology can be built from the mass block. Finally all signal topologies with $(\sigma \times BR)$ below a given value are discarded to speed up the decomposition. This value can be set by the user by setting the variable *sigmacut*. The default value for *sigmacut* is 0.03 fb.

Compression

The decomposition can lead to a great number of more or less complex signal topologies. It is possible, that some of them include decays which are not recognisable in the experiment, e.g. $\tilde{\chi}_2^0 \rightarrow \nu\bar{\nu}\tilde{\chi}_1^0$. In order to eliminate undetectable decays or to reduce the complexity of the signal topology spectrum the signal topologies can be compressed. Within SModelS there are two possible compression processes as described below.

invisible compression: If the last decay of a cascade decay includes invisible particles only, it is discarded. For explanation the T5WW example shown in Figure 5.2 is used. The $\tilde{\chi}^\pm$ can also decay into a $\tilde{\chi}_2^0$ instead of a $\tilde{\chi}_1^0$. The $\tilde{\chi}_2^0$ can further decay by an off-shell Z into $\nu\bar{\nu}$ and the $\tilde{\chi}_1^0$. This last decay includes invisible decay products only and therefore it is discarded. The LSP mass of the corresponding signal

topology in this example is then given by $m_{\tilde{\chi}_2^0}$ instead of $m_{\tilde{\chi}_1^0}$.

mass compression: If two contiguous masses m_i and m_{i+1} in the mass vector are very close to each other the decay $i \rightarrow i + 1$ leads to very soft SM final states. As a show case scenario again a $\tilde{\chi}_2^0$ decaying to an off-shell Z and $\tilde{\chi}_1^0$ is considered, where the off-shell Z is now assumed to decay into $\ell\bar{\ell}$. The leptons are detectable particles but if $m_{\tilde{\chi}_2^0} \sim m_{\tilde{\chi}_1^0}$ their energy might be negligible for all experimental purposes. All decays with $m_{i+1} - m_i$ below a threshold value are discarded by SModelS. This threshold can be set by the user via the variable *minmassgap*. The default value for *minmassgap* is 5 GeV.

5.1.4 Confronting a Full Model with Experimental Results

After the decomposition and compression the model point is given as a spectrum of signal topologies, each of which is described by the constraint, the mass vector and the weight $(\sigma \times BR)$. On the experimental side the topologies for each result are also described by the constraints, whereas $(\sigma \times BR)_{UL}$ for each result is given by the upper limit map. The last remaining step is to confront $(\sigma \times BR)$ of the signal topologies with $(\sigma \times BR)_{UL}$ from the results stored in the database.

Topologies compatible with a signal topology can be identified in the database by their constraints. As mentioned above a signal topology can contribute to more than one topology. Therefore the signal topologies have to be combined, meaning that the individual $(\sigma \times BR)$ are summed up to $(\sigma \times BR)_{theory}$. Every combination for which the value of the fuzzycondition (cf. [subsection 5.1.1](#)) exceeds the value given by *maxcondition* is discarded.

The $(\sigma \times BR)_{UL}$ for the different topologies in the database are stored as upper limit maps. As described in [subsection 4.2.3](#) each topology can be associated with a mass space and upper limit maps are defined in mass planes. For topologies including only one-step decays only one upper limit map is needed to define all $(\sigma \times BR)_{UL}$ in the associated mass space. In this case $(\sigma \times BR)_{theory}$ can directly be compared to $(\sigma \times BR)_{UL}$.

Topologies including cascade decays are defined in a mass space with three dimensions. In this case for each pair of analysis and topology at least two upper limit maps, defined in different mass planes, are needed. In order to compare $(\sigma \times BR)_{theory}$ with $(\sigma \times BR)_{UL}$, SModelS interpolates between the mass planes.

Excluding Model Points

For each combination of analysis and topology in the database the *r*-value (cf. [Equation 5.1](#)) is computed. If at least one *r*-value is greater than one, the model point is excluded. The output of SModelS is given as a text file called *summary.txt*. This file lists the *r*-values and the associated analyses and topologies used to obtain these *r*-values.

$$r = \frac{(\sigma \times BR)_{theory}}{(\sigma \times BR)_{UL}} \quad \begin{cases} r > 1 & \text{model point is excluded by this analysis} \\ r < 1 & \text{model point is not excluded by this analysis} \end{cases} \quad (5.1)$$

Finding Unchallenged Parameter Space

In order to find regions of the parameter space which are so far unchallenged by the experiments SModelS's missing topology tool is used. The missing topologies refer to the signal topologies for which no associated topology could be found in the database. The weight for each missing topology is a sum over all signal topologies described by the same constraints independent of the mass vector. In the *summary.txt* up to ten such missing topologies are listed according to their weights.

5.2 Validation of the SModelS Database

SModelS v1.0.3 is shipped together with a database comprising validated results from ATLAS and CMS SUSY searches. During the development of SModelS 230 results from 98 analysis were collected and stored in an internal database. For each result the implementation in the database and its applicability to SModelS was validated within the scope of this thesis. Therefore SModelS was used to reproduce the official exclusion lines given by the experimentalists. Each reproduced exclusion line was plotted together with the official exclusion line. These plots are called validation plots. Only results showing a very good agreement between the official exclusion line and the reproduced one were incorporated into the public SModelS database. The validation procedure is described in [subsection 5.2.1](#). The outcome of the database validation is discussed in [subsection 5.2.2](#) and [subsection 5.2.3](#).

5.2.1 Validation Procedure

In order to produce validation plots for the huge amount of results in the database a computational working environment was needed. [Figure 5.3](#) depicts the working scheme of this environment. In the first step a template SLHA-file for each topology was created by hand. This template file reflected exactly the assumptions for the topology, made by the experimentalists. For each topology at least one or more mass planes are available in the database. The template SLHA-file was used to create a set of SLHA-files for each of these mass planes. Each file of a set represents a point in the respective mass plane. Such a point in the mass space is also called *mass point*. The SLHA-files were passed to SModelS to derive $(\sigma \times BR)_{theory}$ and to retrieve $(\sigma \times BR)_{UL}$ from the database for each mass point. This information was stored in a grid data file. In the last step the r -value for each point was computed in order to derive the exclusion line. This exclusion line together with the official exclusion line was used to create a validation plot. Some example validation plots are shown and discussed in [subsection 5.2.2](#).

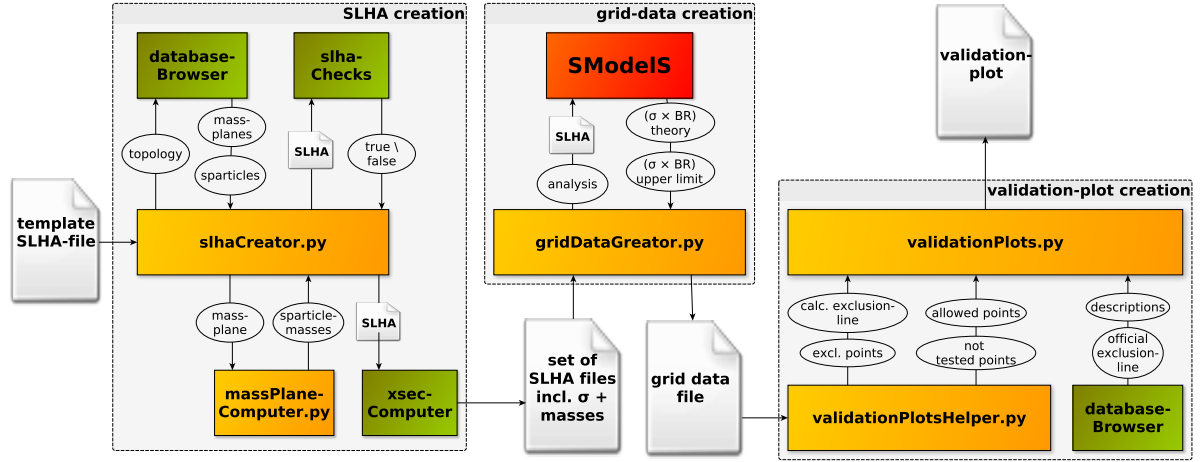


Figure 5.3: Scheme of the work flow used to create the validation plots. Python modules exclusively written for the validation are depicted in orange. Green boxes depict modules from the smodels/tools or smodels-utils packages used by the validation code. The arrows symbolize the transfer of information and files between the modules

Obviously this procedure requires access to the database. Therefore the package `databaseBrowser` was used. It is an object oriented python page which allows a fast and convenient access to the SModelS database. Furthermore it provides additional information about the topologies and analyses comprised in the database e.g. sparticles included in a certain topology. A more detailed description of the `databaseBrowser` can be found elsewhere [70].

In order to validate the complete database, the identification of potential off-shell results was a vital requirement for the design of the computational working environment. The meaning of an off-shell result and the particular steps of the validation procedure are described in more detail below.

Off-shell results

An off-shell result is a result containing $(\sigma \times BR)_{UL}$ for an off-shell topology. As discussed in subsection 5.1.1 an off-shell topology includes off-shell SM particles. Depending on the difference of the masses of the sparticles in a given vertex the SM particles involved can be either on- or off-shell. Hence, the same decay process can either be described by an on- or off-shell topology as the masses vary.

Within SModelS on- and off-shell topologies have to be described by different constraints (cf. subsection 5.1.1). Therefore, for each upper limit map, as given by the experimentalists, it has to be checked if there is an off-shell region. If so, the upper limit map has to be split into two maps: one which contains only $(\sigma \times BR)_{UL}$ for the on-shell topology and the other one for the off-shell topology. The off-shell upper limit map together with the off-shell topology represents the off-shell result.

This so called “splitting” was not done for most of the results comprised in the database when the validation started. Therefore the identification of off-shell regions and the splitting of the results were vital issues during the validation process. It was done during the SLHA creation for the validation plots. The process of creating the SLHA files is described below.

Creation of SLHA Files

The SLHA based decomposition of SModelS was used for the validation. Therefore SLHA files including a mass block, a decay table and an cross section block were needed. As depicted in [Figure 5.3](#) the main module used to create these files was the module `slhaCreator.py`. The creation included several steps:

creating a template SLHA file: First, one template SLHA file for each topology was produced by hand. This file had to reflect the production modes, decays and branching ratios of the topology in question. Therefore only decays described by the topology and their BR were written into the decay table of the file. Separate files with different decay tables were produced for on-shell and off-shell topologies.

As pointed out in [subsection 4.1.1](#) the electroweak production of sparticles depends on their mixing. The SLHA file standard includes so-called mixing blocks to define the mixing of the sparticles. For topologies assuming electroweakly produced sparticles, e.g. neutralinos, the mixing blocks for the sparticles had to be defined. The mixing used for different sparticle production modes is described in [subsection 5.2.2](#).

setting the masses: In the next step the mass table was set and the upper limit maps were split into on-shell and off-shell regions, if necessary. As mentioned in [subsection 5.1.2](#) the upper limit maps are stored in the database. The database contains upper limit maps derived by using different slicing methods. Each upper limit map can be seen as defined in a mass plane given by the slicing method. For one mass plane the database can contains more than one upper limit map. Initially some of these upper limit maps contained on- and off- shell regions and had to be split during the validation.

The `databaseBrowser` was used to collect all mass planes from the database for the topology in question. Each mass plane was passed to the module `massPlaneComputer.py`. This module compared all upper limit maps from the database defined in this mass plane. A mass range which included the mass ranges of all upper limit maps was computed. Then a set of mass points which covered the whole mass range, regardless of the kinematic conditions, was produced.

This set of mass points was passed to the module `slhaCreator.py`. This module created one SLHA file for each mass point in the given set. These SLHA files

were based on the on-shell template SLHA file for the respective topology. The sparticle masses inside the mass block of each file were set to the values given by the respective mass point. All other sparticle masses were decoupled by setting their values to 10^5 GeV. This procedure was repeated for all mass planes of the topology leading to one set of SLHA files for each mass plane.

Since during the computation of the mass range for the SLHA files we did not distinguish between on- and off-shell regions, one set could contain both kinematic regions. Therefore all files with mass configurations of off-shell decays had to be removed from the sets related to the on-shell topology.

To identify these SLHA files the class `SlhaStatus` from the modul `slhaChecks.py` was used. Each SLHA file was passed to an instance of this class. It used the mass block and the decay tables to identify the files describing kinematical forbidden decays. These SLHA files were deleted and the respective upper limit maps were split. Finally the procedure described above was repeated using the off-shell upper limit maps and the template file for the off-shell topology, leading to SLHA sets for the off-shell topology.

calculating the production cross section: In the last step the SLHA files were passed to the internal SModelS cross section computer. All production cross sections were computed at LO order using Pythia 6.4.27 [61] with 10^4 events. The precision of the production cross sections for squarks and gluinos was further increased using NLL-fast [62].

Each set of SLHA files were finally stored in a directory. The topology and the mass plane to which the set belongs is indicated by the name of the directory as well as by the name of the SLHA files.

Creation of Grid data Files

In the next step grid data files were produced. These files hold all information necessary for the production of a validation plot. The creation of grid data files is depicted in the centre of [Figure 5.3](#). Each grid data file represented exactly one result. Therefore SModelS was restricted to the respective analysis. Due to the fact that the SLHA files reflect directly the topology in question, the mass compression and the invisible compression was turned off. The variable *sigmacut* was set to a value close to zero (10^{-5} fb).

The cross section for topologies assuming electroweak production of sparticles were only calculated at LO, whereas the production cross sections used to derive the official exclusion lines are mostly calculated at NLO. Therefore the production cross section for neutralinos, charginos and sleptons were increased by a k-factor of 1.2.

The module `gridDataCreator.py` was used to identify the correct set of SLHA files, associated to the result in question. For each mass point SModelS SLHA based decomposition was used to calculate $(\sigma \times BR)_{theory}$. During this process the computing time

necessary for the decomposition of each file was monitored. SModelS was also used to retrieve $(\sigma \times BR)_{UL}$ from the database.

The sparticle masses, $(\sigma \times BR)_{theory}$ and $(\sigma \times BR)_{UL}$ for each mass point were written to the grid file by the module `gridDataCreator.py`. If SModelS was not able to find $(\sigma \times BR)_{UL}$ for a mass point the entry was set to “None”. In addition the value associated with the violation of the conditions (cf. [subsection 5.1.1](#)) was also written to the file. Due to the nature of the used SLHA files, this value was expected to be very close to zero. Finally the grid files for each result were stored for further usage.

Creation of Validation Plots

The final creation of the validation plots is depicted at the right of [Figure 5.3](#). The modules `validationPlotsHelper.py` and `validationPlots.py` are used. The `validationPlotsHelper.py` used the grid data file for a certain result to compute the r -value. According to this r -value the mass points from the grid data file were sorted into excluded and not excluded points. All mass points for which no $(\sigma \times BR)_{UL}$ was available were marked as “not tested”. The exclusion line was computed by using the shape of the region defined by the excluded points. The excluded, not tested and not excluded points together with the exclusion line were passed to the module `validationPlots.py`. To get the official exclusion line from the database as well as information about the result, e.g. centre-of-mass energy, the `databaseBrowser` was used. The module `validationPlots.py` used all this information to create the final validation plot for the result in question. [Figure 5.4](#) shows an example validation plot for the topology T1 from CMS-SUS-13-012 [\[47\]](#) in the \tilde{g} - $\tilde{\chi}_1^0$ mass plane.

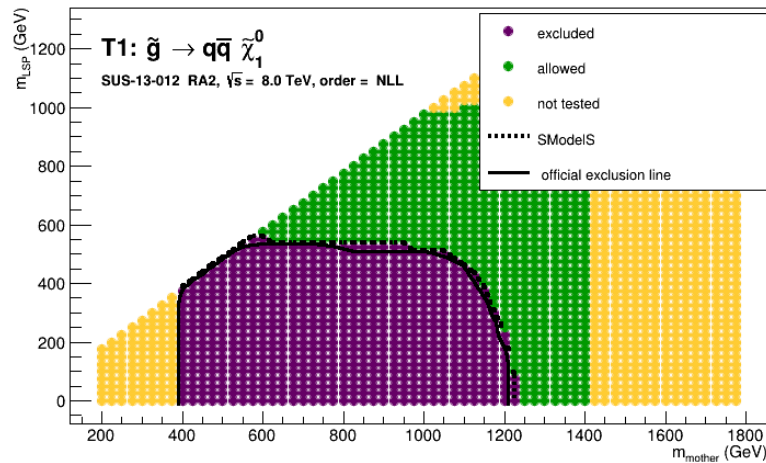


Figure 5.4: Validation plot for the topology T1 from CMS-SUS-13-012 [\[47\]](#).

5.2.2 Discussion of Results

Out of the 230 results comprised in the database 174 results were validated. The number of results was mainly reduced by focusing on results obtained with a centre-of-mass energy of $\sqrt{s} = 8$ TeV. Furthermore only topologies describing one- or two-step decays were taken into account. Due to the vast amount of 174 results only a few example results shall be discussed below.

Strong Production

Gluinos and squarks might be produced by the strong interaction as discussed in [subsection 4.1.1](#). The production cross section σ for strongly produced sparticles depends on their masses only. Therefore the mixing blocks of the SLHA files have no influence on the production cross sections, which were calculated at LO and NLL precision.

It is assumed that sparticle production via strong interaction is dominant at the LHC. Therefore the most frequent results in the database assume the production of squarks and quarks. Below, the validation of some of these results is discussed.

T1tttt: The topology T1tttt describes pair-produced gluinos decaying via $\tilde{g} \rightarrow t\bar{t}\tilde{\chi}_1^0$. Validation plots for 18 results based on this topology were produced. All of them showed a good agreement between the official exclusion line and the one based on SModelS. The upper limit maps of 7 of these results included off-shell regions. According to the procedure described in [subsection 5.2.1](#) these upper limit maps were split and separate validation plots for the off-shell topologies were produced. [Figure 5.5](#) shows the validation plots for T1tttt and T1ttttoff from CMS-SUS-13-007 [22].

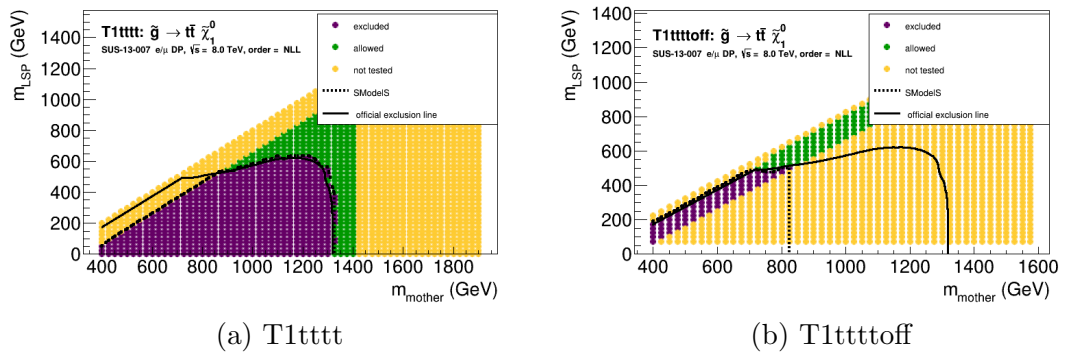
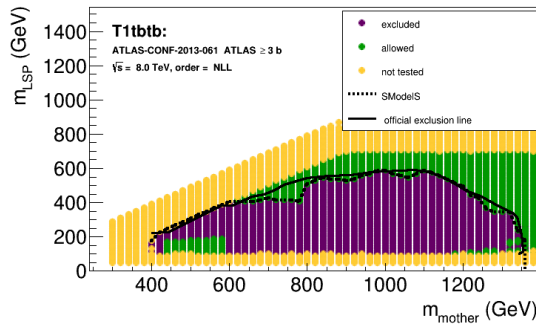


Figure 5.5: Validation plots for the T1tttt result from CMS-SUS-13-007 [22] for the on-shell regime (T1tttt) and off-shell regime (T1ttttoff)

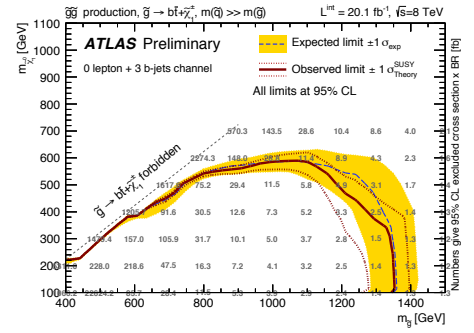
T1btbt: The topology T1btbt is an example for a less common topology. There are only two analyses (ATLAS-CONF-2013-007 [39] and ATLAS-CONF-2013-061 [41]) in the database providing interpretations in terms of this topology. It is defined

by the decay $\tilde{g} \rightarrow t\bar{b}\tilde{\chi}^\pm \rightarrow t\bar{b}(W^*\tilde{\chi}^0)$. Here, $m_{\tilde{\chi}_1^0} \approx m_{\tilde{\chi}_1^\pm}$ is assumed, leading to a very soft off-shell W boson which is not recognisable by the experiment. To validate this topology $(m_{\tilde{\chi}_1^\pm} - m_{\tilde{\chi}_1^0})$ was set to 3 GeV in each SLHA file. In contrast to the computation of $(\sigma \times BR)_{theory}$ for all other results, SModelS's mass compression was turned on. The variable *minmassgap* was set to its default value of 5 GeV. Thus the cascade decay was compressed to a direct, one-step decay by SModelS, matching the assumption of the experiment.

Figure 5.6a shows the validation plot for ATLAS-CONF-2013-061. This result is a good example for the discussion of another issue which occurred during the validation. Some exclusion plots show regions of not excluded points inside the official excluded region. This can be explained by fluctuations of $(\sigma \times BR)_{UL}$ in the upper limit map. Figure 5.6b shows the official upper limit map and exclusion lines from ATLAS-CONF-2013-061. As one can see there is a preponderance of one order of magnitude for the values of $(\sigma \times BR)_{UL}$ near the kinematic edge above all other values. This leads to an under-exclusion in the region close to the point $[m_{\tilde{g}} \approx 750 \text{ GeV}, m_{\tilde{\chi}_1^0} \approx 425 \text{ GeV}]$ in the validation plot. The allowed region near the point $[m_{\tilde{g}} \approx 500 \text{ GeV}, m_{\tilde{\chi}_1^0} \approx 100 \text{ GeV}]$ originated from the fact that $(\sigma \times BR)_{UL}$ in this point is two magnitudes higher than the values for all surrounding points. Both T1tbtb results showed a rather poor agreement of the region excluded by SModelS and the official excluded region.



(a) Validation Plot



(b) Official upper limit map

Figure 5.6: Validation plot (a) and official upper limit map (b) for T1tbtb from ATLAS-CONF-2013-061 [41]. The deviations of the region excluded by SModelS and the official excluded region shown in (a) can be explained by fluctuations of $(\sigma \times BR)_{UL}$ shown in (b)

T6bbWW: This topology is defined by the decay $\tilde{t} \rightarrow b\tilde{\chi}^\pm \rightarrow b(W\tilde{\chi}_1^0)$. The database contains T6bbWW results from 11 different analyses. These analyses comprise upper limit maps in many different mass planes, most of them including off-shell regions. None of these upper limit maps were initially split. The large number of used mass planes made this splitting into on- and off-shell region very lavish.

As an example the $\tilde{b} - \tilde{\chi}_1^0$ – mass plane with the “x-value” slicing method (cf. subsection 4.2.3) is considered. This slicing method defines the mass of the intermediate particle m_{int} according to Equation 5.2. In the case of T6bbWW the intermediate particle is a chargino and therefore $m_{int} \equiv m_{\tilde{\chi}_1^\pm}$. The mass of the mother particle in this topology is equivalent to $m_{\tilde{b}}$ and $m_{LSP} \equiv m_{\tilde{\chi}_1^0}$.

$$m_{int} = x \cdot m_{mother} + (1 - x) \cdot m_{LSP} \quad (5.2)$$

In principle the kinematic edge for the T6bbWW topology containing an off-shell W boson is defined by: Equation 5.3.

$$m_{int} = m_W + m_{LSP} \quad (5.3)$$

Figure 5.7b shows the validation plot for a T6bbWW topology from CMS-SUS-13-011 [25] in the $\tilde{b} - \tilde{\chi}_1^0$ – mass plane with $x = 0.25$. This x-value can be inserted into Equation 5.2. Together with Equation 5.3 this leads to the Equation 5.4 for the kinematic edge in the $\tilde{b} - \tilde{\chi}_1^0$ – mass plane with $x = 0.25$.

$$m_{LSP} = m_{mother} - 4 \cdot m_W \quad (5.4)$$

The kinematic edge in Figure 5.7b is depicted as the edge between the excluded and not tested points.

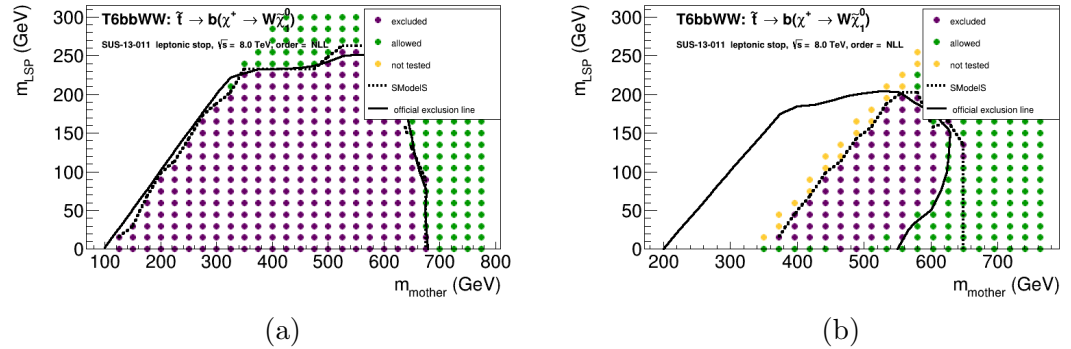


Figure 5.7: Validation plots for T6bbWW from CMS-SUS-13-011 [25] in the $\tilde{b} - \tilde{\chi}_1^0$ – mass plane for $x = 0.75$ (a) and $x = 0.25$ (b). Both figures show on-shell mass points only. The official exclusion line in (b) includes also the off-shell region. The differences between the region excluded by SModelS and the official one at $m_{mother} \sim 650$ GeV is due to the statistical uncertainties of the calculation of the production cross section σ .

Each slicing method leads to a different equation for the kinematic edge in the respective mass plane. Therefore the splitting of the upper limit maps, which are defined in many different mass planes, is very lavish and time consuming and was not done for every result.

Out of all results, for which the kinematic regions were checked and the upper limit maps were split if necessary, 16 results from 5 different analyses could be validated successfully. Besides the problem of the kinematic regions, the number of successful validations was reduced because of fluctuations in the upper limit maps. Moreover, for the production of a validation plot the official exclusion line has to be available in a machine-readable format, which was not the case for all results.

The 5 analyses which were successfully validated are: ATLAS-CONF-2013-037 [71], ATLAS-CONF-2013-048 [24], ATLAS-SUSY-2013-19 [37], ATLAS-CONF-2013-065 [42] and CMS-SUS-13-011 [25]. Figure 5.7 shows two validation plots for CMS-SUS-13-011.

T6ttWW: This topology is very similar to T6bbWW, it describes pair-produced \tilde{b} decaying via $\tilde{b} \rightarrow \tilde{t}\tilde{\chi}^\pm \rightarrow b(W\tilde{\chi}_1^0)$. It shall only be mentioned to demonstrate another problem linked to the splitting of the upper limit maps into on-shell and off-shell regions.

The W boson as well as the top quark are very heavy. Therefore both decays $\tilde{b} \rightarrow \tilde{t}\tilde{\chi}^\pm$ and $\tilde{\chi}^\pm \rightarrow W\tilde{\chi}_1^0$ have large off-shell regions. This leads to three different off-shell regimes, where either one of them or both are off-shell. These three regimes are described by different signal topologies by SModelS's decomposition. Currently, the naming convention for off-shell topologies is not suitable to handle more than one off-shell regime.

Electroweak Production

Neutralinos, charginos, and sleptons might be produced at the LHC by the electroweak interaction (cf. subsection 4.1.1). Out of the 174 validated results only 38 results included electroweakly produced sparticles. The production cross sections of these sparticles are mainly defined by their mixing. To get the same σ as used by the experimentalists to compute the official exclusion lines, the same mixing has to be used for the validation. The settings for this mixing are explained below and the respective blocks of the SLHA files are shown in Listing 5.3.

neutralinos: While the $\tilde{\chi}_1^0$ is assumed to be a bino, the $\tilde{\chi}_2^0$ has equal admixtures from wino and higgsino. The $\tilde{\chi}_3^0$ and $\tilde{\chi}_4^0$ are assumed to be higgsinos. Both have equal admixtures from \tilde{H}_D^0 and \tilde{H}_U^0 . The mixing block used in the SLHA files is depicted in Listing 5.3 on the left.

- charginos:* The $\tilde{\chi}_1^\pm$ are assumed to be winos and the $\tilde{\chi}_2^\pm$ are assumed to be higgsinos. The mixing blocks associated with the chargino mixing are shown in [Listing 5.3](#), indicated with “BLOCK UMIX” and “BLOCK VMIX”
- stau:* The $\tilde{\tau}_1$ is assumed to be purely LH and the $\tilde{\tau}_2$ purely RH. The related mixing block in the SLHA files is called “BLOCK STAUMIX” and is also shown in [Listing 5.3](#).

Listing 5.3: Mixing blocks used in the SLHA files for electroweak production of sparticles

BLOCK NMIX			BLOCK UMIX		
1	1	-1.00000000e+00	1	1	-1.00000000e+00
1	2	0.00000000e+00	1	2	0.00000000e+00
1	3	0.00000000e+00	2	1	0.00000000e+00
1	4	0.00000000e+00	2	2	-1.00000000e+00
2	1	0.00000000e+00	BLOCK VMIX		
2	2	-1.00000000e+00			
2	3	-1.00000000e+00			
2	4	0.00000000e+00			
3	1	0.00000000e+00			
3	2	0.00000000e+00			
3	3	-7.07000000e-01			
3	4	-7.07000000e-01			
4	1	0.00000000e+00	BLOCK STAUMIX		
4	2	0.00000000e+00			
4	3	-7.07000000e-01			
4	4	7.07000000e-01			
			1	1	1.00000000e+00
			1	2	0.00000000e+00
			2	1	0.00000000e+00
			2	2	1.00000000e+00

Due to the fact that the official exclusion lines for the results based on electroweak sparticle productions were calculated with NLO precision, the LO production cross sections obtained from Pythia 6.4.27 [61] were increased by a k-factor of 1.2. It shall also be mentioned again, that the decay tables were written into the SLHA files by hand. Therefore the nature of the sparticles did affect the cross sections exclusively but not the BR of the decays.

The validation for most of the results including electroweak topologies showed a very good agreement between the official exclusion line and the one obtained by using SModelS. Out of 38 results 30 could be validated successfully. [Figure 5.8](#) show two example validation plots for the topology TChiChipmSlepStau from CMS-SUS-13-006 [46]. All analyses and topologies which led to a successful validation plot can be found in [Table 5.1](#).

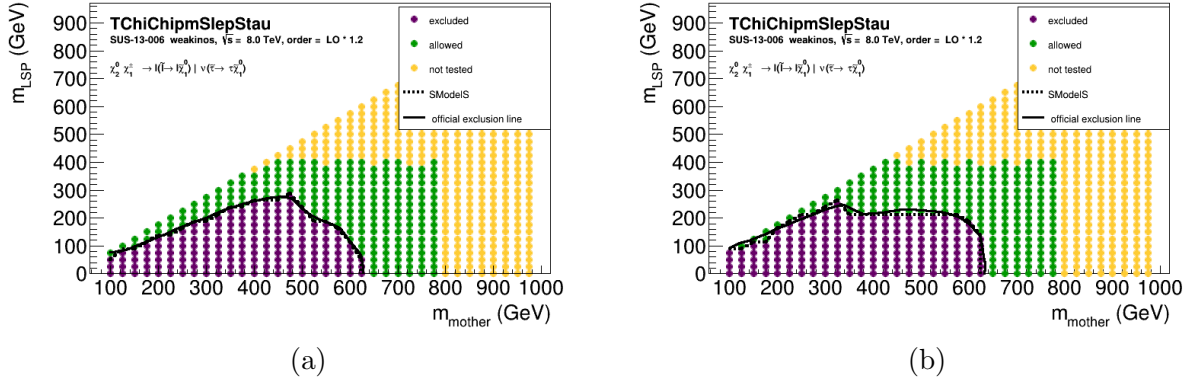


Figure 5.8: Validation plots for TChiChipmSlepStau from CMS-SUS-13-006 [46] in the $\tilde{\chi}_2^0/\tilde{\chi}_1^\pm-\tilde{\chi}_1^0$ mass plane for $x = 0.95$ (a) and $x = 0.50$ (b).

5.2.3 Conclusion

The outcome of the database validation was used to build a public database, which was shipped together with SModelS v.1.0 and all later versions. Some major problems which occurred during the validation procedure were already mentioned in [subsection 5.2.2](#). These problems are summarized below.

- $(\sigma \times BR)_{UL}$ are stored as upper limit maps inside the database. The upper limit maps are given in many different mass planes and some of them contain off-shell regions. The vast number of different mass planes made it nearly unfeasible to split all upper limit maps according to their on- and off-shell regions.
- The SM particles in each vertex of a topology can be off-shell. This can lead to different off-shell regions in the respective upper limit maps defined by different off-shell SM particles. Currently there is no common approach to define more than one off-shell region for a given topology.
- There is no plausibility check of the data when a result is implemented to the database. This can lead to incorrect entries in the database. During the validation most of these errors in the database could be corrected. Nevertheless this manual correction was very time consuming and tedious.
- Fluctuations in the upper limit maps as given by the experimentalists can lead to problems in the interpolation and therefore cause the validation to fail.
- The validation was based on the comparison of an exclusion line obtained by using SModelS and the official exclusion line. Therefore it was necessary to get the official exclusion line in a machine-readable format, e.g. ROOT.TGraph objects. For some results the exclusion line was not available in such a format. These results could not be validated.

After the validation procedure was applied to all results comprised in the unofficial database, a public database for the release of SModelS was built. Only results which passed the validation without problems were used for the public database.

For topologies involving cascade decays, SmodelS needs at least two results from the same analysis in order to interpolate $(\sigma \times BR)_{UL}$ for mass points outside the given mass planes. Therefore analyses which provide only one result for such a topology are not considered in the public database. [Table 5.1](#) in [subsection 5.1.2](#) lists all analyses and topologies in the public database. It contains 62 results from 26 CMS and ATLAS analyses.

Chapter 6

The New SModelS-Database

The validation discussed in [section 5.2](#) revealed weaknesses of the SModelS database, e.g. identification of off-shell regions within the upper limit maps. In addition a new version of SModelS is being developed, while this thesis is written. This new version will use $(\epsilon \times A)$ to calculate $(\sigma \times BR)_{UL}$ and constrain BSM models. The “old” database as used for the validation did not include information about $(\epsilon \times A)$.

Based on the findings of the validation a data standard for a newly structured database, including $(\epsilon \times A)$, was developed. For the implementation of results to the new database an object orientated computational framework - the package `dataPreparation` - was built. It provides python objects to convert the information as given by the experimentalists, e.g. ROOT files containing upper limit maps as ROOT.T2HF objects, into the new data standard.

The development of the new database and the computational framework is motivated in [section 6.1](#). The new data standard and the structure of the database are explained in [section 6.2](#). Eventually, a description of the functionalities of the `dataPreparation` as well as detailed guidelines for its usage for the implementation of new analyses are given in [section 6.3](#).

6.1 Motivation

The development of the new SModelS database was driven by the problems appearing during the validation and the requirements of the new SModelS version, which will be released at the end of this year. The most important problems and their solutions within the new database are discussed below.

Implementation of Data

The SModelS database comprises of information given by ATLAS and CMS analyses, which contain SUSY search results interpreted in terms of various SMS topologies. Each analysis comprises of information about the collected proton-proton collision data and

its interpretation. With respect to the SModelS database this information, given by an analysis, is structured as follows.

analysis related information: Information about the whole analysis valid for all topologies comprised in the analysis. Examples are the corresponding centre-of-mass energy (\sqrt{s}) and the integrated luminosity of the underlying proton-proton collision data.

topology related information: Information related to one topology only. Obviously, one important information about a topology is its name. In [subsection 4.2.2](#) the naming convention for SMS topologies used by SModelS was introduced. Unfortunately, there are analyses which do not follow this convention. Therefore the decays and production modes are of interest. They can be used to identify a topology, link it to the associated name within SModelS and to construct the constraints.

Furthermore, the analysis event selection, e.g. events with jets and a pair of isolated, same-sign leptons, is an important information. In principle, this is an analysis related information. However, it can be seen as topology related information, since the event selection can influence the constraints and conditions (cf. [subsection 5.1.1](#)) of a topology.

mass plane related information: As discussed in [subsection 4.2.3](#), the outcomes of the interpretation of search results in terms of a topology are summarised in two-dimensional plots, e.g. upper limit maps. The information given in such a plot can be seen as related to one specific mass plane, i.e. a slice through the mass space defined by the masses of the involved BSM particles. For each topology, information can be given in many different mass planes. Each mass plane is determined by the sparticle masses on the x- and y- axis of the respective plot and by the slicing method used. The following information is presented in such two dimensional plots and therefore assigned to the respective mass plane:

- $(\epsilon \times A)$ given as efficiency maps. One efficiency map for each signal region is given by the analysis.
- $(\sigma \times BR)_{UL}$ given as upper limit maps. Most analyses contain two different upper limit maps, one observed and one expected upper limit map (cf. [subsection 4.2.3](#)).
- For each mass plane the observed exclusion lines without theoretical uncertainties (σ_{theor}) and with $\pm 1\sigma_{theor}$ are given. Also the expected exclusion lines without experimental uncertainties (σ_{exp}) and with $\pm 1\sigma_{exp}$ are given. This leads to six exclusion lines for each mass plane.

All this information has to be transformed into the data standard used in the SModelS database. The upper limit maps, for example, are given in many different data formats

(e.g. ROOT.TH2F objects or text files) and have to be standardized. Another example was already mentioned: the decays, which define a topology and the event selection are used to construct the constraints and conditions.

In the old database the process of data implementation was poorly standardized and no automatized quality checks of the data were performed. Therefore the `dataPreparation` package was developed. It provides python objects for a simple and standardized implementation of data to the new database, as well as plausibility checks of the data.

Documentation of Data

In order to implement information about $(\epsilon \times A)$, $(\sigma \times BR)_{UL}$ and the exclusion lines into the database, this information must be given in some machine-readable data format. Unfortunately, this is not the case for all analyses. The enormous amount of 230 results from 98 different analyses comprised in the old database made it complicated to get a quick overview of the information available for each result. Therefore a web page on the SModelS wiki server [27] was created. This web page allows to get such an overview. To keep the page up-t-date, each time a new analysis is implemented, the `dataPreparation` package creates a file containing an HTML-string. This string can be uploaded to the wiki page. Figure 6.1 shows two example entries on this wiki page.







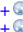






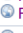
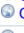

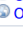

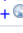
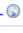

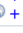






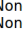









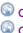





publication/pas	txname	axes (plot information)	Figure	upper limits on production cross sections	efficiency maps	exclusion lines
 CMS-SUS-13-004	T1bbbb	Eq(mother,x)_Eq(lsp,y)	 Figure 12	 OBS  EXP	None	 OBS  +  -  OBS  +  -  EXP  +  -
	T2tt	Eq(mother,x)_Eq(lsp,y)	 Figure 13	 OBS  EXP	None	 OBS  +  -  OBS  +  -  EXP  +  -
	T1tttt	Eq(mother,x)_Eq(lsp,y)	 Figure 14	 OBS  EXP	None	 OBS  +  -  OBS  +  -  EXP  +  -
 CMS-SUS-13-007	T1tttt	Eq(mother,x)_Eq(lsp,y)	 combLimit_T1tttt_b.pdf	 OBS	None	None
	T5tttt	Eq(mother,1000.0)_Eq(inter0,x)_Eq(lsp,y)	 combLimit_T1t1t_b.pdf	 OBS	None	None
	T5tttt	Eq(mother,x)_Eq(inter0,y)_Eq(lsp,50.0)	 combLimit_T5tttt_b.pdf	 OBS	None	None

Figure 6.1: Entries for CMS-SUS-13-004 [72] and CMS-SUS-13-007 [22] on the SModelS wiki page. For each analysis the available topologies and mass planes are listed. The column “Figure” includes the links to the original plots as given by the analysis. Additionally the links to the original data for the upper limit maps, the efficiency maps and exclusion lines are given if available in machine-readable format.

On-shell and Off-shell results

As mentioned in subsection 5.2.1, a result given by the experimentalists can comprise of different kinematic regions. When implementing the results of an analysis into the old database, the kinematic regions comprised in each upper limit map had to be checked manually. Since the kinematic edge looks different for each mass plane, this check is not trivial.

Therefore, a procedure for an automatised recognition of different mass regions was implemented into the `dataPreparation`. It checks the upper limit maps and writes one separate entry for each kinematic region comprised in the upper limit map, into the database.

In contrast to the procedure described in [section 5.2](#), the upper limit maps are no longer split with respect to the kinematic regions. Considering the working procedure of SModelS, as described in [section 5.1](#), this splitting is not necessary. SModelS’ decomposition leads to a signal topology described by an on-shell constraint, only if the underlying model point includes the respective on-shell decay. Furthermore, SModelS keeps the masses for this signal topology as a mass vector. Therefore off-shell $(\sigma \times BR)_{UL}$ included in the respective on-shell topology will be ignored. The same argumentation is true for the off-shell case. Therefore, the entry for the on-shell topology as well as the one for the off-shell topology holds the values of $(\sigma \times BR)_{UL}$ for all masses regardless of the kinematic region and the underlying mass plane.

Upper Limit on $(\sigma \times BR)$

The old database held the $(\sigma \times BR)_{UL}$ for each upper limit map as a nested python dictionary. Each dictionary held $(\sigma \times BR)_{UL}$ corresponding to the x- and y- axes of the upper limit plot, as given by the experimentalists. In order to compute the mass vectors, as used by SModelS, a second database entry, called “axes”, was needed. This second entry defined the mass plane related to the upper limit map, by linking the values for x and y, as stored in the python dictionary, to the BSM particles and defining the slicing method. This information allowed SModelS to compute the respective mass vectors (cf. [subsection 5.1.1](#)).

The “axes” entries were written by hand to the database. To link the “axes” to the python dictionary a labelling system was used. The label for each dictionary was also set by hand. These procedure was highly prone to errors. Furthermore, this data structure demanded a complicated read-out procedure of $(\sigma \times BR)_{UL}$ as encountered during the validation.

The new database no longer contains upper limit maps as python dictionaries. Instead, the upper limits are now stored in lists. These upper limit lists contain all mass vectors for which a value of $(\sigma \times BR)_{UL}$ is available, regardless of the upper limit map it is given in. Hence, all the results for a topology given by an analysis are included in one upper limit list and SModelS no longer needs information about the respective mass planes.

[Listing 6.1](#) shows an example upper limit list for the topology T1tttt from CMS-SUS-12-024 [\[43\]](#). $(\sigma \times BR)_{UL}$ for each mass vector is given in picobarn (pb).

Listing 6.1: upper limit list for T1tttt from CMS-SUS-12-024 [\[43\]](#)

```
[[[400.0*GeV, 0.0*GeV], [400.0*GeV, 0.0*GeV]], 1.815773*pb],
[[[400.0*GeV, 25.0*GeV], [400.0*GeV, 25.0*GeV]], 1.806528*pb],
[[[400.0*GeV, 50.0*GeV], [400.0*GeV, 50.0*GeV]], 2.139336*pb],
.....
```

Efficiency times Acceptance

Currently a new version of SModelS is being developed. It involves a procedure to compute $(\sigma \times BR)_{UL}$ for given values of $(\epsilon \times A)$ and uses this information to constrain a full BSM model. For each pair of analysis and topology this new SModelS version needs the values of $(\epsilon \times A)$ for the different BSM particle masses and signal regions. Furthermore the number of observed events, the expected number of events from the SM background and its uncertainty for each signal region are needed.

In order to handle this new data, the structure of the old database was enhanced (cf. [section 6.2](#)). In analogy to the implementation of $(\sigma \times BR)_{UL}$, a list containing all values of $(\epsilon \times A)$ and the associated mass vectors is computed. For a given pair of analysis and topology several database entries - one for each signal region - are created. [Listing 6.2](#) shows an example efficiency list for a signal region defined by cuts on \cancel{E}_T and H_T plus 3 b-tagged jets for the topology $T1tttt$ from CMS-SUS-12-024 [\[43\]](#).

Listing 6.2: efficiency list for $T1tttt$ from CMS-SUS-12-024 [\[43\]](#)

```
[[[[600.0*GeV, 0.0*GeV], [600.0*GeV, 0.0*GeV]], 0.01209596121],
 [[600.0*GeV, 25.0*GeV], [600.0*GeV, 25.0*GeV]], 0.01212175183],
 [[600.0*GeV, 75.0*GeV], [600.0*GeV, 75.0*GeV]], 0.01275402104],
 .....]
```

Exclusion Lines

In order to produce validation plots (cf. [subsection 5.1.4](#)) and the CMS summary plots (cf. [section 4.3](#)) the official exclusion lines have to be stored in the database. They are given in various data formats by the experimentalists. The `dataPreparation` includes a procedure to convert the exclusion lines into a ROOT.TGraph objects and store them inside a ROOT.TFile.

In contrast to the upper limit maps and efficiency maps, the information about the mass plane, an exclusion line is given in, has to be kept. This information allows to plot the exclusion lines in their associated mass plane, as it is necessary for e.g. the validation plots. Hence, an axes entry is written into the database. This entry holds the same information as the axes entry in the old database, but it is created automatically during the implementation process controlled by the `dataPreparation` and is not used by SModelS, but is only used to produce the validation plots and the CMS summary plots.

In order to cure the problems discussed above and to prepare the database considering the inclusion of $(\epsilon \times A)$ and the implementation of the $\sqrt{s} = 13$ TeV results to come, a new structure was developed. This improved database structure will be described in the next section.

6.2 Database Structure

The new SModelS database is designed to hold all information needed by SModelS and to create the validation plots as well as the CMS summary plots. For each analysis this information is stored in a standardized data format inside four different files: *globalInfo.txt*, *sms.root*, *dataInfo.txt* and *txName.txt*. These standardized data files are created utilising the `dataPreparation` package (cf. [section 6.3](#)). It is used within the python scripts, to convert the original data given by the experimentalists (e.g. files containing upper limit maps) into the database standard. These scripts are *template.py*, *utilsPath.py* and *convert.py*. In order to keep track of the origin of the standardized data, these scripts as well as the original data files, are stored inside the database, whereby the original data files are located in sub-folders called “orig”.

To guarantee the quality of the implemented data, each result is validated right after its implementation. The outcome of this validation (e.g. validation plots), is stored in sub-folders called “validation”. Eventually, the database contains the *tWiki.txt* used to create entries on the SModelS wiki web page. This web page gives a quick overview of the data comprised in the database.

The new SModelS database provides a clear structure (cf. [Figure 6.2](#)) to store all the files mentioned above, as explained in more detail below.

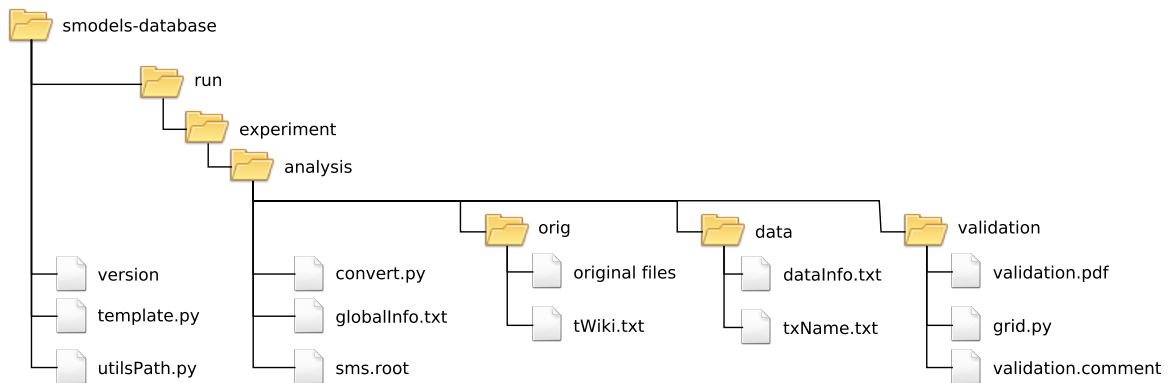


Figure 6.2: Structure of the new SModelS database

6.2.1 General Structure

The complete database is located inside a folder called `smodels-database`. Most files inside the database are divided into sub-folders. Nevertheless three files are located directly at the top level of the database. These three files are:

version: A text file containing a string with the version name. While this thesis is written the first version of the new database is constantly filled with new data and validated. The working name of this first version is “new style test-version”.

utilsPath.py: contains the path to smodels-utils, where the `dataPreparation` is located.

This path is used by the files *template.py* and *convert.py*.

template.py A python script which creates the folder structure and a template *convert.py* to implement a new analysis. The functionality of this script is described in more detail in [subsection 6.3.1](#).

The files associated with a particular analysis are located in so-called analysis folders. These folders are grouped by the run folders and the experiment folders. The run folders are named with respect to the centre-of-mass energy of the respective data sample, e.g. 8TeV. The experiment folders are named after the two general-purpose experiments ATLAS and CMS. The substructure inside one analysis folder is described below.

6.2.2 Analysis Folder

To store $(\sigma \times BR)_{UL}$ as well as $(\epsilon \times A)$ given by an analysis, the experimental data is split and stored in two different analysis folders, the “upper limit analysis” and “efficiency analysis” folder. These folders follow the naming convention of the respective collaboration, whereby the postfix “-eff” is used to identify an efficiency analysis folder. For example, the folder ATLAS-SUSY-2013-04 contains the upper limit lists for the respective analysis [32] and the folder ATLAS-SUSY-2013-04-eff contains the efficiency lists. In addition, both folders contain information related to the whole analysis (e.g. \sqrt{s}) and to the topologies (e.g. constraints) comprised in the analysis.

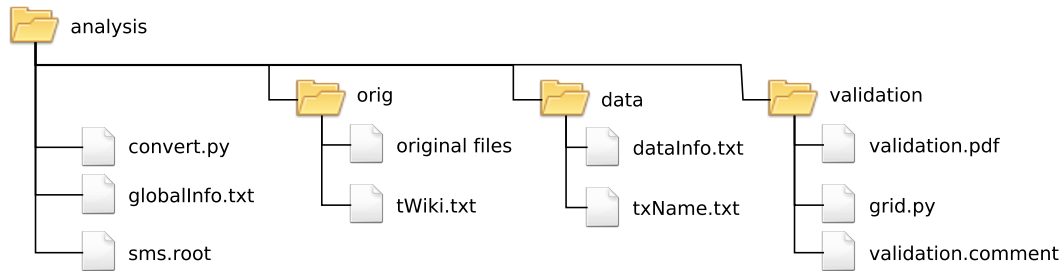


Figure 6.3: Structure of an arbitrary analysis folder.

The data inside an analysis folder is located in different files. These files are further organised in a substructure (cf. [Figure 6.3](#)) of three sub-folders: “data”, “orig” and “validation”. The sub-folders and their file content is described below. A complete list of all information stored inside the standardized data files can be found in [Appendix A](#). Three files are located directly inside the analysis folders:

convert.py: The *convert.py* is one of the first files which is created during the implementation of data from a new analysis. It is a python script which uses the objects

defined within the `dataPreparation` package to produce the internal analysis file structure, as well as the files *globalInfo.txt*, *sms.root*, *dataInfo.txt*, *txName.txt* and *tWiki.txt*. For a detail description see [subsection 6.3.2](#).

globalInfo.txt: This text file contains the analysis related information, e.g. the integrated luminosity of the data sample used in the analysis. An example *globalInfo.txt* for ATLAS-SUSY-2013-04 [31] is shown in [Listing 6.9](#). The \sqrt{s} is labelled with “sqrts” and the luminosity with “lumi”. A complete explanation of all possible information comprised by the *globalInfo.txt* can be found in [section A.4](#)

Listing 6.3: *globalInfo.txt* entries for ATLAS-SUSY-2013-04 [31]

```
sqrts: 8.0*TeV
lumi: 20.1/fb
id: ATLAS-SUSY-2013-05
prettyName: ATLAS 2b
url: https://atlas.web.cern.ch/Atlas/GROUPS/PHYSICS/PAPERS/SUSY-2013-05/
arxiv: http://arxiv.org/abs/1308.2631
publication: http://link.springer.com/article/10.1007/JHEP10%282013%29189
supersedes: ATLAS_CONF_2013_001;ATLAS_CONF_2013_053
comment: upper limits for T6bbWWC150 are not public
private: False
implementedBy: Wolfgang Waltenberger
lastUpdate: 2015/5/6
```

sms.root: A ROOT.TFile containing exclusion lines as ROOT.TGraph objects. The exclusion lines are grouped inside the file with respect to the corresponding topology. As discussed in [subsection 4.2.3](#) six exclusion lines for each topology and mass plane are given by the experimentalists. To distinguish between them a naming convention is used. For example “exclusionP1” denotes the observed exclusion line including theory uncertainties of $+1\sigma_{theor}$.

Listing 6.4: *exclusion lines for T6bbWW for ATLAS-SUSY-2013-05 [32]*

```
TFile*          sms.root
TDirectoryFile* T6bbWW
  exclusion_2*Eq(mother,300.0)_Eq(inter0,x)_Eq(lsp,y)
  exclusionP1_2*Eq(mother,300.0)_Eq(inter0,x)_Eq(lsp,y)
  exclusionM1_2*Eq(mother,300.0)_Eq(inter0,x)_Eq(lsp,y)
  expectedExclusion_2*Eq(mother,300.0)_Eq(inter0,x)_Eq(lsp,y)
  expectedExclusionP1_2*Eq(mother,300.0)_Eq(inter0,x)_Eq(lsp,y)
  expectedExclusionM1_2*Eq(mother,300.0)_Eq(inter0,x)_Eq(lsp,y)
```

The respective mass plane for each exclusion line is indicated by a postfix. This postfix corresponds to the “axis string” readable by the `dataPreparation`. The

respective object (the `OrigPlot`) and the axis string are explained in [subsection 6.3.3](#). [Listing 6.4](#) shows the content of the ROOT.TFile from the analysis folder ATLAS-SUSY-2013-05 [32], containing exclusion lines for T6bbWW in the $\tilde{\chi}^\pm - \tilde{\chi}_1^0$ - mass plane with $m_{\tilde{\tau}} = 300$ GeV.

The orig-Folder

The folder called `orig`, contains the upper limit maps, efficiency maps and exclusion lines as given by the experimentalists. These original data files can have various data formats. The `convert.py` script uses objects from the `dataPreparation` package to read this original files and store them in the standard data format.

Furthermore, the `orig`-folder also contains the `tWiki.txt`. It holds the HTML-string used to create an entry for the respective analysis on the SModelS wiki page. This file is created by the `convert.py` file. The wiki page links the information inside the database to the web page where the original data is provided by the experimentalists. Therefore the `tWiki.txt` is located in the `orig`-folder.

The data Folders

The data folders hold information about the signal regions and the topologies. Since, an upper limit analysis does not depend on the signal region, each upper limit analysis folder contains exactly one data folder named “data”. Whereas each efficiency analysis folder contains one data folder for each signal region. These folders are named using an abbreviation for the signal region. One simple example is MET2_HT1_nb3, which describes a signal region defined by cuts on \cancel{E}_T and H_T plus 3 b-tagged jets. Inside each data folder the files `dataInfo.txt` and `txName.txt` are located. Their content is described below.

dataInfo.txt: The future SModelS version will use this file to identify if the information inside the data folder is related to an upper limit or an efficiency analysis. For efficiency analyses it holds additional information needed for the calculation of $(\sigma \times BR)_{UL}$ for a given $(\epsilon \times A)$, e.g events observed in the signal region. A full list is given in [section A.4](#). [Listing 6.5](#) and [6.6](#) show example *dataInfo.txt* files for the upper limit analysis and efficiency analysis based on CMS-SUS-12-024 [43].

Listing 6.5: dataInfo.txt entries for CMS-SUS-12-024 [43]; upper limit analysis

```
dataType: upperLimit
dataId: None
.
```

Listing 6.6: globalInfo.txt entries for CMS-SUS-12-024 [43]; efficiency analysis

```
dataType: efficiencyMap
dataId: MET2_HT1_nb3
observedN: 161
expectedBG: 157
bgError: 13
```

txName.txt: Most analyses include interpretations in terms of different topologies. Each data folder contains one *txName.txt* for each of these topologies. The files are named after the topologies using the naming convention introduced in [subsection 4.2.2](#). They contain all information about the respective topology, e.g. constraints. A complete list of possible information stored in the *txName.txt* files can be found in [section A.3](#).

txName.txt files in the data folder of an upper limit analysis contain the upper limit lists. Whereas for efficiency analyses the data folders hold *txName.txt* files containing efficiency lists. [Listing 6.7](#) shows the entries of *T1ttttoff.txt* for the upper limit analysis based on CMS-SUS-12-024 [\[43\]](#). The label “conditionDescription” indicates the conditions as described in [subsection 5.1.1](#), whereas the label condition indicates the “fuzzyconditions” within the new database.

Listing 6.7: T1ttttoff.txt entries for CMS-SUS-12-024 [\[43\]](#); upper limit analysis

```
txName: T1ttttoff
conditionDescription: None
condition: None
constraint: [[['b','b','W','W']], [['b','b','W','W']]]
checked: AL
figureUrl: https://twiki.cern.ch/twiki/pub/CMSPublic/
           PhysicsResultsSUS12024/T1tttt_exclusions_corrected.pdf
validated: True
axes: 2*Eq(mother,x)_Eq(lsp,y)
publishedData: True
upperLimits: [[[[400.0*GeV, 0.0*GeV], [400.0*GeV, 0.0*GeV]],
                1.815773*pb],
               [[400.0*GeV, 25.0*GeV], [400.0*GeV, 25.0*GeV]], 1.806528*pb],
               [[400.0*GeV, 50.0*GeV], [400.0*GeV, 50.0*GeV]], 2.139336*pb],
               ....
```

The Validation Folder

The implementation of data into the new database is an ongoing process. Each result from a newly implemented analysis is immediately validated and the outcome of this validation is stored in the validation folder. Each validation plot is named after the respective topology and the axis string describing the respective mass plane. The new validation procedure uses python objects developed for the `dataPreparation` (e.g. `OrigPlot`). Two validation plots produced by using the new database and the future SModelS version are shown and described in [Figure 6.4](#).

For each validation plot a python file (*grid.py*) containing the grid data for the plot is stored. Furthermore the folder contains a comment file, containing comments about the validation, e.g. the reason why the validation of a result was not successful.

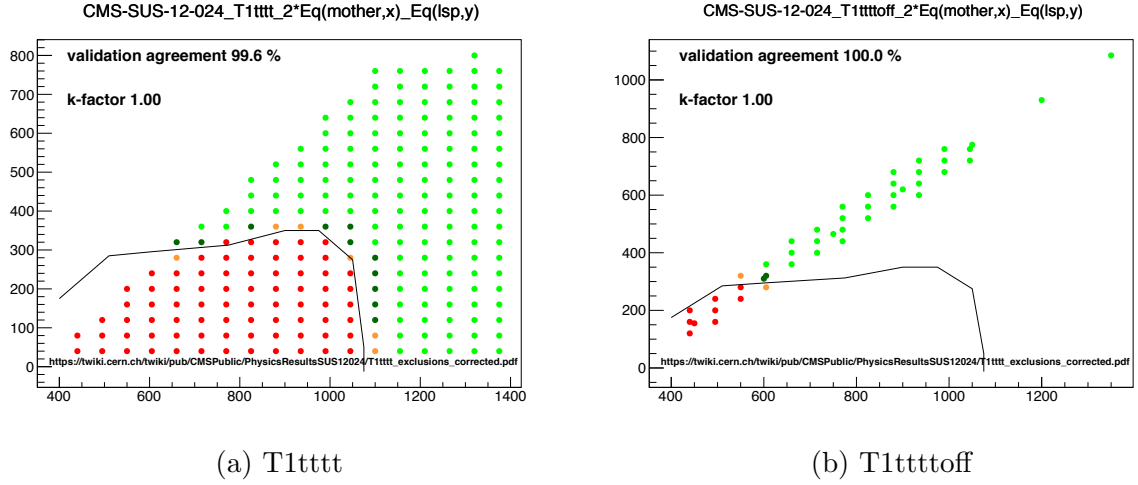


Figure 6.4: Validation plots for the T1tttt result from CMS-SUS-12-024 [43] for the on-shell regime (T1tttt) and off-shell regime (T1ttttoff), respectively. The plots show points which can be excluded (red) and points which can not be excluded (light green), even if an uncertainty of 10 % is introduced to $(\sigma \times BR)_{UL}$. Excluded and not excluded points computed without uncertainties are shown in orange and dark green. The validation agreement refers to the ratio of wrong assigned red and light green points (e.g. light green points inside the official excluded region) to the overall number of points. The official exclusion line does not distinguish between on- and off-shell region.

The entire new database described above, the process of data implementation and the automatised checks performed during this implementation, are based on the `dataPreparation`. Hence, the next section is dedicated to a detailed description of this package.

6.3 Implementation of Data - the `dataPreparation` package

The `dataPreparation` is an object-oriented python package, providing powerful objects for the implementation and standardization of data with respect to the new SModelS database.

As described in section 6.1, the development of the `dataPreparation` was driven by the experiences made during the validation of the old SModelS database (cf. section 5.2). Besides the identification of different kinematic regions comprised in the upper limit maps, incorrectly implemented data was one of the most frequent problems within the old database. To avoid these problems the `dataPreparation` performs several checks of the data during the implementation.

In particular, the constraints have to be given within a well defined structure, consisting of a system of nested brackets (cf. subsection 5.1.1). Therefore the constraints for all

topologies, are checked for consistency with this structure.

Another procedure which was highly prone to errors was the definition of the mass planes. Within the `dataPreparation` the mass plane is used to compute the mass vectors. Therefore an incorrect mass plane may cause an erroneous mass vector. For example, the mass of the second particle may exceed the mass of the mother particle, which is kinematically forbidden. Therefore one of the checks which is performed to verify a given mass plane is to compare all masses inside a mass vector.

This section demonstrates the utilisation of the `dataPreparation` package for the implementation of new analyses into the database.

6.3.1 Preparatory Settings

The `dataPreparation` package is located inside the `smodels-utils` folder and is not part of the SModelS database. It is recommended to place the folders `smodels-database` and `smodels-utils` into the same directory. If this is not the case, `utilsPath.py` can be used to set the relative path from `smodels-database` to `smodels-utils`.

Once the path is properly set, data from a new analysis can be implemented into the database. The first steps for this implementation are described below.

- An upper limit analysis folder and an efficiency analysis folder inside the database structure have to be created.
- Inside each of these folders an `orig`-folder and the `convert.py` file have to be created.
- The original data files have to be downloaded from the respective web page and stored inside the `orig` folder. The search results are mostly presented at the CERN twiki [8, 19] web page or the HepData [73] web page.

For an upper limit analysis the first two steps can be automatised by using the executable python script `template.py`, which takes the following command line arguments:

- id* : Identification of the analysis corresponding to the analysis naming convention from ATLAS (ATLAS-CONF or ATLAS-SUSY) or CMS (CMS-PAS or CMS-SUS-PAS).
- CMS*; -*ATLAS* : To define the name of the experiment, either the CMS or the ATLAS flag has to be set.
- sqrts* : Center of mass energy of the data sample used for the analysis.
- txNames* : A list of topologies comprised in the analysis. If the publication provides more than one mass plane for a given topology the number of mass planes can be defined in square brackets. e.g: T1 T5WW[3]

Listing 6.8 shows an example for the usage of these command line options for the implementation of a new CMS analysis including two topologies.

Listing 6.8: Example for the usage of *template.py*

```
python template.py -CMS -id PAS-13-008 -sqrts 8.0 -txNames T2bb
T6bbWW [2]
```

The given topologies are checked using the class `txDecay` from module `txDecays.py` comprised in the `dataPreparation` package. In case a topology is unknown, the process is interrupted. Also the predefined number of mass planes is checked by `txDecay`. Topologies describing a one step decay can not have additional mass planes. The user input is corrected automatically and a warning is printed to the screen.

When *template.py* is executed, a new folder structure is created for the upper limit analysis. This folder structure is defined by the command line attributes described above and follows the structure discussed in [section 6.2](#). If the run- or experiment-folder does not exist, the respective folders are created. If the complete publication path already exists, an error message is raised and the process is interrupted to avoid data loss. In addition, a *convert.py* is created, which contains a predefined code skeleton that has to be completed by the user.

Currently the implementation of efficiency map - based analysis lacks this automated creation procedure. The folder structure and the *convert.py* skeleton for efficiency map - based analysis have to be created manually.

6.3.2 Convert File

The script *convert.py* is the central file for the implementation of a new analysis. Within this file objects from the `dataPreparation` page are used to create the folder structure and the files *info.txt*, *datainfo.txt*, *txNames.txt*, *sms.root* and *tWiki.txt* inside an analysis folder.

A *convert.py* is structured in several blocks, each of these blocks is linked to objects of the `dataPreparation` package. These blocks are:

- The first block contains the import statements of the objects from the `dataPreparation` package.
- The next block is the global info block. Inside this block an instance of the class `MetaInfoObject` is used to implement information (e.g luminosity) related to the whole analysis.
- For each topology contained in the analysis, the *convert.py* contains a topology block. Each block uses an instance of the class `TxNameInput` for the implementation of information valid for the topology, e.g. constraints.
- Each topology block contains at least one mass plane block. These blocks use instances of the class `MassPlane` for implementation of the data related to a mass plane, e.g. upper limit maps.

- At the bottom of the file the creation of the database files is initialised by calling the method “create” of the class `databaseCreator`.

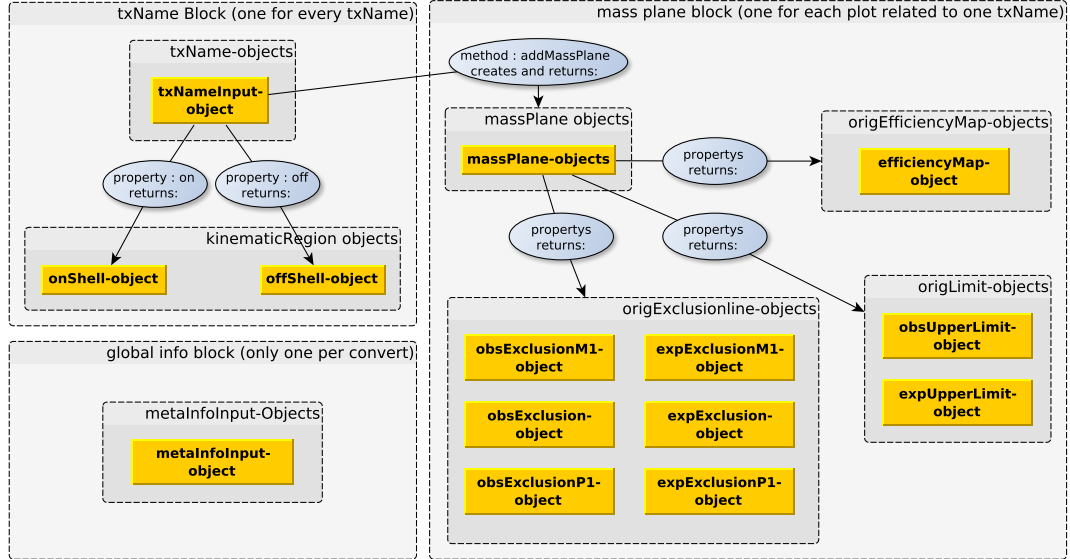


Figure 6.5: Assignment of the `dataPreparation` classes to the blocks of a `convert.py`. The substructure of the objects is shown.

The classes `TxNameInput` and `MassPlane` comprise several objects, as depicted in Figure 6.5. The blocks inside the `convert` files are described in detail below.

Global Info Block

This block is controlled by the `MetaInfoInput` object, which is initialized with the id of the analysis, e.g. ATLAS-SUSY-2013-05 [32]. The object provides several attributes and properties to write information valid for the entire analysis to the database. The information related to the attributes and properties of this object is listed below. Listing 6.9 shows example global info settings.

sqrts : center of mass energy in TeV,

lumi : integrated luminosity in fb^{-1} ,

prettyname : L^AT_EX readable string describing the search strategy,

arxiv : link to the corresponding arXiv [74] article, if it exists,

publication : link to the corresponding publication article if it exists,

superseded_by : ids of the analysis which supersedes this publication, if it exists,

supersedes : names of all analysis, separated by semicolons superseded by this one,

comment : internal comments about the publication ,

private : indicates if an analysis is made public by the collaboration. Set to “False” if the analysis is public, else set to “True”.

Listing 6.9: Example global info settings for ATLAS-SUSY-2013-05 [32]

```
info = MetaInfo('ATLAS-SUSY-2013-05')
info.url = 'https://atlas.web.cern.ch/Atlas/GROUPS/PHYSICS/PAPERS/
           SUSY-2013-05/'
info.sqrts = '8.0'
info.lumi = 20.1
info.prettyname = 'ATLAS 2b'
info.private = False
info.arxiv = 'http://arxiv.org/abs/1308.2631'
info.publication = 'http://link.springer.com/article/10.1007/JHEP10
                   %282013%29189'
info.comment = 'not all upper limit maps for T6bbWW are public'
info.supersedes = 'ATLAS_CONF_2013_001;ATLAS_CONF_2013_053'
```

Topology Block

Each topology block starts with the initialization of a `TxNameInfo` object with the name of the topology. The `TxName` is used to implement information related to the on-shell and off-shell region of a topology. Listing 6.10 shows a complete topology block for the example topology T6bbWW from the analysis ATLAS-SUSY-2013-05 [32]. To set the values for the two possible kinematic regions, `TxNameInfo` contains two `KinematicRegion` objects. They are returned and set by the following properties:

on : returns the `KinematicRegion` object related to the on-shell topology,

off : returns the `KinematicRegion` object related to the off-shell topology,

onShell : switch for the on-shell topology, possible values: “True”, “False” or “auto”,

offShell : switch for the off-shell topology, possible values: “True”, “False” or “auto”,

The switches are set to “auto” by default. If the default is used the automatised recognition of kinematic regions within the `dataPreparation` is performed. A *txName.txt* for the on-shell topology and a *txName.txt* for the off-shell topology is produced if the respective kinematic region exists within the given upper limit maps or efficiency maps.

The values True or False can be used to overrule this automation. For example, if *onShell* is set to “True” the creation of a *txName.txt* for the on-shell topology is forced and no *txName.txt* for the off-shell case is created.

Listing 6.10: Example txName setting for ATLAS-SUSY-2013-05 [32], T6bbWW

```

T6bbWW = TxName('T6bbWW')
T6bbWW.on.checked = 'VM'
T6bbWW.off.checked = 'VM'
T6bbWW.on.constraint = "[['b'], ['W']], [['b'], ['W']]"
T6bbWW.off.constraint = "[['b'], ['L', 'nu']], [['b'], ['L', 'nu']] +
    [['b'], ['L', 'nu']], [['b'], ['jet', 'jet']] + [['b'], ['jet', 'jet']] +
    [['b'], ['jet', 'jet']]"
T6bbWW.condition = None
T6bbWW.off.condition = None
T6bbWW.on.conditionDescription = None
T6bbWW.off.conditionDescription = None

```

The `KinematicRegion` objects returned by the `txNameInfo` object provide attributes to set the following information:

constraint : constraint as described in [subsection 5.1.1](#),

condition : fuzzycondition as described in [subsection 5.1.1](#)

conditionDescription : condition as described in [subsection 5.1.1](#),

checked : name of a third person who checked the implementation of the data for this kinematic region,

Mass Plane Block:

Every mass plane block belongs to a topology block and corresponds to a 2D-plot given by the analysis. For upper limit analysis this plot is an upper limit map and for efficiency analysis it is an efficiency map. By using the method “addMassPlane” of the `TxName` object a new `MassPlane` object is initialized and assigned to the `TxName`. To define the mass plane, the method takes a set of optional arguments. These arguments represent the masses of the sparticles within the associated decay. The predefined variables `x` and `y` are used to assign the masses to the axes of the plot. Available parameters are:

motherMass : mass of the mother particle of the decay chain,

lspMass : mass of the LSP,

interMass0,...,interMassN : masses of the particles between the mother particle and the LSP, numbered by an index,

Since, every decay chain needs a beginning and an end, `motherMass` and `lspMass` have to be set in every case. The `interMass` parameters have to be set if the respective topology describes a cascade decay. The method “addMassPlane” sets both branches to the same masses. To define mass planes corresponding to asymmetric topologies, the methods “setBranch_1” or “setBranch_2” can be used to reset one of the branches. Listing

Listing 6.11: Example mass plane initialization for an asymmetric decay

```

T4tbW_1 = T4tbW.addMassPlane(motherMass = x, interMass0 = y + 5.,
    lspMass = y)
T4tbW_1.setBranch_2(motherMass = x, lspMass = y)

```

6.11 shows the initialization of a mass plane with a two-step decay in one branch and a one-step decay in the other branch.

The upper limit maps and the efficiency maps are presented as plots by the collaborations on the respective result web pages, e.g CMS Supersymmetry Physics Results at the CERN twiki. Information related to these plots can be stored inside the database by using the following attributes of the **MassPlane**:

figureUrl : string containing the link to the plot on the respective web page,

figure : string containing the name of the plot on the respective web page,

In addition, the information comprised in an upper limit map or an efficiency map as well as the exclusion lines are needed in some machine-readable format. Within the database the original files, providing this machine-readable information, are stored inside the orig-folder (cf. subsection 6.2.2). To read these files the **MassPlane** includes three different types “OrigData” objects:

- The **OrigLimit** objects are designed to read original files containing the upper limit maps. The **MassPlane** object provides two properties to return the **OrigLimit** objects:

obsUpperLimit : returns an **OrigLimit** to read the observed upper limit map,

expUpperLimit : returns an **OrigLimit** to read to the expected upper limit map,

- The **OrigEfficiencyMap** object is designed to read original files containing the efficiency maps for exactly one signal region. To return this object the property *efficiencyMap* is used.
- The **OrigExclusion** objects are designed to read original files containing the exclusion lines. The **MassPlane** object provides six properties to return the **OrigExclusion** objects for the different exclusion lines:

obsExclusion : observed exclusion line, with $\sigma_{theor} = \pm 0$,

obsExclusionM1 : observed exclusion line with $\sigma_{theor} = +1$,

obsExclusionP1 : observed exclusion line with $\sigma_{theor} = -1$,

expExclusion : expected exclusion line, $\sigma_{exp} = \pm 0$,

expExclusionM1 : expected exclusion line with $\sigma_{exp} = +1$,

expExclusionP1 : expected exclusion line with $\sigma_{exp} = -1$,

In order to use these objects, a distinction between implementation of an upper limit analysis and an efficiency analysis needs to be made.

For **upper limit analysis**, the `OrigLimit` objects and `OrigExclusion` objects are used. After using the respective properties to return an “OrigData” object, the method “set-Source” is used to assign it to the original data, stored in the orig-folder (cf. [Listing 6.12](#)).

Listing 6.12: Example source setting

```
#settings for a text file containing observed upper limit:
T1tttt_1.obsUpperLimit.setSource( 'orig/T1tttt.txt', 'txt')
#settings for a root file containing an observed exclusion line as
  ROOT-object:
T1bbbb_1.obsExclusion.setSource( './orig/xsecUL_SMS_Razor.root', '
  root', objectName = 'Obs_T1bbbb_MultiJet_Jet2b')
```

This method takes the arguments “path” and “fileType”, as well as the optional arguments “objectName” and “index”. The argument “path” takes a string referring to the path of the data file. “fileType” takes a string describing the type of the file. The available values for “fileType” are:

- txt*: Text file containing columns with floats only. The first column holds the values of the x-axis and the second the values for the y-axis. In case of upper limit maps a third column is required. This column holds the $(\sigma \times BR)_{UL}$. No settings for “objectName” or “index” are required.
- svg*: Text file holding information as scalable vector graphic (svg). Available for exclusion lines only. No settings for “objectName” or “index” are required.
- root*: ROOT.TFile containing data as a ROOT object. In case of exclusion lines a ROOT.TGraph object is required and a 2D ROOT histogram for the upper limit maps. “objectName” must be set to the name of the ROOT object. No setting for “index” is required.
- cMacro*: ROOT macro containing data as ROOT objects. In case of exclusion lines a ROOT.TGraph object is required and a 2D ROOT histogram for the upper limit maps. “objectName” must be set to the name of the ROOT object. No setting for “index” is required.
- canvas*: ROOT.TFile containing a ROOT.TCanvas object. The data is stored in this ROOT.TCanvas object as sub-objects. In case of exclusion lines a ROOT.TGraph object is required and a 2D ROOT histogram for the upper limit maps. “object-Name” must be set to the name of the ROOT.TCanvas. “Index” has to be set to the index of the required sub-object in the “listOfPrimitives” of the TCanvas.

In order to keep track of the data source and to handle the data more precisely, the “OrigData” object provides several attributes:

dataUrl: Download link for the original data provided by the experimentalists.

unit: Available for upper limits only. Unit of the cross sections as a string. The strings “fb” and “pb” can be used. By default the unit is set to “fb”.

reverse: Available for exclusion lines only. The given points of the exclusion lines are reversed when set to “True”.

sort: Available for exclusion lines only. The given points of the exclusion lines are ordered by x-values when set to “True”.

Since the original exclusion lines are given in various formats, the options *reverse* and *sort* may be necessary to guarantee a uniform appearance in the summary and validation plots. Instead of setting the download link for every “OrigData” object, the **MassPlane** object can be used to set the link for an entire set of original data. This is useful in case all exclusion lines are provided within a single ROOT.TFile, for example. Hereby the following properties are available:

dataUrl: sets the download link for all “OrigData” objects related to the mass plane,

histDataUrl: sets the download link for all **OrigLimit** objects related to the mass plane,

exclusionDataUrl: sets the download link for all **OrigExclusion** objects related to the mass plane,

Listing [Listing 6.13](#) and [Listing 6.14](#) together show an entire example mass plane block for T6bbWW from ATLAS-SUSY-2013-05 [32].

Listing 6.13: Example mass plane setting for ATLAS-SUSY-2013-05 [32], T6bbWW

```
T6bbWW_1 = T6bbWW.addMassPlane(motherMass = x, interMass0 = y + 5.,
    lspMass = y)
T6bbWW_1.figure = 'Fig.(aux) 8a'
T6bbWW_1.figureUrl = 'https://atlas.web.cern.ch/Atlas/GROUPS/PHYSICS/
    PAPERS/SUSY-2013-05/figaux_08a.png'
#-----limits-----
T6bbWW_1.obsUpperLimit.setSource('orig/T6bbWWoffD005_2014-09-22.dat',
    'txt')
T6bbWW_1.obsUpperLimit.dataUrl = 'http://hepdata.cedar.ac.uk/view/
    ins1247462/d37'
#-----exclusions-----
T6bbWW_1.obsExclusion.setSource('orig/T6bbWWoffD005_exc.dat', 'txt')
T6bbWW_1.obsExclusionM1.setSource('orig/T6bbWWoffD005_excMinusSigma.
    dat', 'txt')
T6bbWW_1.obsExclusionP1.setSource('orig/T6bbWWoffD005_excPlusSigma.
    dat', 'txt')
T6bbWW_1.expExclusion.setSource('orig/T6bbWWoffD005_excExpected.dat',
    'txt')
```

Listing 6.14: Continuation of the example from Listing 6.13 for ATLAS-SUSY-2013-05 [32], T6bbWW

```

T6bbWW_1.expExclusionM1.setSource('orig/
    T6bbWWoffD005_excExpectedMinusSigma.dat', 'txt')
T6bbWW_1.expExclusionP1.setSource('orig/
    T6bbWWoffD005_excExpectedPlusSigma.dat', 'txt')
#-----exclusions.dataUrl-----
T6bbWW_1.obsExclusion.dataUrl = 'http://hepdata.cedar.ac.uk/view/
    ins1247462/d19'
T6bbWW_1.obsExclusionM1.dataUrl = 'http://hepdata.cedar.ac.uk/view/
    ins1247462/d20'
T6bbWW_1.obsExclusionP1.dataUrl = 'http://hepdata.cedar.ac.uk/view/
    ins1247462/d21'
T6bbWW_1.expExclusion.dataUrl = 'http://hepdata.cedar.ac.uk/view/
    ins1247462/d22'
T6bbWW_1.expExclusionM1.dataUrl = 'http://hepdata.cedar.ac.uk/view/
    ins1247462/d23'
T6bbWW_1.expExclusionP1.dataUrl = 'http://hepdata.cedar.ac.uk/view/
    ins1247462/d24'

```

For **efficiency analyses** the `OrigEfficiencyMap` objects and `OrigExclusion` objects are used. Like for the other “OrigData” objects, within the `OrigEfficiencyMap` the method “setSource” is used to assign the original data to the object. To set the argument “fileType” the strings *txt*, *root*, *cMacro* and *canvas* are available. In addition the string *effi* can be used for efficiency maps produced by Fastlim [75].

The method “setSource” for `OrigEfficiencyMap` includes the additional argument “dataset”. This argument takes a string describing the signal region. Eventually, additional data related to this signal region can be set by the method “setStatistics”. It takes three optional arguments:

observedN: number of observed events in the signal region,

expectedBG: number of events expected from SM background,

bgError: uncertainties on the SM background,

Listing 6.15 shows example settings for efficiency maps for two T1tttt signal regions from the efficiency analysis folder CMS-SUS-12-024-eff.

In order to create database entries for more than one signal region, the `OrigEfficiencyMap` object is used iteratively. After using the methods to set the data related to the efficiency maps for one mass plane and signal region, the creation of the respective database entries is started. The line “databaseCreator.create(True)” (cf. Listing 6.15) initializes the creation of a data-folder, a *dataInfo.txt* and a *txName.txt* file for each topology inside the efficiency analysis folder. After this is done, the same `OrigEfficiencyMap` object can be used for the implementation of data corresponding to another signal region. By using this iteration, arbitrary numbers of signal regions can be created by using one `OrigEfficiencyMap` object for each `MassPlane`.

Listing 6.15: Example efficiency map settings for CMS-SUS-12-024-eff, T1tttt

```

T1tttt.efficiencyMap.setSource("orig/efficiency_T1tttt_multi.root", "
    root", objectName = "heff_MET2_HT4_nb3", dataset="MET2_HT4_nb3")
T1tttt.efficiencyMap.setStatistics (observedN=14, expectedBG=12.3,
    bgError=2.7)

databaseCreator.create(True)

T1tttt.efficiencyMap.setSource("orig/efficiency_T1tttt_multi.root", "
    root", objectName = "heff_MET3_HT1_nb3", dataset="MET3_HT1_nb3")
T1tttt.efficiencyMap.setStatistics (observedN=15, expectedBG=15.5,
    bgError=3.0)

databaseCreator.create(True)

```

The last step for the implementation of a new analysis is to execute the *convert.py* file.

6.3.3 Creating the Database

When a *MetaInfoInput* or *TxNameInput* object is initialised within the *convert.py*, these objects are automatically written into an instance of the class *DatabaseCreator*. This object controls the standardization of the data and creates the internal folder structure of the analysis folder, as well as the standard data files. The creation of the database entries is initialized by the line “*databaseCreator.create()*”¹ at the end of each *convert* file.

The *dataPreparation* package is not only used for the implementation of new analyses, but also to update an existing analysis folder. This is done by editing the respective *convert.py* and executing it again. Therefore the first step when creating database entries is to delete the old standard data files, if they are existing. It is important to note that for the iterative implementation of different signal regions this deletion has to be turned off to avoid data loss. Therefore the attribute “createAdditional” of the method “create” is set to “True” (cf. Listing 6.15).

Within the *dataPreparation* package the following steps are performed to create the database entries:

- The information from *MetaInfoInput* is used to create the *globalInfo.txt* file.
- The original exclusion lines, assigned to the *OrigExclusion* objects, are standardized as *ROOT.TGraph* objects and stored inside *sms.root*.
- The information necessary to create the *tWiki.txt* is collected from *MetaInfoInput* and all *txNameInput* objects. This information (e.g. *dataUrl*) is used to create an HTML string, which is written to the *tWiki.txt*.

¹for efficiency map analysis, this command is used iteratively, as discussed in subsection 6.3.2.

- For an upper limit analysis only one data folder, called “data” and a default *dataInfo.txt* (cf. [Listing 6.5](#)) is created. For an efficiency analysis one data folder and one *dataInfo.txt* for each signal region is written into the database. The name of the data folder is given by the attribute “dataSet” of the `OrigEfficiencyMap` object. The content of the *dataInfo.txt* files is given by the attributes of the “setStatistics” method (cf. [Listing 6.15](#))
- The *txName.txt* files are created by using the `txNameInput` objects and the associated sub-objects.

The conversion of the data assigned to the `txNameInput` objects into the data standard used inside the *txName.txt* was one of the most challenging tasks during the development of the `dataPreparation` package and shall therefore be described in more detail.

Upper Limit and Efficiency Lists

Within the *convert.py* the original upper limit maps and efficiency maps for the different mass planes, are assigned to the “original data objects” inside the `MassPlane` objects. These maps have to be converted into one upper limit or efficiency list for each topology, which is finally stored in the *txName.txt* files. This process is alike for efficiency maps and all types of upper limit maps and shall therefore be exemplified by observed upper limit maps.

When creating the *convert.py* each `MassPlane` is defined and assigned to a `TxNameInput` object by using the method “addMassPlane” (cf. [Listing 6.11](#)). This method passes the equations used to define the mass plane on to an object of type `OrigPlot`. This is exemplified in [Listing 6.16](#).

Listing 6.16: Example OrigPlot settings

```
origPlot = OrigPlot()
origPlot.setBranch_2(motherMass = x, interMass0 = y + 5., lspMass = y)
origPlot.setBranch_1(motherMass = x, lspMass = y)
```

To create the observed upper limit list, every mass point given by the original upper limit map related to the `MassPlane` is read out and passed on to the respective `origPlot`. This object converts these two-dimensional mass points into mass vectors. (cf. [Listing 6.17](#))

Listing 6.17: Conversion of the two dimensional mass point (500,100) into a mass vector.

```
In : origPlot.getParticleMasses(500.0,100.0)
Out: [[500.0, 100.0], [500.0, 105.0, 100.0]]
```


This process is repeated for the observed upper limit maps of all `MassPlane` objects inside a `TxNameInput`. Finally all the mass vectors together with the respective $(\sigma \times BR)_{UL}$ are written into the upper limit list.

Axis String

The upper limit and efficiency lists no longer contain any information about the original mass planes. To keep track of this information, the `OrigPlot` is used to create the so-called axis string (cf. [Listing 6.18](#)).

Listing 6.18: Getting the axis string for a mass plane

```
In : str(origPlot)
Out: 'Eq(mother,x)_Eq(lsp,y)+Eq(mother,x)_Eq(inter0,y+5.0)_Eq(lsp,y)'
```

The string represents the equations which were initially passed on to the `origPlot`. For each `MassPlane` inside a `txNameInfo` the axis string is computed and written into the respective `txName.txt`. These strings hold the information about the mass planes originally used by the experimentalists. They can be used to reconvert a mass vector into a two dimensional mass point inside the respective mass plane (cf. [Listing 6.19](#)). For example this is used to create the validation plots for the new database.

Listing 6.19: Using the `OrigPlot` to get a point inside a mass plane from the data stored in the database

```
# initializing the OrigPlot object with an axis string
In : origPlot = OrigPlot.fromString('Eq(mother,x)_Eq(lsp,y)
    +Eq(mother,x)_Eq(inter0,y+5.0)_Eq(lsp,y)')
# reconvert a mass vector into an two dimensional mass point
In : origPlot.getXYValues([[500.0, 100.0], [500.0, 105.0, 100.0]])
Out: [500.0, 100.0]
```

On- and off-shell topologies

After computing the upper limit and efficiency lists, as well as the axis strings, the last remaining step to create the `txName.txt` files is to distinguish between on- and off-shell topologies. Therefore, for a given topology each mass vector is passed on to an instance of the class `VertexChecker`.

The working scheme of the `VertexChecker` is depicted in [Figure 6.6](#). It uses the constraints stored inside the `KinematicRegion` object related to the on-shell topology, to find all vertices containing off-shell SM particles for a given mass vector. For each vertex the mass difference ($\Delta m_i = m_i - m_{i-1}$) of the BSM particles is computed. This mass difference is then compared with the masses of the SM particles in this vertex, as given by the constraints. In order to be conservative the masses of the SM particles are set to

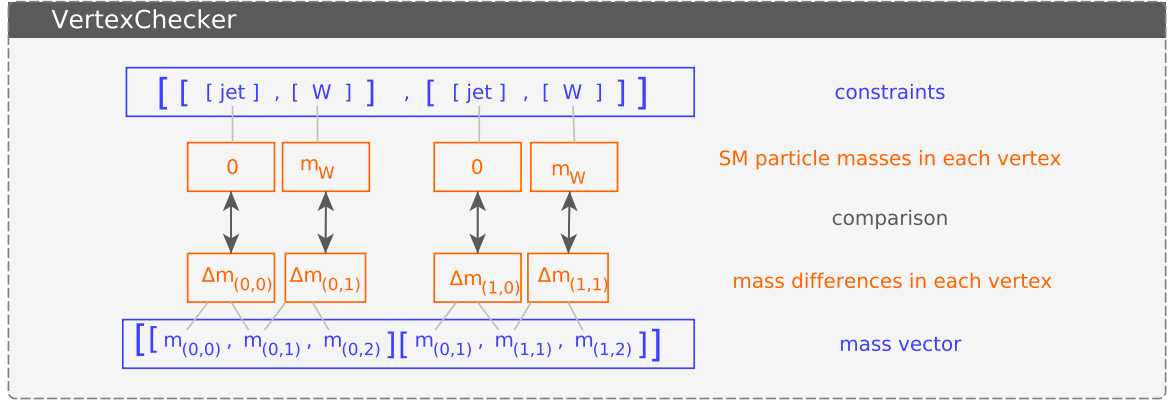


Figure 6.6: Working scheme of the class **VertexChecker**, exemplified by the constraints for T6WW; the constraints are used to calculate the masses of the SM particles in each vertex (m_{SM}). The light flavoured quarks (jets) are ignored and their mass is set to zero. The mass vector is used to compute the mass splitting in each vertex ($\Delta m_{(i,j)}$). Finally, m_{SM} is compared with $\Delta m_{(i,j)}$.

$m_{SM} = m - 2 \cdot \Gamma$, where m denotes the mass of the particle as given by the particle data group and Γ denotes its decay width. If $m_{SM} \leq \Delta m$, the corresponding vertex is off-shell. The **VertexChecker** can handle the off-shell regimes for vector bosons, the Higgs boson and the top quark. The masses of all other SM particles are neglected.

If the upper limit or efficiency list for a given topology contains at least one mass vector leading to a vertex with off-shell SM particles, a `txName.txt` for the off-shell topology is created. The upper limit or efficiency lists, as well as the axis strings are written into the file. Eventually, the information stored in the **KinematicRegion** object related to the off-shell topology (e.g. constraint and conditionDescription) is written to the file.

If the lists contain at least one mass vector including exclusively vertices with on-shell SM particles, a `txName.txt` for the on-shell topology is created. This file contains the same upper limit or efficiency list as the one for the off-shell case, but the on-shell constraints and conditionDescription stored in the respective **KinematicRegion** are used.

To date, the **dataPreparation** was used to implement 35 upper limit analysis folders and 17 efficiency analysis folders into the database. All data comprised in these folders is correctly implemented and validated. All SMS topologies as given by the experimentalists are split into on- and off-shell topologies if necessary.

Chapter 7

Conclusion

During the development of SModelS a database containing results from ATLAS and CMS analyses providing interpretations of SUSY searches in terms of different SMS topologies was built. In order to validate all results based on data samples collected at $\sqrt{s} = 8$ TeV, a computational working environment was written. This working environment made it possible to create validation plots for each of the 174 upper limit maps inside the database. A public database containing 62 validated results from 26 analyses was built and shipped with the first release of SModelS 1.0.

The validation was based on the comparison between an exclusion line derived by SModelS and the official exclusion line. Results for which this exclusion line was not available in a machine-readable format could not be validated. Another frequent reason for failed validations were fluctuations in the upper limit maps.

During the validation also some weaknesses of the implementation of the data were revealed. For example the implementation of $(\sigma \times BR)_{UL}$ as upper limit maps and the respective axes and slicing methods as strings made it difficult to access the data within the validation working environment. Due to the fact that these entries were implemented by hand, they were highly prone to errors. Eventually the large number of different slicing methods made it nearly unfeasible to recognize the off-shell regions inside all upper limit maps.

These problems led to the development of a restructured SModelS database including data in a new data standard. For example the $(\sigma \times BR)_{UL}$ for one topology and one analysis are no longer stored as different upper limit maps. Instead one upper limit list containing all $(\sigma \times BR)_{UL}$ for this topology is stored inside the database. The new database also provides a clear structure for the implementation of $(\epsilon \times A)$ for different signal regions. To prevent errors during the data implementation, this process was standardized and highly automatized. To this end an object oriented python package called **dataPreparation** was developed. This package automatizes also the identification of off- and on-shell regimes within the upper limit and efficiency lists.

The implementation of data into the new database is an ongoing process. To date, the **dataPreparation** package was used to implement data from 37 ATLAS and CMS

analyses. The implementation of the data from these analyses is checked and validated. A new version of SModelS which will be able to use $(\epsilon \times A)$ to constrain given BSM model points, is currently under development. This new version including the new database will eventually be released at the end of this year.

Appendix A

Content Of The SModelS Database Files

A.1 Information Comprised in the globalInfo.txt File

id	Identification corresponding to the analyses naming conventions from ATLAS (ATLAS-CONF or ATLAS-SUSY) or CMS (CMS-PAS or CMS-SUS-PAS).
sqrts	Centre-of-mass energy of the data sample used by the analysis.
lumi	Integrated luminosity of the data sample used by the analysis.
prettyname	L ^A T _E X readable string describing the event selection used for the analysis.
url	Link to the analysis on the CMS or ATLAS result web page [8],[19].
arxiv	Link to the publication on arXiv [74], if it exists.
publication	Link to the corresponding journal publication article, if it exists.
superseded_by	Identification of the analysis which supersedes this analysis, if existing.
supersedes	Identifications of all analyses superseded by this one.
comment	Internal comments about the analysis.
private	Indicates if an analysis is made public by the collaboration. “False” means the analysis is public. “True” indicates an analysis which is presented within the collaboration only.
implemented_by	Name of the person who created or updated the analysis folder.
lastUpdate	Date of creation or update of the analysis folder.

A.2 Naming Convention For the Exclusion Lines Stored in the sms.root File

exclusion	observed exclusion line without theory uncertainties (σ_{theor})
exclusionP1	observed exclusion line including $\sigma_{theor} = +1$
exclusionM1	observed exclusion line including $\sigma_{theor} = -1$
expectedExclusion	expected exclusion line without experimental uncertainties (σ_{exp})
expectedExclusionP1	expected exclusion line including $\sigma_{exp} = +1$
expectedExclusionM1	expected exclusion line including $\sigma_{exp} = -1$

A.3 Information Comprised in the txName.txt File

txName	Name of the the topology according to the naming convention given in subsection 4.2.2 . The postfix “off” is used to identify an off-shell topology. Topologywithout a postfix refer to on-shell topologies.
conditionDescription	The conditions, explained in subsection 5.1.1 are renamed to conditionDescription within the new database.
conditions	The fuzzyconditions, explained in subsection 5.1.1 are renamed to condition within the new database.
constraint	constraint of the respective topology (cf. subsection 5.1.1)
checked	After the implementation of a new topology for a given analysis it has to be checked by a third person of the SModelS group. This entry shows the initials of this person.
figureUrl	Link to the original plots showing the upper limit maps or efficiency maps for this topology as given by the experimentalists
validated	Describes if the topology is successfully validated
axes	String describing the mass planes originally used for the plots given by experimentalist for this topology. Classes from the <code>dataPreparation</code> package can be used to read this string and to convert the mass vectors from the e.g. upper limit map, back into two dimensional points inside the mass planes. This is e.g. used to produce the validation plots for example.
published data	This entry is set to “True” if the upper limit maps or efficiency maps are available for public download in a machine-readable format.
upperLimits	Contains the observed upper limit list. This is used for upper limit only
expUpperLimits	Contains the expected upper limit list. Used for upper limits only.
efficiencies	Contains the efficiency list for a given signal region. Used for efficiency maps only.

A.4 Information Comprised In the dataInfo.txt File

dataType	The dataType entry can hold two different strings, “efficiencyMap” or “upperLimit”. This string defines the type of the analysis.
dataId	The dataID for upper limit analyses is set to “None”. For efficiency analyses the dataId is given by an abbreviation for the signal region.
observedN	Number of observed events in the signal region.
expectedBG	Number of events expected from SM background.
bgError	Uncertainties on the SM background estimate.

List of Figures

2.1	The CERN accelerator Complex [4]	5
2.2	Overview of the ATLAS detector [7]	7
2.3	Overview of the CMS detector [7]	8
3.1	Particle content of the SM [10]. The outer ring depicts the fermions. Quarks are depicted in red and leptons in green. The inner blue ring shows the bosons and in the centre the Higgs boson is depicted in black. .	11
3.2	Illustration of the Higgs potential [12]. The blue pellet indicates the stable, non vanishing ground state, whereas the yellow pellet marks the unstable vanishing vacuum expectation value.	16
3.3	Extension of Figure 3.1. The particles of the SM shown in the circle are extended by their superpartners. The new particles are denoted by the symbol of their SM partner with a tilde. [10]	19
3.4	Dependency of the coupling constants for the electromagnetic α_1 , weak α_2 and strong interaction α_3 on the energy scale Q in the SM (left) and the MSSM (right). [17]	21
4.1	Examples for strong sparticle productions. From the left to the right: gluon-gluon fusion in s-channel, gluon-quark fusion in t-channel, quark-antiquark annihilation in s-channel, quark-quark scattering in t-channel. . .	26
4.2	Examples for production of electroweak sparticles. From the left to the right: neutralino pair production in s- and t-channel, chargino-neutralino associated production in s- and t-channel	26
4.3	Feynman graphs for topologies with gluino productions	31
4.4	Feynman graphs for topologies with squark productions	32
4.5	Feynman graphs for topologies with neutralino and chargino production . .	33

4.6	Efficiency map (a) and upper limit map including exclusion line (b) for the T1tttt topology from CMS-SUS-13-007 [22] in the gluino-LSP mass plane. Figure (a) shows $(\epsilon \times A)$ for a signal region determined by jets and selections on \cancel{E}_T and H_T . Figure (b) shows the 95 % C.L. upper limits on the production cross section assuming $BR = 100\%$, obtained from the combination of different signal regions. For the exclusion lines, next to leading logarithmic (NLL) SUSY production cross sections are computed and compared with the 95 % CL upper limits. To this end, a BR of 100 % into the SMS topology is assumed	34
4.7	Upper limit map and exclusion lines for the T6ttWW topology from ATLAS-SUSY-2013-09 [23] in two different mass planes. Figure (a) shows a mass plane defined by the mass of the sbottom (x-axis) and the mass of the chargino (y-axis). The mass of the LSP is set to 60 GeV. Figure (b) depicts a mass plane defined by the mass of the sbottom (x-axis) and the mass of the LSP (y-axis). The mass of the chargino is set to two times the mass of the LSP.	35
4.8	CMS summary bar plot produced for the 37th International Conference on High Energy Physics (ICHEP 2014) at Valencia. The plot shows a comparison of the exclusion limits for the mother particles of different SMS topologies. The string inside the bars refers to the CMS notification of the respective CMS Physic Analysis Summary.	37
5.1	SModelS working procedure [29]. The experimental side (right) contains σ_{UL} for different SMS topologies. On the theory side (left) a BSM model can be decomposed into its signal topologies. The signal topologies can be combined and their weights are compared to σ_{UL} uppcase of the SMS topologies.	39
5.2	Comparison between the topology T5WW as used in the analyses and its signal topology analogue as used in SModelS. The signal topology is defined by the constraint $[[[jet, jet], [W]], [[jet, jet], [W]]]$ and the mass vector $[[M_1^I, M_2^I, M_3^I], [M_1^{II}, M_2^{II}, M_3^{II}]]$	40
5.3	Scheme of the work flow used to create the validation plots. Python modules exclusively written for the validation are depicted in orange. Green boxes depict modules from the smodels/tools or smodels-utils packages used by the validation code. The arrows symbolize the transfer of information and files between the modules	48
5.4	Validation plot for the topology T1 from CMS-SUS-13-012 [47].	51
5.5	Validation plots for the T1tttt result from CMS-SUS-13-007 [22] for the on-shell regime (T1tttt) and off-shell regime (T1ttttoff)	52

5.6	Validation plot (a) and official upper limit map (b) for T1tbtb from ATLAS-CONF-2013-061 [41]. The deviations of the region excluded by SModelS and the official excluded region shown in (a) can be explained by fluctuations of $(\sigma \times BR)_{UL}$ shown in (b)	53
5.7	Validation plots for T6bbWW from CMS-SUS-13-011 [25] in the $\tilde{b} - \tilde{\chi}_1^0$ - mass plane for $x = 0.75$ (a) and $x = 0.25$ (b). Both figures show on-shell mass points only. The official exclusion line in (b) includes also the off-shell region. The differences between the region excluded by SModelS and the official one at $m_{mother} \sim 650$ GeV is due to the statistical uncertainties of the calculation of the production cross section σ	54
5.8	Validation plots for TChiChipmSlepStau from CMS-SUS-13-006 [46] in the $\tilde{\chi}_2^0/\tilde{\chi}^\pm - \tilde{\chi}_1^0$ - mass plane for $x = 0.95$ (a) and $x = 0.50$ (b).	57
6.1	Entries for CMS-SUS-13-004 [72] and CMS-SUS-13-007 [22] on the SModelS wiki page. For each analysis the available topologies and mass planes are listed. The column “Figure” includes the links to the original plots as given by the analysis. Additionally the links to the original data for the upper limit maps, the efficiency maps and exclusion lines are given if available in machine-readable format.	61
6.2	Structure of the new SModelS database	64
6.3	Structure of an arbitrary analysis folder.	65
6.4	Validation plots for the T1tttt result from CMS-SUS-12-024 [43] for the on-shell regime (T1tttt) and off-shell regime (T1ttttoff), respectively. The plots show points which can be excluded (red) and points which can not be excluded (light green), even if an uncertainty of 10 % is introduced to $(\sigma \times BR)_{UL}$. Excluded and not excluded points computed without uncertainties are shown in orange and dark green. The validation agreement refers to the ratio of wrong assigned red and light green points (e.g light green points inside the official excluded region) to the overall number of points. The official exclusion line does not distinguish between on- and off-shell region.	69
6.5	Assignment of the <code>dataPreparation</code> classes to the blocks of a <code>convert.py</code> . The substructure of the objects is shown.	72
6.6	Working scheme of the class <code>VertexChecker</code> , exemplified by the constraints for T6WW; the constraints are used to calculate the masses of the SM particles in each vertex (m_{SM}). The light flavoured quarks (jets) are ignored and their mass is set to zero. The mass vector is used to compute the mass splitting in each vertex ($\Delta m_{(i,j)}$). Finally, m_{SM} is compared with $\Delta m_{(i,j)}$	82

List of Tables

2.1	Acceleration steps at CERN accelerator complex	4
3.1	Overview of the three fundamental interactions in the SM.	12
3.2	SM lepton and quark fields grouped into the three generations.	13
3.3	chiral supermultiplets in the MSSM	22
3.4	gauge supermultiplets in the MSSM	22
5.1	List of analyses contained in the public database [28]. A detailed description of each analysis can be found in the respective publication.	43

Listings

5.1	Example decay table for the three body decays $\tilde{g} \rightarrow d\bar{d}\tilde{\chi}^0$ and $\tilde{g} \rightarrow u\bar{u}\tilde{\chi}^0$ with $BR = 50\%$	45
5.2	Example XSECTION table for gluino pair-production with $\sqrt{s} = 8$ TeV at NLO and NLL	45
5.3	Mixing blocks used in the SLHA files for electroweak production of sparticles	56
6.1	<i>upper limit list for T1tttt from CMS-SUS-12-024 [43]</i>	62
6.2	<i>efficiency list for T1tttt from CMS-SUS-12-024 [43]</i>	63
6.3	<i>globalInfo.txt entries for ATLAS-SUSY-2013-04 [31]</i>	66
6.4	<i>exclusion lines for T6bbWW for ATLAS-SUSY-2013-05 [32]</i>	66
6.5	<i>dataInfo.txt entries for CMS-SUS-12-024 [43]; upper limit analysis</i>	67
6.6	<i>globalInfo.txt entries for CMS-SUS-12-024 [43]; efficiency analysis</i>	67
6.7	<i>T1ttttoff.txt entries for CMS-SUS-12-024 [43]; upper limit analysis</i>	68
6.8	Example for the usage of template.py	71
6.9	Example global info settings for ATLAS-SUSY-2013-05 [32]	73
6.10	Example txName setting for ATLAS-SUSY-2013-05 [32], T6bbWW	74
6.11	Example mass plane initialization for an asymmetric decay	75
6.12	Example source setting	76
6.13	Example mass plane setting for ATLAS-SUSY-2013-05 [32], T6bbWW	77
6.14	Continuation of the example from Listing 6.13 for ATLAS-SUSY-2013-05 [32], T6bbWW	78
6.15	Example efficiency map settings for CMS-SUS-12-024-eff, T1tttt	79
6.16	<i>Example OrigPlot settings</i>	80
6.17	<i>Conversion of the two dimensional mass point (500,100) into a mass vector.</i>	80
6.18	<i>Getting the axis string for a mass plane</i>	81
6.19	<i>Using the OrigPlot to get a point inside a mass plane from the data stored in the database</i>	81

Bibliography

- [1] G. Aad *et al.* Observation of a new particle in the search for the Standard Model Higgs boson with the ATLAS detector at the LHC. *Physics Letters B*, 716(1):1 – 29, 2012.
- [2] S. Chatrchyan *et al.* Observation of a new boson at a mass of 125 GeV with the CMS experiment at the LHC. *Physics Letters B*, 716(1):30 – 61, 2012.
- [3] CERN. About cern. <http://home.web.cern.ch/about>. Accessed 14 July 2015.
- [4] Christiane Lefèvre. The CERN accelerator complex. Complexe des accélérateurs du CERN. Dec 2008.
- [5] ATLAS. Public Results. <https://twiki.cern.ch/twiki/bin/view/AtlasPublic>. Accessed 25 May 2015.
- [6] G. Aad *et al.* The ATLAS Experiment at the CERN Large Hadron Collider. *JINST*, 3:S08003, 2008.
- [7] CERN AC. Layout of ATLAS. Dessin representant le detecteur ATLAS. Mar 1998.
- [8] CMS. CMS Supersymmetry Physics Results. <https://twiki.cern.ch/twiki/bin/view/CMSPublic/PhysicsResultsSUS>. Accessed 25 May 2015.
- [9] S. Chatrchyan *et al.* The CMS experiment at the CERN LHC. *JINST*, 3:S08004, 2008.
- [10] Mark Levinson. Particle Fever. <http://particlefever.com/>. Accessed 25 May 2015.
- [11] H. Fritzsch, M. Gell-Mann, and H. Leutwyler. Advantages of the color octet gluon picture. *Phys. Lett.*, B47:365–368, 1973.
- [12] Joseph Lykken and Maria Spiropulu. The future of the Higgs boson. *Physics Today*, 66:28, December 2013.
- [13] NASA. Wilkinson Microwave Anisotropy Probe. <http://map.gsfc.nasa.gov/>. Accessed 26 May 2015.

- [14] ESA. PLANCK Space Observatory. http://www.esa.int/Our_Activities/Space_Science/Planck/. Accessed 26 May 2015.
- [15] B. T. Cleveland et al. Measurement of the solar electron neutrino flux with the homestake chlorine detector. *Astrophys. J.*, 496:505, 1998.
- [16] Stephen P. Martin. A Supersymmetry primer. 1997.
- [17] D. I. Kazakov. Beyond the standard model: In search of supersymmetry. In *2000 European School of high-energy physics, Caramulo, Portugal, 20 Aug-2 Sep 2000: Proceedings*, pages 125–199, 2000.
- [18] Chatrchyan, S. *et al.* Interpretation of searches for supersymmetry with simplified models. *Phys. Rev. D*, 88:052017, Sep 2013.
- [19] ATLAS. Supersymmetry Public Results. <https://twiki.cern.ch/twiki/bin/view/AtlasPublic/SupersymmetryPublicResults>. Accessed 24 May 2015.
- [20] Daniele Alves. Simplified Models for LHC New Physics Searches. *J. Phys.*, G39:105005, 2012.
- [21] A L Read. Presentation of search results: the cl s technique. *Journal of Physics G: Nuclear and Particle Physics*, 28(10):2693, 2002.
- [22] Serguei Chatrchyan et al. Search for supersymmetry in pp collisions at $\sqrt{s}=8$ TeV in events with a single lepton, large jet multiplicity, and multiple b jets. *Phys.Lett.*, B733:328–353, 2014.
- [23] Georges Aad et al. Search for supersymmetry at $\sqrt{s}=8$ TeV in final states with jets and two same-sign leptons or three leptons with the ATLAS detector. *JHEP*, 06:035, 2014.
- [24] Search for direct top squark pair production in final states with two leptons in $\sqrt{s} = 8$ TeV pp collisions using 20fb⁻¹ of ATLAS data. Technical Report ATLAS-CONF-2013-048, CERN, Geneva, May 2013. Not published in the proceedings.
- [25] Serguei Chatrchyan et al. Search for top-squark pair production in the single-lepton final state in pp collisions at $\sqrt{s} = 8$ TeV. *Eur.Phys.J.*, C73(12):2677, 2013.
- [26] CMS. CMS summary of comparison plots in simplified models spectra for the 8TeV dataset. <https://twiki.cern.ch/twiki/bin/view/CMSPublic/SUSYSMSSummaryPlots8TeV>. Accessed 24 May 2015.
- [27] Sabine Kraml, Suchita Kulkarni, Ursula Laa, Andre Lessa, Veronika Magerl, Wolfgang Magerl, Doris Proschofsky, Michael Traub, and Wolfgang Waltenberger. SModels: A tool for interpreting simplified-model results from the LHC. <http://smodels.hephy.at>. Accessed 26 May 2015.

- [28] Sabine Kraml, Suchita Kulkarni, Ursula Laa, Andre Lessa, Veronika Magerl, Wolfgang Magerl, Doris Proschofsky, Michael Traub, and Wolfgang Waltenberger. SModelS v1.0: a short user guide. 2014.
- [29] Sabine Kraml, Suchita Kulkarni, Ursula Laa, Andre Lessa, Wolfgang Magerl, Doris Proschofsky, and Wolfgang Waltenberger. SModelS: a tool for interpreting simplified-model results from the LHC and its application to supersymmetry. *Eur.Phys.J.*, C74:2868, 2014.
- [30] Georges Aad et al. Search for squarks and gluinos with the ATLAS detector in final states with jets and missing transverse momentum using $\sqrt{s} = 8$ TeV proton–proton collision data. *JHEP*, 1409:176, 2014.
- [31] Georges Aad et al. Search for new phenomena in final states with large jet multiplicities and missing transverse momentum at $\sqrt{s}=8$ TeV proton-proton collisions using the ATLAS experiment. *JHEP*, 1310:130, 2013.
- [32] Georges Aad et al. Search for direct third-generation squark pair production in final states with missing transverse momentum and two b -jets in $\sqrt{s} = 8$ TeV pp collisions with the ATLAS detector. *JHEP*, 1310:189, 2013.
- [33] Georges Aad et al. Search for direct production of charginos, neutralinos and sleptons in final states with two leptons and missing transverse momentum in pp collisions at $\sqrt{s} = 8$ TeV with the ATLAS detector. *JHEP*, 1405:071, 2014.
- [34] Georges Aad et al. Search for direct production of charginos and neutralinos in events with three leptons and missing transverse momentum in $\sqrt{s} = 8$ TeV pp collisions with the ATLAS detector. *JHEP*, 1404:169, 2014.
- [35] Georges Aad et al. Search for the direct production of charginos, neutralinos and staus in final states with at least two hadronically decaying taus and missing transverse momentum in pp collisions at $\sqrt{s} = 8$ TeV with the ATLAS detector. *JHEP*, 1410:96, 2014.
- [36] Georges Aad et al. Search for top squark pair production in final states with one isolated lepton, jets, and missing transverse momentum in $\sqrt{s} = 8$ TeV pp collisions with the ATLAS detector. 2014.
- [37] Georges Aad et al. Search for direct top-squark pair production in final states with two leptons in pp collisions at $\sqrt{s} = 8$ TeV with the ATLAS detector. *JHEP*, 1406:124, 2014.
- [38] Search for Supersymmetry in final states with two same-sign leptons, jets and missing transverse momentum with the ATLAS detector in pp collisions at $\sqrt{s} = 8$ TeV. Technical Report ATLAS-CONF-2012-105, CERN, Geneva, Aug 2012.

- [39] Search for strongly produced superpartners in final states with two same sign leptons with the ATLAS detector using 21 fb^{-1} of proton-proton collisions at $\sqrt{s} = 8 \text{ TeV}$. Technical Report ATLAS-CONF-2013-007, CERN, Geneva, Mar 2013.
- [40] Search for direct production of the top squark in the all-hadronic $t\bar{t}b + \text{etmiss}$ final state in 21 fb^{-1} of p-p collisions at $\sqrt{s} = 8 \text{ TeV}$ with the ATLAS detector. Technical Report ATLAS-CONF-2013-024, CERN, Geneva, Mar 2013.
- [41] Search for strong production of supersymmetric particles in final states with missing transverse momentum and at least three b-jets using 20.1 fb^{-1} of pp collisions at $\sqrt{s} = 8 \text{ TeV}$ with the ATLAS Detector. Technical Report ATLAS-CONF-2013-061, CERN, Geneva, Jun 2013.
- [42] Searches for direct scalar top pair production in final states with two leptons using the transverse mass variable and a multivariate analysis technique in $\sqrt{s} = 8 \text{ TeV}$ pp collisions using 20.3 fb^{-1} of ATLAS data. Technical Report ATLAS-CONF-2013-065, CERN, Geneva, Jul 2013.
- [43] Serguei Chatrchyan et al. Search for gluino mediated bottom- and top-squark production in multijet final states in pp collisions at 8 TeV. *Phys.Lett.*, B725:243–270, 2013.
- [44] Serguei Chatrchyan et al. Search for supersymmetry in hadronic final states with missing transverse energy using the variables α_T and b-quark multiplicity in pp collisions at $\sqrt{s} = 8 \text{ TeV}$. *Eur.Phys.J.*, C73(9):2568, 2013.
- [45] Serguei Chatrchyan et al. Search for anomalous production of events with three or more leptons in pp collisions at $\sqrt{s} = 8 \text{ TeV}$. *Phys.Rev.*, D90:032006, 2014.
- [46] Vardan Khachatryan et al. Searches for electroweak production of charginos, neutralinos, and sleptons decaying to leptons and W, Z, and Higgs bosons in pp collisions at 8 TeV. *Eur.Phys.J.*, C74(9):3036, 2014.
- [47] Serguei Chatrchyan et al. Search for new physics in the multijet and missing transverse momentum final state in proton-proton collisions at $\sqrt{s} = 8 \text{ TeV}$. *JHEP*, 1406:055, 2014.
- [48] Serguei Chatrchyan et al. Search for new physics in events with same-sign dileptons and jets in pp collisions at $\sqrt{s} = 8 \text{ TeV}$. *JHEP*, 1401:163, 2014.
- [49] Search for supersymmetry in pp collisions at $\sqrt{s} = 8 \text{ TeV}$ in events with three leptons and at least one b-tagged jet. Technical Report CMS-PAS-SUS-13-008, CERN, Geneva, 2013.

- [50] Search for supersymmetry in pp collisions at $\sqrt{s} = 8$ TeV in events with two opposite sign leptons, large number of jets, b-tagged jets, and large missing transverse energy. Technical Report CMS-PAS-SUS-13-016, CERN, Geneva, 2013.
- [51] Search for direct production of bottom squark pairs. Technical Report CMS-PAS-SUS-13-018, CERN, Geneva, 2014.
- [52] Search for supersymmetry in hadronic final states using MT2 with the CMS detector at $\sqrt{s} = 8$ TeV. Technical Report CMS-PAS-SUS-13-019, CERN, Geneva, 2014.
- [53] Exclusion limits on gluino and top-squark pair production in natural SUSY scenarios with inclusive razor and exclusive single-lepton searches at 8 TeV. Technical Report CMS-PAS-SUS-14-011, CERN, Geneva, 2014.
- [54] Johan Alwall, A. Ballestrero, P. Bartalini, S. Belov, E. Boos, et al. A Standard format for Les Houches event files. *Comput.Phys.Commun.*, 176:300–304, 2007.
- [55] Peter Z. Skands, B.C. Allanach, H. Baer, C. Balazs, G. Belanger, et al. SUSY Les Houches accord: Interfacing SUSY spectrum calculators, decay packages, and event generators. *JHEP*, 0407:036, 2004.
- [56] particle data group. Monte carlo numbering scheme 2014. http://pdg.lbl.gov/2014/mcdata/mc_particle_id_contents.html. Accessed 20 August 2015.
- [57] Les Houches. Extending the SLHA: cross section information. <http://phystev.cnrs.fr/wiki/2013:groups:tools:slha>. Accessed 26 May 2015.
- [58] B.C. Allanach. SOFTSUSY: a program for calculating supersymmetric spectra. *Comput.Phys.Commun.*, 143:305–331, 2002.
- [59] A. Djouadi, M.M. Mühlleitner, and M. Spira. Decays of supersymmetric particles: The Program SUSY-HIT (SUspect-SdecaY-Hdecay-InTerface). *Acta Phys.Polon.*, B38:635–644, 2007.
- [60] Werner Porod. SPheno, a program for calculating supersymmetric spectra, SUSY particle decays and SUSY particle production at e+ e- colliders. *Comput.Phys.Commun.*, 153:275–315, 2003.
- [61] Torbjörn Sjöstrand, Stephen Mrenna, and Peter Z. Skands. PYTHIA 6.4 Physics and Manual. *JHEP*, 0605:026, 2006.
- [62] Christoph Borschensky *et al.* NLL-fast. <http://pauli.uni-muenster.de/~akule.01/nllwiki/index.php/NLL-fast>. Accessed 26 May 2015.
- [63] W. Beenakker, R. Hopker, M. Spira, and P.M. Zerwas. Squark and gluino production at hadron colliders. *Nucl.Phys.*, B492:51–103, 1997.

- [64] W. Beenakker, M. Krämer, T. Plehn, M. Spira, and P.M. Zerwas. Stop production at hadron colliders. *Nucl.Phys.*, B515:3–14, 1998.
- [65] A. Kulesza and L. Motyka. Threshold resummation for squark-antisquark and gluino-pair production at the LHC. *Phys.Rev.Lett.*, 102:111802, 2009.
- [66] A. Kulesza and L. Motyka. Soft gluon resummation for the production of gluino-gluino and squark-antisquark pairs at the LHC. *Phys.Rev.*, D80:095004, 2009.
- [67] Wim Beenakker, Silja Brensing, Michael Krämer, Anna Kulesza, Eric Laenen, et al. Soft-gluon resummation for squark and gluino hadroproduction. *JHEP*, 0912:041, 2009.
- [68] Wim Beenakker, Silja Brensing, Michael Krämer, Anna Kulesza, Eric Laenen, et al. Supersymmetric top and bottom squark production at hadron colliders. *JHEP*, 1008:098, 2010.
- [69] W. Beenakker, S. Brensing, M. Krämer, A. Kulesza, E. Laenen, et al. Squark and Gluino Hadroproduction. *Int.J.Mod.Phys.*, A26:2637–2664, 2011.
- [70] Veronika Magerl. Constraining Low Fine Tuned Supersymmetric Models With Simplified Models Spectra Results Based On CMS And ATLAS Searches. Master’s thesis, Technische Universität Wien, 2015.
- [71] Search for direct top squark pair production in final states with one isolated lepton, jets, and missing transverse momentum in $\sqrt{s} = 8, \text{TeV}$ pp collisions using 21 fb^{-1} of ATLAS data. Technical Report ATLAS-CONF-2013-037, CERN, Geneva, Mar 2013.
- [72] Search for supersymmetry using razor variables in events with b-jets in pp collisions at 8 TeV. Technical Report CMS-PAS-SUS-13-004, CERN, Geneva, 2013.
- [73] Durham University. The durham hepdata project. <http://hepdata.cedar.ac.uk/>. Accessed 09 September 2015.
- [74] Cornell University Library. arXiv document server. <http://arxiv.org/>. Accessed 31 August 2015.
- [75] Michele Papucci, Kazuki Sakurai, Andreas Weiler, and Lisa Zeune. Fastlim: a fast LHC limit calculator. *Eur. Phys. J.*, C74(11):3163, 2014.